Aus der Kinderklinik und Kinderpoliklinik im Dr. von Haunerschen Kinderspital
der Ludwig-Maximilians-Universität München
Direktor: Prof. Dr. med. Dr. sci. nat. C. Klein
Abteilung: Neonatologie am Perinatalzentrum Großhadern

Mesenchymale Stromazellen aus der Lunge extrem unreifer Frühgeborener und ihre Wechselwirkung mit der pulmonalen Entzündungsreaktion

Dissertation
zum Erwerb des Doktorgrades der Medizin
an der Medizinischen Fakultät der
Ludwig–Maximilians–Universität zu München

vorgelegt von
Tobias Reicherzer
aus
München
2020

Berichterstatter: PD Dr. med. Harald Ehrhardt

Mitberichterstatter: Prof. Dr. Jürgen Behr

                                     Prof. Dr. Alexander Bartelt

                                     PD Dr. Gerhard Wolf

Dekan: Prof. Dr. med. dent. Reinhard Hickel

Tag der mündlichen Prüfung: 16.01.2020

Für meinen Vater
Konrad Reicherzer
1942 – 2002
in Liebe und Dankbarkeit

und für meine Söhne
Konrad und Franz
in Liebe und Zuversicht

Inhaltsverzeichnis

1 Einleitung

1.1 Hintergrund

Frühgeburtlichkeit ist in Deutschland, wie in praktisch allen westlichen Industriestaaten, ein zunehmendes Problem. Besonders die Zahl der extrem kleinen Frühgeborenen unter vollendeten 28 Schwangerschaftswochen (SSW) ist in den letzten Jahren gestiegen. Allein in Deutschland kamen im Jahr 2014 4242 Kinder als extreme Frühgeborene vor der 28. SSW zur Welt (AQUA, Institut für angewandte Qualitätsförderung und Forschung im Gesundheitswesen GmbH 2015). Die Bronchopulmonale Dysplasie (BPD) ist in dieser Patientengruppe als eine besonders häufige und schwerwiegende Konsequenz der Frühgeburt mit lebenslang fortbestehender Lungenfunktionseinschränkung verbunden mit einem erhöhten Risiko für eine Vielzahl von Morbiditäten und auch Mortalität (Gough u. a. 2014; Islam u. a. 2015). Um die langandauernden Auswirkungen der neonatalen BPD zu betonen, sprechen manche Autoren, wie auch hier in der zweiten vorgestellten Veröffentlichung, von „Neonatal Chronic Lung Disease" (nCLD – Chronische Lungenerkrankung des Neugeborenen).

Die BPD bewirkt eine Störung der normalen Lungenentwicklung im sakkulären Stadium. Die Ursachen der BPD liegen in zahlreichen prä-, peri- und postnatalen Faktoren: Plazentainsufffizienz und Wachstumsrestriktion des Feten, genetische Prädisposition, Tabakrauchexpostition in der Schwangerschaft, sowie der durch die Frühgeburtlichkeit bedingte Surfactant-Mangel, prä- und postnatale Infektionen, Beatmung und Sauerstoffexposition.(Gronbach u. a. 2018) Allen diesen Faktoren ist gemeinsam, dass sie eine Inflammationsreaktion in der sich entwickelnden Lunge hervorrufen, die das für die Lungenentwicklung notwendige Gleichgewicht stört und für die Pathogenese der BPD eine zentrale Rolle spielt. (Shahzad u. a. 2016; Hilgendorff u. a. 2014)

Seit Mesenchymale Stromazellen (MSCs, zur Nomenklatur dieser Zellen siehe weiter unten) erstmals im Trachealsekret Frühgeborener nachgewiesen wurden (Hennrick u. a. 2007), haben mehrere Arbeiten die Rolle dieser Zellen bei der Entstehung der BPD untersucht (Popova u. a. 2010a; Bozyk u. a. 2011). MSCs wurde darüber hinaus eine zentrale Rolle bei der Organogenese und Regeneration vieler Organe sowie bedeutende immunmodulatorische Effekte bei Entzündungsreaktionen zugeschrieben (Silva Meirelles u. a. 2006; Aggarwal und Pittenger 2005) . Eine erste Phase I Studie untersuchte bereits den Einsatz allogener MSCs aus der Nabelschnur bei Kindern mit sich abzeichnender schwerer BPD, wobei sich zwar

ein vielversprechender Effekt auf die BPD-Entstehung zeigte (Chang u. a. 2014), es aber auch zu einem nicht gut erklärten Todesfall durch eine Sepsis kam (Ahn u. a. 2017). In einer anschließenden Phase II-Studie zeigten sich allerdings keine statistisch relevanten Vorteile (Park 2017).

Die genauen Mechanismen, wie residente MSCs in der Lunge, aber auch Spender-MSCs die Inflammationsreaktion, die letzten Endes zur BPD-Entstehung führt, beeinflussen, sind noch nicht gut verstanden.

Die hier vorgestellten Arbeiten wollen die Rolle der MSCs bei der BPD-Entstehung weiter aufschlüsseln, indem sie die Funktion der an Inflammationsreaktionen beteiligten Signalwege NFκB, PDGF, VEGF sowie TGF-β im Rahmen der BPD untersuchen.

1.2 Die BPD und ihre Pathologie

Die BPD war bei ihrer Erstbeschreibung durch Northway eine vor allem radiologische Diagnose (Northway u. a. 1967). Histopathologisch war bei Patienten, die an BPD litten, eine Fibrose der Lunge und eine Hypertrophie der glatten Muskelzellen der Atemwege zu sehen (Philip 2012). Durch tiefgreifende Änderungen in der Versorgung Frühgeborener, z.B durch die Einführung von exogenem Surfactant (Speer u. a. 1992), antenatalen Kortikosteroiden – und der auch dadurch ermöglichten schonenderen Beatmung – hat sich das Krankheitsbild deutlich gewandelt. Die „neue" BPD betrifft unreifere Kinder und zeigt histopathologisch deutlich weniger Fibrose, sondern in erster Linie eine Störung der Alveolarisierung und der Vaskulogenese in der Lunge (Jobe 1999).

Zum Zeitpunkt der extremen Frühgeburt befindet sich die Lunge im sakkulären Stadium ihrer Entwicklung. Mensenchymale Stammzellen sind die Vorläuferzellen mehrerer Zellpopulationen, die in diesem Stadium der Lungenentwicklung eine sehr wichtige Rolle spielen. Es wurde u.a. gezeigt, dass Zellen, die als Myofibroblasten bezeichnet wurden und die in vielen Aspekten den MSCs gleichen bzw. eventuell sogar entsprechen (siehe 1.3), eine wichtige Rolle bei der Alveolarisierung spielen und bei deren Fehlen bzw. gestörter Funktion es im Tiermodell zu abnorm weiten Alveolarsäcken kommt (Boström u. a. 1996; Lindahl u. a. 1997). Es existieren Hinweise, dass sich Lungen-MSCs zu diesen Myofibroblasten differenzieren (Popova u. a. 2010b).

Nach den Kriterien von Jobe und Bancalari wird die Diagnose BPD klinisch gestellt. Eine BPD liegt definitionsgemäß dann vor, wenn das Kind mehr als 28 Tage Sauerstoffbedarf zeigt. Der Schweregrad wird nach dem Sauerstoffbedarf bei 36 SSW bzw. bei Entlassung (je nachdem, was früher ist) eingeteilt: Kinder mit

milder BPD haben bei 36 SSW bzw. Entlassung keinen Sauerstoffbedarf, Kinder mit moderater BPD benötigen eine $F_I O_2$ von weniger als 0,3 und Kinder mit schwerer BPD eine $F_I O_2$ von mehr als 0,3 und/oder Überdruckbeatmung. (Jobe und Bancalari 2001) Eine ernste Limitation dieser Definition für die Forschung besteht darin, dass das Ausmaß von langfristigen Komplikationen und das Ausmaß einer eventuellen Erholung der Lungenfunktion durch sie nicht abgebildet werden kann. Aber auch wenn mittlerweile andere Definitionen vorgeschlagen wurden, ist die Definition von Jobe und Bancalari nach wie vor die, die sowohl im klinischen Alltag, als auch in der Literatur überwiegend verwendet wird, so auch in den hier vorgestellten Arbeiten.

1.3 Mesenchymale Stromazellen, Mesenchymale Stammzellen, Fibroblasten, Myofibroblasten: Unterschiedliche Zellpopulationen?

Die Zellen, die in den hier vorliegenden Arbeiten untersucht werden, zeigen ein spindelförmiges Aussehen, adhärieren an Plastik, proliferieren in Kultur und lassen sich in Osteoblasten und Adipozyten ausdifferenzieren. Außerdem zeigen sie in unterschiedlicher Ausprägung Expression von αSMA, was gemeinhin als Merkmal von Myofibroblasten gilt (Desmoulière u. a. 2005). Aufgrund der Expression der Oberflächenmarker CD 90, CD 13, CD 73 und CD 105 konnten sie als Zellen mesenchymalen Ursprungs identifiziert werden. Bis auf die Expression von αSMA gelten diese Kriterien ebenso für Fibroblasten, wie für Mesenchymale Stammzellen, so dass unklar bleibt, ob diese zwei Zellpopulationen in vitro sicher zu unterscheiden sind. Da diesen Zellpopulationen auch funktionell die gleichen Aufgaben – insbesondere während Verletzung und Inflammation – zugeschrieben wird, ist eine Unterscheidung im Einzelfall für die meisten Fragestellung auch nicht zwingend notwendig. (Haniffa u. a. 2009)

Der Begriff Mesenchymale Stromazellen trägt dieser Unschärfe Rechnung, da er, ohne eine klare Unterscheidung zu suggerieren, die unterschiedlichen Zellpopulationen zusammenfasst. Aufgrund der Expression von αSMA, die auch von den Erstbeschreibern der Lungen-MSCs gesehen wurde (Hennrick u. a. 2007), werden die Zellen in der zweiten Publikation als Myofibroblasten bezeichnet. In der sich entwickelnden Lunge wird den Myofibroblasten in den aussprossenden Alveolarsepten eine zentrale Rolle bei der Alveolarisierung und bei der Angiogenese zugesprochen. Sie spielen also wahrscheinlich eine Schlüsselrolle bei der Entstehung der BPD (Li u. a. 2015). Da die hier vorgestellten Daten dafür sprechen, dass ein Kontinuum der Myofibroblasten-Differenzierung im mesenchymalen Kompartment der fetalen
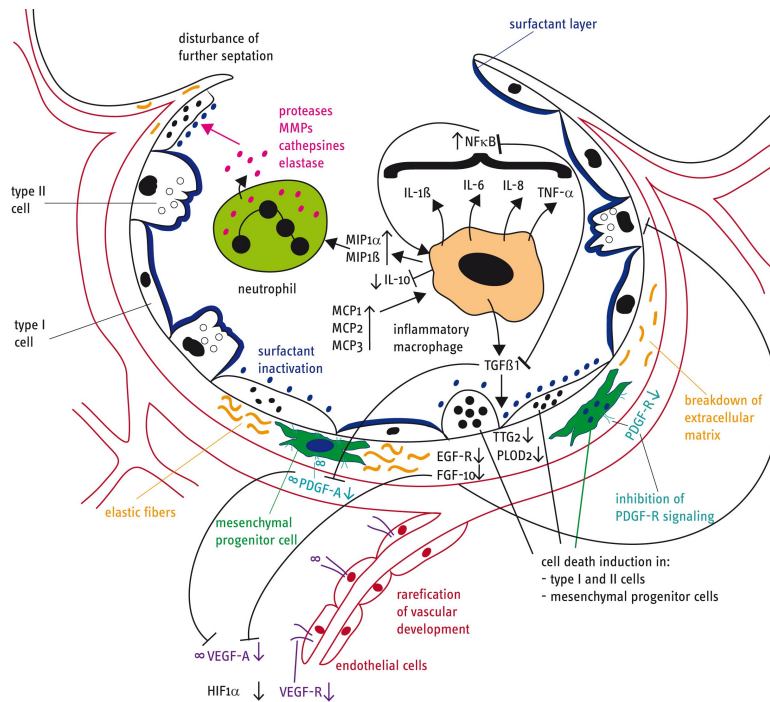
Abbildung 1.1: Pathogenese der BPD (aus: Gronbach u. a. 2018)

Lunge besteht, denke ich, dass die Bezeichnungen MSCs und Myofibroblasten sich auf eine zumindest in weiten Teilen identische Zell-Population mit variablem Differenzierungsgrad beziehen und deswegen hier ohne Widerspruch beide für die aus dem Trachealsekret gewonnenen Zellen verwendet werden können.

1.4 MSCs im inflammatorischen Millieu der BPD-Entstehung

Es scheint wenig überraschend, dass in der Lunge des Frühgeborenen komplexe Inflammationsprozesse vonstatten gehen (Abb.1.1). Untersuchungen des Trachealsekrets Frühgeborener haben gezeigt, dass mit der BPD-Entstehung ein Überwiegen pro-inflammatorischer Zytokine, wie IL-1β, IL-6, IL-8, TNF-α, Monocyte Chemoattractant Proteins (MCP), und Macrophage Inflammatory Proteins (MIPs) vergesellschaftet ist (Shahzad u. a. 2016), während sich im Trachealsekret und in pathologischen Lungen-Schnitten von Kindern mit sich entwickelnder BPD geringere Mengen von anti-inflammatorischen Proteinen, wie IL-10 und von Wachsumsfaktoren wie VEGF-A und PDGF-A befinden (Popova u. a. 2014; Bhatt u. a. 2001; Speer 2006). Eine simple Dosis-Wirkung-Beziehung in dem Sinne, dass weniger pro-inflammatorische Signalmoleküle in der fetalen/frühgeborenen Lunge zu weniger Krankheitsausprägung führt, besteht allerdings wohl nicht. Das wird besonders klar, betrachtet man NfκB und TGF-β. Der exzesssiven NfκB-Aktivierung wird eine zentrale Rolle bei der Entstehung der BPD zugeschrieben, die Inhibierung von

NfκB zeigte in Vitro eine positive Auswirkung auf die Alveologenese (Blackwell u. a. 2011). Allerdings ist NfκB, als ubiquitär exprimierter Transkriptionsfaktor mit zahlreichen Zielgenen, auch ein wichtiger Faktor bei der physiologischen Entwicklung der Lunge (wie auch anderer Organe) und eine Inhibierung von NfκB zeigte wiederum auch eine negative Auswirkung auf die Entwicklung der Lunge (Iosef u. a. 2012). Für TGF-β gilt Ähnliches: Sowohl ein Überwiegen, als auch ein Mangel an TGF-β geht mit einer Störung der Lungenentwicklung einher (Gauldie u. a. 2003; Bonniaud u. a. 2004).

So, wie die reine Anwesenheit von NfκB und TGF-β keine per se negative oder positive Wirkung auf die BPD-Entstehung hat, so ist auch die Rolle der MSCs nicht einfach zu definieren. Während einige Arbeiten die bloße Anwesenheit von MSCs im Trachealsekret mit der Entstehung der BPD assoziierten (Popova u. a. 2010a), so betonen andere Arbeiten die Rolle der MSCs als mögliche Therapeutika (Möbius und Thébaud 2015). Es steht zu vermuten, dass der Unterschied in der Rolle der MSCs bei der BPD-Entstehung in der Ausprägung des inflammatorischen Milieus besteht. So stammen die therapeutischen MSCs bisher aus der Nabelschnur bzw. dem peripheren Blut von Spendern, mithin also aus einer nicht-inflammatorischen Umgebung.

2 Ziele dieser Arbeit

Die hier vorgelegten Arbeiten sollen zum einen eine molekulare Charakterisierung der MSCs aus dem Trachealsekret liefern und zum anderen helfen, die Marker oder Eigenschaften von MSCs, die mit einem ungünstigen klinischen Verlauf assoziiert sind, zu identifizieren, indem sie weiter aufklären, wie das inflammatorische Milieu in der frühgeborenen Lunge mit MSCs wechselwirkt.

In bisherigen Arbeiten wurde zwar ein Zusammenhang zwischen der Präsenz von Lungen-MSCs im Trachealsekret und der Entstehung von BPD postuliert (Popova u. a. 2010a), die oben dargestellte möglicherweise zwiespältige Rolle der MSCs in der Inflammation aufzuklären gelang bisher aber noch nicht zufriedenstellend. Hier soll deshalb versucht werden, zumindest anhand molekularer Marker einen Phänotyp zu identifizieren, der sich mit einem schlechten pulmonalen Outcome assoziieren lässt.

In den hier vorgelegten Arbeiten wurde die Hypothese überprüft, dass sich MSCs von Kindern, die schwerer von einer BPD betroffen waren, durch ihre Suszeptibilität gegenüber inflammatorischen Reizen von den MSCs weniger schwer betroffener Kinder unterscheiden. Durch die Definition der Unterschiede zwischen den Phänotypen sollte es dann möglich sein, molekulare Mechanismen zu identifizieren, die möglicherweise entweder die MSCs daran hindern, ihre anti-inflammatorische Funktion auszuüben, oder die MSCs dazu prädisponiert, selbst proinflammatorische Signale auszusenden. Die Identifikation möglicherweise von der Inflammation betroffener oder sogar dafür ursächlicher Signalwege könnte dabei helfen, die Rolle der Lungen-MSCs bei der pulmonalen Inflammation besser zu verstehen.

3 Ergebnisse eigener wissenschaftlicher Arbeiten

3.1 Die spezifische Phänotypveränderung der MSC ist prädiktiv für die BPD-Entstehung

Reicherzer T., Häffner S., Shahzad T., Gronbach J., Mysliwietz J., Hübener C., Hasbargen U., Gertheiss J., Schulze A., Bellusci S., Mort y R.E., Hilgendorff A. und Ehrhardt H. (2018). „Activation of the NFκB pathway alters the phenotype of MSCs in the tracheal aspirates of preterm infants with severe BPD". In: *American Journal of Physiology-Lung Cellular and Molecular Physiology.* L87-L101

Im Gegensatz zu Vorarbeiten (Hennrick u. a. 2007; Popova u. a. 2010a) konnt hier kein Zusammenhang zwischen BPD-Ausprägung und der Präsenz der MSCs nachgeweisen werden (Fig. 2). Bei allen Kindern, die mindestens sieben Tage lang invasiv beatmet wurden, konnten wir MSCs aus dem Trachealaspirat isolieren, auch wenn sich im weiteren Verlauf nur eine milde BPD entwickelte.

Allerdings zeigten sich deutliche Unterschiede zwischen den MSC-Kulturen der verschiedenen Kinder. Mithilfe von automatisierter Lichtmikroskopie (Cellscreen, Fig. 3a) wurde die Ausbreitung der MSCs in Zellkultur überprüft. Es zeigte sich, dass ein verstärktes Ausbreiten im Kultur-Well tatsächlich durch Proliferation und nicht durch Hypertrophie der Zellen oder geringere Apoptose bedingt war (Fig. 3c-e). Mit dem Parameter Proliferationsindex (PI), der den Vergleich verschiedener Versuchsansätze ermöglicht, wurde das Proliferationsverhalten der Zellkulturen von Patienten mit schwerer und milder BPD verglichen. Es zeigte sich, dass ein hoher PI prädiktiv für eine schwerere BPD-Ausprägung ist (Fig. 4).

Auf Proteinebene gab es einen Unterschied in der Expression des Myofibroblasten-Markers αSMA, der in MSCs von weniger schwer von BPD betroffenen Patienten stärker exprimiert wurde. Eine starke αSMA-Expression war prädiktiv für eine weniger starke Ausprägung der BPD (Fig 4).

Als mögliche Ursache der Unterschiede im Phänotyp der MSCs konnte der Transkriptionsfaktor NFκB identifiziert werden. Eine hohe nukleäre Akkumulation von NFκB ging mit einer schwereren BPD-Ausprägung einher (Fig. 6b). Ein Score, der höher war, je höher der PI und die Expression von NFκB und je niedriger die Expression von αSMA war, erwies sich in einer Receiver Operating Characteristic (ROC) als gutes Prognose-Werkzeug, um eine schwere BPD vorherzusagen (Area under the Curve (AUC) 0,847).

NFκB ist als Transkriptionsfaktor zentraler Bestandteil in zahlreichen pro-in-

flammatorischen Signalwegen (Baeuerle und Baichwal 1997). Um zu belegen, dass die Aktivierung von NFκB nicht nur mit der BPD-Ausprägung lediglich korreliert, sondern als zentraler Bestandteil der von den pro-inflammatorischen Zytokinen in Gang gebrachten Signalwege tatsächlich zumindest mit-ursächlich für den unterschiedlichen Phänotyp der MSCs ist, wurde der Phänotyp durch Inhibierung der Expression von NFκB durch Transfektion mit siRNA gezielt verändert. Nach Knock-down von NFκB zeigte sich eine geringere Proliferation der MSCs (Fig. 7).

Dass die NFκB-Akkumulation Teil des Phänotypes war, der sich als prädiktiv für ein schlechtes pulmonales Outcome erwies, führte zu der Vermutung, dass die Unterschiede im MSC-Phänotyp zumindest teilweise bedingt waren durch die unterschiedliche Ausprägung der Inflammationsreaktion, der die MSCs in vivo vor Inkulturnahme ausgesetzt waren.

Passend dazu zeigte sich, dass die Menge an dem pro-inflammatorischen Protein Il-1β im Trachealaspirat mit dem PI der MSCs, die aus diesem Trachealaspirat isoliert wurden, positiv korreliert war (Fig. 8a). Der mit einem schlechten pulmonalen Outcome vergesellschafteten MSC-Phänotyp ließ sich durch Stimulation der MSCs mit TNFα und IL-1β induzieren: In einer Dosis-abhängigen Weise stieg der PI nach Stimulation mit Il-1β an, auch nach Stimulation mit TNFα ließ sich eine verstärkte Proliferation zeigen. Wie zu erwarten war, führte die Stimulation mit beiden Zytokinen zu einer Aktivierung von NFκB, die Expression von αSMA nahm nach Stimulation ab. Eine einmalige Stimulation der Zellen führte mindestens noch nach 120 Stunden zu einer erhöhten Proliferationsrate der MSCs. Das inflammatorische Milieu in der neonatalen Lunge konnte also den Phänotyp der MSC auch noch lange nach Inkulturnahme der Zellen stabil beeinflussen (Fig. 8). Ein Knockdown von NFκB durch siRNA konnte die Steigerung der Proliferation durch Il-1β und TNFα verhindern.

Schlussfolgernd führte also die Simulation einer pro-inflammatorischen Umgebung in vitro bei pulmonalen MSCs zu Phänotyp-Veränderungen, die auch bei MSCs von Kindern mit einem schlechten pulmonalen Outcome bestehen. Außerdem ist die nukleäre Akkumulation von NFκB nötig, um die Phänotypveränderungen durch pro-inflammatorische Zytokine zu induzieren.

Eigener Anteil an der Arbeit: Nach Einarbeitung durch Harald Ehrhardt etablierte ich die MSC-Kultur und erhob die klinischen Daten (Fig 1, 2, Tabellen). Die Charakterisierung der kultivierten Zellen als MSCs (Durchflusszytometrie, Fig. 1) wurde von mir nach Anleitung durch Josef Mysliewitz durchgeführt. Die weiteren Experimente, nachdem sich phänotypische Unterschiede zwischen den MSC-Kulturen angedeutet hatten, wurden von Harald Ehrhardt und mir geplant.

Die Etablierung und Validierung der CellScreen-Messungen (Fig. 3) wurde von mir mit Unterstützung von Susanne Häffner durchgeführt. Die Bestimmung des Phänotypes der MSCs (Immunfluoreszenz-Mikroskopie, Bestimmung der Proliferation, Western-Blot, Fig 4, 5, 6) wurde von mir mit Unterstützung von Harald Ehrhardt durchgeführt, ebenso die Etablierung des siRNA-Knockdowns (Fig 7). Die Zytokin-Stimulationen (Fig 8, 9) wurden größtenteils von Susanne Häffner, Tayyab Shahzad und Judith Gronbach durchgeführt. Die statistische Auswertung führte ich nach Beratung und mit wertvollem Input von Jan Gertheiss zusammen mit Harald Ehrhardt und Suanne Häffner durch. Bei der Interpretation der Daten unterstützen uns Andreas Schulze, Uwe Hasbargen und Christoph Hübner. Harald Ehrhardt und ich verfassten das Manuskript, das von Anne Hilgendorff, Rory E. Morty, Saverio Bellusci und Jan Gertheiss durch Anmerkungen und Korrekturen verbessert wurde.

3.2 Auch Veränderungen im PDGF-Signalweg führen zu einem ungünstigen Phänotyp

Oak P., Pritzke T., Thiel I., Koschlig M., Mous D. S., Windhorst A., Jain N., Eickelberg O., Förster K., Schulze A., Goepel W., **Reicherzer T.**, Ehrhardt H., Rottier R.J., Ahnert P., Gortner L., Desai T.J. und Hilgendorff A. (2017). „**Attenuated PDGF signaling drives alveolar and microvascular defects in neonatal chronic lung disease**" In: *EMBO molecular medicine* 9(11), S. 1504-1520.

Die Entstehung der Pathologie der neuen BPD mit gestörter Alveolarisierung und Vaskularisierung wurde in der Vergangenheit, wie oben beschrieben, auch auf das Fehlen, bzw. die Fehlfunktion von PDGF-Rα-positiven mesenchymalen Zellen zurückgeführt. Untersuchungen konnten zeigen, dass sowohl im Tiermodell (Bland u. a. 2003; Bland u. a. 2007; Bland u. a. 2008), als auch bei Frühgeborenen (Popova u. a. 2014) die Menge an PDGF-A und PDGF-Rα durch mechanische Beatmung vermindert wurde und MSCs von Kindern, die BPD entwickeln, weniger PDGF-Rα exprimieren. Jedoch ist im Tiermodell in der Vergangenheit auch bereits eine überschießende Inflammationsreaktion mit einer PDGF-Überexpression in Verbindung gebracht worden (Hoyle u. a. 1999). Das Ziel dieser Arbeit war es, mit dem PDGF-Signalweg die Rolle eines weiteren, nicht von vornherein als primär gut oder schlecht für die Lungenentwicklung einzuschätzenden und von der pulmonalen Inflammationsreaktion beeinflussten Signalweges weiter zu erhellen.

Die vorgelegte Arbeit zeigte, dass in den MSCs von beatmeten Kindern über die Dauer der Beatmung – und damit auch über die Dauer der die pulmonale Inflam-

mation auslösenden Stimuli - wie mechanische Belastung und Sauerstoff - die Expression von PDGF-Rα abnimmt (Fig 1a). In einer Fall-Kontroll-Analyse von 1061 Neugeborenen konnten drei single nucleotid polymorphisms (SNPs) im PDGF-Rα Gen identifiziert werden, die, falls mindestens einer von ihnen vorlag, mit einer geringeren Expression von PDGF-Rα und einer geringeren Migrationsfähigkeit der MSCs assoziiert waren. Es konnten also genetische Risikofaktoren identifiziert werden, die teilweise die unterschiedliche Suszeptibilität für Lungenveränderungen im Sinne einer BPD erklären könnten.

In einem Mausmodell, das haploinsuffizient für PDGF-Rα war, zeigte sich, dass die Wildtypmäuse weniger anfällig für Lungenveränderungen durch Beatmung waren, als die PDGF-Rα-haploinsufffizienten. Interessanterweise zeigten die PDGF-Rα-haploinsuffizienten Mäuse auch eine verminderte Vaskularisierung der Lunge nach Beatmung, möglicherweise bedingt durch eine verringerte Expression von VEGF-A (Fig. 3). Diese Veränderungen ließen sich teilweise durch endotracheale Verabreichung von PDGF-A verhindern (Fig. 4).

Ein starker Hinweis auf einen Mechanismus, der die unterschiedliche Reaktion Frühgeborener auf pulmonale inflammatorische Reize bedingt, liegt darin, dass wir zeigen konnten, dass bei Patienten mit BPD zum einen in Lungenschnitten signifikant weniger Expression von PDGF-Rα festzustellen war, zum anderen diese Patienten mit ansteigenden TGF-β-Spiegeln weniger PDGF-Rα exprimierten, Patienten die klinisch weniger beeinträchtigt waren (und keine BPD entwickelten) allerdings mit ansteigenden TGF-β-Spiegel mehr PDGF-Rα-Expression zeigten (Fig. 5 a+b). Dieser Unterschied unterstreicht, dass auch formal pro-inflammatorischen Zytokinen wie TGF-β nicht eindeutig eine Rolle zugeschrieben werden kann, sondern dass in diesem Fall insbesondere TGF-β je nach Kontext und Gesamtsituation in einem komplexen Netzwerk aus Signalwegen die Inflammation einerseits befördern, andererseits aber auch zur normalen Lungenentwicklung und sogar zur Reparatur von Gewebeschäden beitragen kann (Bartram und Speer 2004).

Dass die verminderte PDGF-Rα-Expression in mesenchymalen Lungen-Zellen tatsächlich (zumindest auch) auf den Einfluss von TGF-β zurückzuführen ist, wurde mit einem Luciferase-Assay nachgewiesen: Ich transfizierte CCL206-Zellen mit einem pGal-Vektor, der den PDGF-Rα-Promotor enthielt. In Zellen, die mit TGF-β stimuliert wurden, zeigte sich eine deutlich reduzierte Promotor-Aktivität.

Die vorliegende Arbeit zeigt, dass der PDGF-Signalweg von dem pro-inflammatorischen Zytokin TGF-β beeinflusst werden kann, und dass dieser Mechanismus eine mögliche (zumindest teilweise) Erklärung für die krankhaft verminderte Alveolisierung und – durch Beeinflussung des VEGF-Signalweges – die verminderte Dichte an Kapillaren, die für die BPD kennzeichnend ist, sein kann. Allerdings zeigt

sich diese Korrelation nicht bei allen Patienten, sondern es scheint Situationen zu geben, in denen die Empfindlichkeit für pro-inflammatorische Zytokine nicht gegeben ist. Ob die PDGF-Effekte lediglich auch oder sogar vor allem in MSCs zu Tage treten, konnte allerdings mit dieser Arbeit nicht nachgewiesen werden.

Eigener Anteil an der Arbeit: Ich stellte die von mir etablierten MSC-Kulturen und die klinischen Daten der Patienten für die in Fig 1a, Fig 5 i-m und Fig 6 l+m sowie im Anhang in S3a und in Tabelle S3c gezeigten Ergebnisse zur Verfügung. Außerdem wirkte ich an der Auswertung der Versuche mit und führte das Experiment aus Fig. 5d einschließlich Auswertung durch. Das Konzept des Papers wurde größtenteils von Anne Hilgendorff, Oliver Eickelberg und Tushar Desai erstellt. Der Großteil der Experimente wurde von Prajakta Oak, Tina Pritzke, Markus Koschlig und Isabella Thiel durchgeführt. Die anderen Co-Autoren stellten Patientendaten und Probenmaterial zur Verfügung, beziehungsweise wirkten an der Versuchsauswertung mit oder lieferten Anregungen für das Manuskript.

4 Schlussfolgerung und Ausblick: Modulation des Phänotyps residenter MSC eröffnet neue therapeutische Möglichkeiten

Die vorgelegten Arbeiten konnten zum einen zeigen, dass ein bestimmter Phänotyp von MSCs, der durch eine hohe Spontanproliferation, hohe NfκB-Aktivierung und geringe αSMA-Expression charakterisiert ist, mit einer schwereren Ausprägung der BPD vergesellschaftet ist, zum anderen, dass bei Kindern, die eine BPD entwickeln, ein hoher TGF-β-Spiegel mit einer geringen PDGF-Rα-Expression vergesellschaftet ist, während die Korrelation bei Kindern ohne BPD genau umgekehrt ist. Da sich außerdem zeigte, dass der Phänotyp der MSCs durch pro-inflammatorische Zytokine in Richtung des mit schwerer BPD vergesellschafteten Phänotyps verschoben werden kann, und da eine Störung des PDGF-Signalweges zu verminderter Alveolarisierung und Kapillarisierung führt, konnten zwei potentiell ineinandergreifende Mechanismen identifiziert werden, die zur BPD-Entstehung beitragen können. Offensichtlich scheint es entweder eine intrauterine Prägung der MSCs zu geben (etwa durch intrauterine Infektion oder Zytokinausschüttung bei Plazentainsuffizienz (Bartha u. a. 2003)), oder eine individuelle Veranlagung, die zu gesteigerter Empfindlichkeit gegenüber Inflammationsreizen führt, demonstriert zum einen durch den veränderten Phänotyp, zum anderen durch die unterschiedliche Korrelation von pro-inflammatorischem TGF-β und PDGF-Rα. Diese Erkenntnisse ermöglichen ein besseres Verständnis der Rolle der MSCs bei der BPD-Entstehung Dieses wird dringend benötigt, um den Funktionsmechanismus von therapeutischen MSCs zu verstehen und zu kontrollieren. Zukünftige Arbeiten sollten darauf zielen, die Mechanismen, die der unterschiedlichen Prägung zugrunde liegen zu identifizieren und so eventuell kontrollieren zu können. Dadurch könnte nicht nur die Therapie mit Spender-MSCs verbessert werden, etwa in dem die zu transplantierenden MSCs anhand ihres anti-inflammatorischen Phänotyps selektiert werden, es könnten auch neue Zielmoleküle für eine Therapie der BPD vor ihrer Entstehung identifiziert werden. Außerdem sollte das therapeutische Potential von PDGF, das gezeigt hat, das es im PDGF-Rα haploinsuffizienten Mausmodell die Ausprägung der BPD-Pathologie vermindern kann, weiter untersucht werden.

Eine Unterdrückung von NFκB um den mit der BPD-Entstehung vergesellschafteten MSC-Phänotyp zu verhindern, stellt dagegen sicher keine Therapiemöglichkeit dar: NFκB hat unzählige Funktionen bei der Entwicklung mehrerer Organsysteme (u.a. der Leber (Beg u. a. 1995), des Gehirns (O'Neill und Kaltschmidt

1997) und des Immunsystems (Snapper u. a. 1996)), so dass eine therapeutische Inhibierung unkontrollierbare Nebenwirkungen hätte. Jedoch könnte die Identifizierung eines distinkten MSC-Phänotyps als Prädiktor für BPD-Entstehung in der Zukunft durch den Einsatz neuer Techniken, die eine Untersuchung des Transkriptoms einzelner Zellen ermöglichen, helfen, durch Untersuchung von MSCs aus Trachealaspirat diejenigen extremen Frühgeborenen zu identifizieren, die ein hohes Risiko für die Entstehung einer BPD haben und diese z.B. prophylaktisch mit Glukokortikoiden (Doyle u. a. 2010) zu behandeln, um die BPD-Entstehung zu verhindern.

Zusammengefasst bestärken die beiden vorgelegten Arbeiten die aktuelle Lehrmeinung, dass die Störung des komplexen Signalwegnetzwerkes, das für die Lungenentstehung mit den drei Kompartimenten Epithel, Mesenchym und Endothel benötigt wird, das kritische Ereignis für die Entstehung der BPD darstellt und dass therapeutische Modulationen darauf abzielen müssen, die physiologische Balance wiederherzustellen.

5 Zusammenfassung

Die BPD ist eine wichtige Ursache langanhaltender Morbidität bei Frühgeborenen. Während viele Faktoren identifiziert wurden, die prä- und postnatal zu einer an der BPD-Entstehung beteiligten Inflammationsreaktion führen, ist die Rolle von Lungen-MSCs dabei weitgehend unverstanden. Ein genaueres Verständnis der MSCs ist besonders vor dem Hinblick, dass diese Zellen als Therapeutikum untersucht werden, ein wichtiges Ziel.

Eine inadäquate Ausprägung der Signalkaskaden der neben ihrer Rolle in inflammatorischen Prozessen auch an der Lungenentwicklung beteiligten Proteine NFκB, TGF-β, VEGFA und PDGF-A kann zur Entstehung der BPD-typischen Veränderungen beitragen. Inwieweit die zugrundeliegenden Prozesse der Inflammationsreaktion von MSCs beeinflusst werden, oder selbst MSCs beeinflussen, ist noch weitestgehend unklar.

In den vorgelegten Arbeiten konnte nachgewiesen werden, dass MSCs aus Trachealaspirat Frühgeborener regelhaft isoliert werden können. Zeigten die MSCs einen Phänotyp mit hoher Spontanproliferation, hoher NFκB-Aktivierung und geringer αSMA-Expression, so war das prädiktiv für eine schwerere BPD-Ausprägung. Durch Stimulation mit pro-inflammatorischen Zytokinen (TNFα, IL-1β) konnte dieser Phänotyp induziert werden. NFκB wurde als zentrales Signalmolekül bei seiner Entstehung identifiziert, indem der Phänotyp durch Inhibierung bzw. siRNA-knockdown von NFκB umgekehrt wurde.

In einer weiteren Arbeit konnten der PDGF-Signalweg als (zumindest auch) von MSCs ausgehenden Einflussfaktor auf die BPD-Entstehung identifiziert werden. Es konnte nachgewiesen werden, dass in MSCs über die Dauer der Beatmung die Expression von PDGF-Rα abnimmt. Außerdem konnten genetische Polymorphismen im PDGF-Rα-Gen identifiziert werden, die mit einer schwereren BPD-Ausprägung vergesellschaftet waren. TGF-β spielt dabei als Inhibitor der PDGF-Rα-Expression im Rahmen der Inflammationsreaktion eine wichtige Rolle: Nach Stimulation nahm die PDGF-Rα-Promotor-Aktivität in MSCs ab.

Mit dem Nachweis des Einflusses, den die Expression von PDGF-Rα und die Aktivierung von NFκB in MSCs auf Inflammations- und Entwicklungsprozesse der Lunge Frühgeborener wurden zwei Mechanismen identifiziert, die an der Funktion der MSCs bei BPD-Entstehung oder -Verhinderung teilhaben. Die Ergebnisse könnten in der Zukunft zur Verbesserung der MSC-Zelltherapie dienen, aber auch helfen, diagnostische Werkzeuge zu entwickeln, die Kinder mit besonders hohem BPD-Risiko frühzeitig identifizieren und einer gezielten Therapie zuführen.

6 Summary

BPD is a major cause for long-term morbidity in preterm infants. While many pre and postnatal factors leading to the inflammatory response which contributes to BPD development have been identified, the role of lung MSCs in these processes are poorly understood. A more precise understanding of MSCs and their role is important, especially because MSCs have been used as promising therapeutic agents to treat BPD. Inadequate signaling in the NFκB, TGF-β, VEGFA and PDGF-A pathways all contribute to both lung development, as well as to inflammation of the lung, and can aid in the development of pathologic alterations in lung architecture characteristic for BPD. However, to what extent the underlying processes leading to inflammation are affected by MSCs or affect MSCs themselves is not well understood.

This work demonstrates that MSCs from preterm infants' tracheal aspirates can, as a rule, be isolated. In these MSCs, a phenotype characterized by a high capacity for spontaneous proliferation, high NFκB activation and low levels of αSMA expression was predictive for more severe BPD. By stimulating the MSCs with pro-inflammatory cytokines (TNF-α, IL-1β), this phenotype could be induced. NFκB was identified as the central agent in the development of this phenotype. The phenotype was reversible by chemical inhibition or siRNA-knockdown of NFκB.

Furthermore, PDGF signaling could be identified as another contributor to the onset of BPD development (at least partially) from MSCs. It was shown that in lung MSCs, PDGF-Rα expression decreases with the increased duration of mechanical ventilation. Additionally, genetical polymorphisms in the PDGF-Rα gene were identified that correlated with severe BPD.

TGF-β played an important role as an inhibitor of PDGF-Rα expression in the context of inflammatory response: After stimulation with TGF-β, the activity of a PDGF-Rα promotor decreased in MSCs.

By proving the influence of PDGF-Rα expression and NFκB activation on lung inflammation and development in preterm infants, two mechanisms were identified, which contribute to the MSCs' role in BPD development or its prevention. These results could help improve MSC therapy. Moreover, they could also contribute to the design of diagnostic tools to identify children at high risk for BPD at an early stage and enable timely and targeted treatment.

7 Literatur

Aggarwal S. und Pittenger M. F. (2005). „Human mesenchymal stem cells modulate allogeneic immune cell responses". In: *Blood* 105(4), S. 1815–1822.

Ahn S. Y., Chang Y. S., Kim J. H., Sung S. I. und Park W. S. (2017). „Two-year follow-up outcomes of premature infants enrolled in the phase I trial of mesenchymal stem cells transplantation for bronchopulmonary dysplasia". In: *The Journal of pediatrics* 185, S. 49–54.

AQUA, Institut für angewandte Qualitätsförderung und Forschung im Gesundheitswesen GmbH (2015). *Bundesauswertung zum Erfassungsjahr2014 16/1 –Geburtshilfe.* `https://sqg.de/downloads/Bundesauswertungen/2014/bu_Gesamt_16N1-GEBH_2014.pdf`, aufgerufen am 05.02.2019.

Baeuerle P. A. und Baichwal V. R. (1997). „NF-kB as a frequent target for immunosuppressive and anti-inflammatory molecules". In: *Advances in immunology* 65, S. 111–138.

Bartha J. L., Romero-Carmona R. und Comino-Delgado R. (2003). „Inflammatory cytokines in intrauterine growth retardation". In: *Acta obstetricia et gynecologica Scandinavica* 82(12), S. 1099–1102.

Bartram U. und Speer C. P. (2004). „The role of transforming growth factor β in lung development and disease". In: *Chest* 125(2), S. 754–765.

Beg A. A., William C. S., Bronson R. T., Ghosh S. und Baltimore D. (1995). „Embryonic lethality and liver degeneration in mice lacking the RelA component of NF-κB". In: *Nature* 376(6536), S. 167–170.

Bhatt A. J., Pryhuber G. S., Huyck H., Watkins R. H., Metlay L. A. und Maniscalco W. M. (2001). „Disrupted pulmonary vasculature and decreased vascular endothelial growth factor, Flt-1, and TIE-2 in human infants dying with bronchopulmonary dysplasia". In: *American journal of respiratory and critical care medicine* 164(10), S. 1971–1980.

Blackwell T. S., Hipps A. N., Yamamoto Y., Han W., Barham W. J., Ostrowski M. C., Yull F. E. und Prince L. S. (2011). „NF-κB signaling in fetal lung macrophages disrupts airway morphogenesis". In: *The Journal of Immunology,* S. 1101495.

Bland R. D., Albertine K. H., Pierce R. A., Starcher B. C. und Carlton D. P. (2003). „Impaired alveolar development and abnormal lung elastin in preterm lambs with chronic lung injury: potential benefits of retinol treatment". In: *Neonatology* 84(1), S. 101–102.

Bland R. D., Ertsey R., Mokres L. M., Xu L., Jacobson B. E., Jiang S., Alvira C. M., Rabinovitch M., Shinwell E. S. und Dixit A. (2008). „Mechanical ventilation uncouples synthesis and assembly of elastin and increases apoptosis in lungs of newborn mice. Prelude to defective alveolar septation during lung development?" In: *American Journal of Physiology-Lung Cellular and Molecular Physiology* 294(1), S. L3–L14.

Bland R. D., Mokres L. M., Ertsey R., Jacobson B. E., Jiang S., Rabinovitch M., Xu L., Shinwell E. S., Zhang F. und Beasley M. A. (2007). „Mechanical ventilation with 40% oxygen reduces pulmonary expression of genes that regulate lung development and impairs alveolar septation in newborn mice". In: *American Journal of Physiology-Lung Cellular and Molecular Physiology* 293(5), S. L1099–L1110.

Bonniaud P., Kolb M., Galt T., Robertson J., Robbins C., Stampfli M., Lavery C., Margetts P. J., Roberts A. B. und Gauldie J. (2004). „Smad3 null mice develop airspace enlargement and are resistant to TGF-β-mediated pulmonary fibrosis". In: *The Journal of Immunology* 173(3), S. 2099–2108.

Boström H., Willetts K., Pekny M., Levéen P., Lindahl P., Hedstrand H., Pekna M., Hellström M., Gebre-Medhin S., Schalling M. u. a. (1996). „PDGF-A signaling is a critical event in lung alveolar myofibroblast development and alveogenesis". In: *Cell* 85(6), S. 863–873.

Bozyk P. D., Popova A. P., Bentley J. K., Goldsmith A. M., Linn M. J., Weiss D. J. und Hershenson M. B. (2011). „Mesenchymal stromal cells from neonatal tracheal aspirates demonstrate a pattern of lung-specific gene expression". In: *Stem cells and development* 20(11), S. 1995–2007.

Chang Y. S., Ahn S. Y., Yoo H. S., Sung S. I., Choi S. J., Oh W. I. und Park W. S. (2014). „Mesenchymal stem cells for bronchopulmonary dysplasia: phase 1 dose-escalation clinical trial". In: *The Journal of pediatrics* 164(5), S. 966–972.

Desmoulière A., Chaponnier C. und Gabbiani G. (2005). „Tissue repair, contraction, and the myofibroblast". In: *Wound repair and regeneration* 13(1), S. 7–12.

Doyle L. W., Ehrenkranz R. A. und Halliday H. L. (2010). „Dexamethasone treatment in the first week of life for preventing bronchopulmonary dysplasia in preterm infants: a systematic review". In: *Neonatology* 98(3), S. 217–224.

Gauldie J., Galt T., Bonniaud P., Robbins C., Kelly M. und Warburton D. (2003). „Transfer of the active form of transforming growth factor-β1 gene to newborn rat lung induces changes consistent with bronchopulmonary dysplasia". In: *The American journal of pathology* 163(6), S. 2575–2584.

Gough A., Linden M., Spence D., Patterson C. C., Halliday H. L. und McGarvey L. P. (2014). „Impaired lung function and health status in adult survivors of bronchopulmonary dysplasia". In: *European Respiratory Journal* 43(3), S. 808–816.

Gronbach J., Shahzad T., Radajewski S., Chao C.-M., Bellusci S., Morty R. E., Reicherzer T. und Ehrhardt H. (2018). „The Potentials and Caveats of Mesenchymal Stromal Cell-Based Therapies in the Preterm Infant". In: *Stem cells international* 2018.

Haniffa M. A., Collin M. P., Buckley C. D. und Dazzi F. (2009). „Mesenchymal stem cells: the fibroblasts' new clothes?" In: *Haematologica* 94(2), S. 258–263.

Hennrick K. T., Keeton A. G., Nanua S., Kijek T. G., Goldsmith A. M., Sajjan U. S., Bentley J. K., Lama V. N., Moore B. B., Schumacher R. E. u. a. (2007). „Lung cells from neonates show a mesenchymal stem cell phenotype". In: *American journal of respiratory and critical care medicine* 175(11), S. 1158–1164.

Hilgendorff A., Reiss I., Ehrhardt H., Eickelberg O. und Alvira C. M. (2014). „Chronic lung disease in the preterm infant. Lessons learned from animal models". In: *American journal of respiratory cell and molecular biology* 50(2), S. 233–245.

Hoyle G. W., Li J., Finkelstein J. B., Eisenberg T., Liu J.-Y., Lasky J. A., Athas G., Morris G. F. und Brody A. R. (1999). „Emphysematous lesions, inflammation, and fibrosis in the lungs of transgenic mice overexpressing platelet-derived growth factor". In: *The American journal of pathology* 154(6), S. 1763–1775.

Iosef C., Alastalo T.-P., Hou Y., Chen C., Adams E. S., Lyu S.-C., Cornfield D. N. und Alvira C. M. (2012). „Inhibiting NF-κB in the developing lung disrupts angiogenesis and alveolarization". In: *American Journal of Physiology-Lung Cellular and Molecular Physiology* 302(10), S. L1023.

Islam J. Y., Keller R. L., Aschner J. L., Hartert T. V. und Moore P. E. (2015). „Understanding the short-and long-term respiratory outcomes of prematurity and bronchopulmonary dysplasia". In: *American journal of respiratory and critical care medicine* 192(2), S. 134–156.

Jobe A. H. (1999). „The new BPD: an arrest of lung development". In: *Pediatric research* 46(6), S. 641.

Jobe A. H. und Bancalari E. (2001). „Bronchopulmonary dysplasia". In: *American journal of respiratory and critical care medicine* 163(7), S. 1723–1729.

Li C., Li M., Li S., Xing Y., Yang C.-Y., Li A., Borok Z., De Langhe S. und Minoo P. (2015). „Progenitors of secondary crest myofibroblasts are developmentally committed in early lung mesoderm". In: *Stem Cells* 33(3), S. 999–1012.

Lindahl P., Karlsson L., Hellstrom M., Gebre-Medhin S., Willetts K., Heath J. K. und Betsholtz C. (1997). „Alveogenesis failure in PDGF-A-deficient mice is coupled to lack of distal spreading of alveolar smooth muscle cell progenitors during lung development". In: *Development* 124(20), S. 3943–3953.

Möbius M. A. und Thébaud B. (2015). „Stem cells and their mediators–next generation therapy for bronchopulmonary dysplasia". In: *Frontiers in medicine* 2, S. 50.

Northway Jr. W. H., Rosan R. C. und Porter D. Y. (1967). „Pulmonary disease following respirator therapy of hyaline-membrane disease: bronchopulmonary dysplasia". In: *New England Journal of Medicine* 276(7), S. 357–368.

O'Neill L. A. und Kaltschmidt C. (1997). „NF-kB: a crucial transcription factor for glial and neuronal cell function". In: *Trends in neurosciences* 20(6), S. 252–258.

Park W. S. (2017). *Stem cell therapy for neonatal disorders; Prospects and challenges.* Mündlicher Konferenzbeitrag, Zweiter Kongress der Joint European Neonatal Societies JENS, Venedig, 01.11.2017.

Philip A. G. (2012). „Bronchopulmonary dysplasia: then and now". In: *Neonatology* 102(1), S. 1–8.

Popova A. P., Bentley J. K., Cui T. X., Richardson M. N., Linn M. J., Lei J., Chen Q., Goldsmith A. M., Pryhuber G. S. und Hershenson M. B. (2014). „Reduced platelet-derived growth factor receptor expression is a primary feature of human bronchopulmonary dysplasia". In: *American Journal of Physiology-Lung Cellular and Molecular Physiology* 307(3), S. L231–L239.

Popova A. P., Bozyk P. D., Bentley J. K., Linn M. J., Goldsmith A. M., Schumacher R. E., Weiner G. M., Filbrun A. G. und Hershenson M. B. (2010a). „Isolation of tracheal aspirate mesenchymal stromal cells predicts bronchopulmonary dysplasia". In: *Pediatrics*, e1127–e1133.

Popova A. P., Bozyk P. D., Goldsmith A. M., Linn M. J., Lei J., Bentley J. K. und Hershenson M. B. (2010b). „Autocrine production of TGF-β1 promotes myofibroblastic differentiation of neonatal lung mesenchymal stem cells". In: *American Journal of Physiology-Lung Cellular and Molecular Physiology* 298(6), S. L735–L743.

Shahzad T., Radajewski S., Chao C.-M., Bellusci S. und Ehrhardt H. (2016). „Pathogenesis of bronchopulmonary dysplasia: when inflammation meets organ development". In: *Molecular and cellular pediatrics* 3(1), S. 23.

Silva Meirelles L. da, Chagastelles P. C. und Nardi N. B. (2006). „Mesenchymal stem cells reside in virtually all post-natal organs and tissues". In: *Journal of cell science* 119(11), S. 2204–2213.

Snapper C. M., Zelazowski P., Rosas F. R., Kehry M. R., Tian M., Baltimore D. und Sha W. C. (1996). „B cells from p50/NF-kappa B knockout mice have selective defects in proliferation, differentiation, germ-line CH transcription, and Ig class switching." In: *The Journal of Immunology* 156(1), S. 183–191.

Speer C. P. (2006). „Inflammation and bronchopulmonary dysplasia: a continuing story". In: *Seminars in Fetal and Neonatal Medicine.* Bd. 11. 5. Elsevier, S. 354–362.

Speer C. P., Robertson B., Curstedt T., Halliday H. L., Compagnone D., Gefeller O., Harms K., Herting E., McClure G., Reid M. u. a. (1992). „Randomized European multicenter trial of surfactant replacement therapy for severe neonatal respiratory distress syndrome: single versus multiple doses of Curosurf". In: *Pediatrics* 89(1), S. 13–20.

8 Abbildungsverzeichnis

9 Sonderdrucke der Publikationen im Rahmen der Promotionsarbeit

Publikation 1: **Reicherzer T.**, Häffner S., Shahzad T., Gronbach J., Mysliwietz J., Hübener C., Hasbargen U., Gertheiss J., Schulze A., Bellusci S., Morty R.E., Hilgendorff A. und Ehrhardt H. (2018). „**Activation of the NFκB pathway alters the phenotype of MSCs in the tracheal aspirates of preterm infants with severe BPD**". In: *American Journal of Physiology-Lung Cellular and Molecular Physiology.* L87-L101

Publikation 2: Oak P., Pritzke T., Thiel I., Koschlig M., Mous D. S., Windhorst A., Jain N., Eickelberg O., Förster K., Schulze A., Goepel W., **Reicherzer T**., Ehrhardt H., Rottier R.J., Ahnert P., Gortner L., Desai T.J. und Hilgendorff A. (2017). „**Attenuated PDGF signaling drives alveolar and microvascular defects in neonatal chronic lung disease**" In: *EMBO molecular medicine* 9(11), S. 1504-1520.

RESEARCH ARTICLE

Activation of the NF-κB pathway alters the phenotype of MSCs in the tracheal aspirates of preterm infants with severe BPD

Tobias Reicherzer,[1,2] Susanne Häffner,[1,2] Tayyab Shahzad,[3] Judith Gronbach,[3] Josef Mysliwietz,[4] Christoph Hübener,[5] Uwe Hasbargen,[5] Jan Gertheiss,[6] Andreas Schulze,[1] Saverio Bellusci,[7] ⓘ Rory E. Morty,[8] Anne Hilgendorff,[1,2] and ⓘ Harald Ehrhardt[1,3]

[1]*Division of Neonatology, University Children's Hospital, Perinatal Center, Ludwig-Maximilians-University, Campus Grosshadern, Munich, Germany;* [2]*Comprehensive Pneumology Center, Ludwig-Maximilians-University, Asklepios Hospital, and Helmholtz Center Munich, Munich, Germany;* [3]*Department of General Pediatrics and Neonatology, Justus-Liebig-University and Universities of Giessen and Marburg Lung Center, Member of the German Lung Research Center (DZL), Giessen, Germany;* [4]*Institute of Molecular Immunology, Helmholtz Center Munich, Munich, Germany;* [5]*Department of Obstetrics and Gynecology, Perinatal Center, University Hospital, Ludwig-Maximilians-University, Munich, Germany;* [6]*Institute of Applied Stochastics and Operations Research, Research Group Applied Statistics, Clausthal University of Technology, Clausthal-Zellerfeld, Germany;* [7]*Universities of Giessen and Marburg Lung Center, Excellence Cluster Cardio-Pulmonary System, Member of the German Center for Lung Research (DZL), Department of Internal Medicine II, Giessen, Germany; and* [8]*Department of Lung Development and Remodeling, Max Planck Institute for Heart and Lung Research, Member of the German Lung Center (DZL), Bad Nauheim, Germany*

Reicherzer T, Häffner S, Shahzad T, Gronbach J, Mysliwietz J, Hübener C, Hasbargen U, Gertheiss J, Schulze A, Bellusci S, Morty RE, Hilgendorff A, Ehrhardt H. Activation of the NF-κB pathway alters the phenotype of MSCs in the tracheal aspirates of preterm infants with severe BPD. *Am J Physiol Lung Cell Mol Physiol* 315: L87–L101, 2018. First published April 12, 2018; doi:10.1152/ajplung.00505.2017.—Mesenchymal stromal cells (MSCs) are released into the airways of preterm infants following lung injury. These cells display a proinflammatory phenotype and are associated with development of severe bronchopulmonary dysplasia (BPD). We aimed to characterize the functional properties of MSCs obtained from tracheal aspirates of 50 preterm infants who required invasive ventilation. Samples were separated by disease severity. The increased proliferative capacity of MSCs was associated with longer duration of mechanical ventilation and higher severity of BPD. Augmented growth depended on nuclear accumulation of NFκBp65 and was accompanied by reduced expression of cytosolic α-smooth muscle actin (α-SMA). The central role of NF-κB signaling was confirmed by inhibition of IκBα phosphorylation. The combined score of proliferative capacity, accumulation of NFκBp65, and expression of α-SMA was used to predict the development of severe BPD with an area under the curve (AUC) of 0.847. We mimicked the clinical situation in vitro, and stimulated MSCs with IL-1β and TNF-α. Both cytokines induced similar and persistent changes as was observed in MSCs obtained from preterm infants with severe BPD. RNA interference was employed to investigate the mechanistic link between NFκBp65 accumulation and alterations in phenotype. Our data indicate that determining the phenotype of resident pulmonary MSCs represents a promising biomarker-based approach. The persistent alterations in phenotype, observed in MSCs from preterm infants with severe BPD, were induced by the pulmonary inflammatory response. NFκBp65 accumulation was identified as a central regulatory mechanism. Future preclinical and clinical studies, aimed to prevent BPD, should focus on phenotype changes in pulmonary MSCs.

INTRODUCTION

Bronchopulmonary dysplasia (BPD) is caused by injury to the developing lung, leading to life-long sequelae (14, 20). Histopathology of BPD shows simplified alveolar structures and dysmorphic capillary configuration (7). The disturbance of lung development and severity of BPD are caused by perinatal and postnatal factors, including prematurity, genetic susceptibility, prenatal and postnatal infections, mechanical ventilation, and oxygen toxicity. These factors cause a pulmonary inflammatory response that is central to the pathogenesis of BPD. BPD is characterized by an imbalance between pro- and anti-inflammatory cytokines, downregulation of vascular and tissue growth factors, influx of inflammatory cells, formation of reactive oxygen species, and activation of proteases (17, 43).

The transcription factor NF-κB is essential for normal lung development, but excessive signaling during pulmonary inflammation is a critical mechanism in abnormal lung development (15, 19, 27, 41). In line with this, the accumulation of proinflammatory cytokines, such as IL-1β or TNF-α, which activate NF-κB, perturbs normal lung development. Conversely, mechanical ventilation in an oxygen-rich environment can also lead to increased lung damage when NF-κB signaling and levels of TNF-α are reduced (4, 11). Therefore, therapeutic targeting of NF-κB signaling needs to be critically reevaluated.

In recent years, pioneering studies have focused on MSCs obtained from the tracheal aspirates of ventilated preterm infants. These cells fulfilled the classical criteria of MSCs and displayed a lung-specific phenotype, which distinguished them from nonresident MSCs (3, 8, 9, 16, 29, 39). Isolation of MSCs from tracheal aspirates of ventilated preterm infants in these

27

Table 1. *Patient characteristics of the study cohort*

	Complete Study Cohort	Preterm Infants Fulfilling Inclusion Criteria
No. of children	112	49
Gestational age , wk	26 + 0 (1 + 4)	25 + 6 (1 + 3)
Birth weight, g	786 (241)	709 (279)
Male sex	70 (62.5%)	31 (63.3%)
Twin birth	46 (41.7%)	24 (48%)
Early onset infection	63 (56.3%)	31 (62%)
Antenatal steroids	103 (92%)	46 (92%)
Mechanical ventilatory support, days	61 (28)	70 (22)
Any BPD	106 (94.6%)	49 (100%)
No BPD	6 (5.4%)	not included
Mild BPD	43 (38.4%)	19 (38%)
Moderate BPD	25 (22.3%)	16 (32%)
Severe BPD	24 (21.4%)	14 (28%)
Deceased	14 (12.5%)	not included

The relevant characteristics of the entire patient cohort of 112 preterm infants ($<$29 wk of gestational age) and of the subgroup of patients fulfilling study inclusion criteria (see MATERIALS AND METHODS for details) are presented. Children who died during intensive care therapy as a result of sepsis or severe intracranial bleeding before 36 + 0 wk of gestational age were excluded (n = 4). The mean values and standard deviations, or the percentage of children, are depicted. Higher order multiples were not present within the study cohort. Early onset infection was diagnosed if the infants showed two typical clinical signs of infection and a pathological immature-to-total neutrophils ratio (I/T) ($\geq$ 0.2) and/or an increase in C-reactive protein (CRP) $\geq$ 6 mg/l in the first 72 h of life. A positive history of antenatal steroids included the application of a complete course of betamethasone or dexamethasone not longer than 7 days before birth. None of the children within the "no antenatal steroids group" were born beyond 12 h of the initiation of the first course. The parameter "days of mechanical ventilatory support" includes any form of mechanical ventilation or continuous positive airway pressure (CPAP). The severity of bronchopulmonary dysplasia (BPD) was classified according to the definition established by Jobe and Bancalari (21).

studies was particularly successful from tracheal aspirates of infants who later developed BPD. This finding led to the conclusion that the release of MSCs into the airway is the result of lung injury. These MSCs demonstrated substantial alterations in the pathways controlled by PDGF receptor-α, β-catenin, and TGF-β1, which regulate the differentiation of MSCs into myofibroblasts. These alterations were associated with distortion of further septation and interstitial fibrosis (16, 29, 33, 37, 38, 40).

We performed detailed descriptive, functional, and molecular studies on MSCs obtained from the tracheal aspirates of preterm infants. We identified a combination of new phenotypic characteristics predictive of a prolonged need for mechanical ventilation and higher severity of BPD. Finally, we mimicked the effects of an inflammatory milieu in vivo by exposing MSCs to proinflammatory cytokines in vitro. This induced phenotype alterations similar to those observed in MSCs isolated from preterm infants with severe BPD.

MATERIALS AND METHODS

For flow cytometry, the antibodies anti-CD45 (1:50, MHCD4518), anti-CD13 (1:50, MHCD1301), anti-CD105 (1:50, MHCD10505), anti-CD34 (1:50, CD34-581-18), and anti-CD14 (1:50, MHCD1427) were obtained from Caltag (Towcester, UK); anti-CD73 (1:50, 550257), anti-CD90 (1:50, 559869), anti-CD11b (1:50, 557743), and anti-CXCR4 (1:50, 555974) were obtained from BD Biosciences (San Diego, CA). Isotype control antibodies were obtained from BD Biosciences. For Western blot analysis, the antibodies anti-histone H1 (1:500, sc-10806), anti-lamin A/C (1:1,000, sc-6214), and anti-NFκBp65 (1:500, sc-372) were obtained from Santa Cruz (Santa Cruz, CA); anti-α-SMA (1:1,000, 113200) was obtained from Cal-biochem (San Diego, CA), anti-p-IκBα (1:1,000, 2859) and anti-IκBα (1:1,000, 9242) were obtained from Cell Signaling Technology (Danvers, MA), anti-GAPDH (1:2,500, MA1-22670) and fluorochrome-conjugated secondary antibodies were obtained from Thermo Fisher (Waltham, MA). Cytokines were obtained from PeproTech (Hamburg, Germany). All other reagents were obtained from Sigma-Aldrich (Munich, Germany). All antibodies used in the manuscript can be found in SciCrunch database.

Study Cohort, Cell Culture, and Study Parameters

A cohort of 112 preterm infants ($<$29 wk of gestational age) from the PROTECT (PROgress in the molecular understanding of The evolution of Chronic lung disease in premature infants Trial) study was eligible for this study. Of these patients, five were excluded because of fungal or bacterial cell culture contamination. No child was excluded because of insufficient sampling. A total of 50 preterm infants met the evaluation criteria of *1*) mechanical ventilation for $\geq$7 days and *2*) routine suctioning performed at least every other day until successful establishment of MSC cultures. Chorioamnionitis was proven by histopathologic examination. All experiments were approved by the ethics committees of the Ludwig-Maximilians-University Munich (no. 195-07) and the Justus-Liebig-University Gießen (no. 135/12). All MSC samples subjected to cohort analyses were collected at the Munich site. No changes in the ventilation strategies were introduced into the clinical routine during the study period. All procedures involving human subjects were in accordance with the principles of the Helsinki Declaration. Written informed consent was obtained from the parents of all infants.

Preservation of Primary Samples, Cell Culture, Transfection Experiments, and Experimental Readouts

Cell culture. Cell pellets from tracheal aspirates were resuspended in MesenCult medium supplemented with 20% fetal calf serum (FCS; StemCell Technologies, Vancouver, Canada), 2 mM L-glutamine, 10 mM HEPES buffer solution, 50 U/ml penicillin, 50 μg/ml streptomycin, and 50 μg/ml gentamicin (Invitrogen, Carlsbad, CA). MSCs were allowed to grow to confluence. Established cultures were maintained under constant growth. The purity of $>$95% of MSC cultures was determined by cell-surface staining assay described below (3, 16, 33, 39). Experiments were conducted between passages 2 and 6 in DMEM medium (PAN Biotech, Aidenbach, Germany) without FCS. The area of the well, covered by cells at the start of experiments, ranged between 10 and 25%.

Fig. 1. Characterization of mesenchymal stromal cells (MSCs). Isolated cells displayed a homogeneous and stable MSC phenotype. *A*: description of the experimental procedure. MSCs were detected 1−4 days after cultivation of tracheal aspirates. MSCs were allowed to grow to confluence within 10−16 days before passaging. Experimental procedures were performed between passages 2 and 6. *B*: using flow cytometry, cells expressed the surface receptors CD13, CD73, CD90, and CD 105 which are typically expressed on MSCs, while they were not expressing markers of hematopoetic or myelopoetic cells (CD11b, CD14, CD34, CD45, and CXCR4). *C*: cell differentiation into adipogenic (*top*), osteogenic (*middle*), and myofibroblastic (*bottom*) cells was confirmed using Oil Red O staining, alizarin red staining, or immunofluorescence labeling for α-smooth muscle actin (α-SMA). *D*: stability of cell characteristics was ensured until passage 6 for the proliferation index in n = 20 different MSC cultures (*top*) and for the content of α-SMA (*bottom*). Statistical analysis was performed using an ANOVA and Bonferroni post hoc adjusted pairwise comparison. NS, not significant.

Cell transfection. Transient transfection was performed with Lipofectamine 2000 (Life Technologies) according to the manufacturer's instructions. siRNA against NFκBp65 (5′-GCCCUAUCCCUUUAC-GUCA-3′ (MWG Biotech, Ebersberg, Germany) and AllStars nega- tive control siRNA (Qiagen, Hilden, Germany) was used at a concentration of 20 nM. Experiments were started 24 h after transfection. Iκκ2 inhibitor IV (Merck KGaA) was used to inhibit the phosphorylation of IκBα.
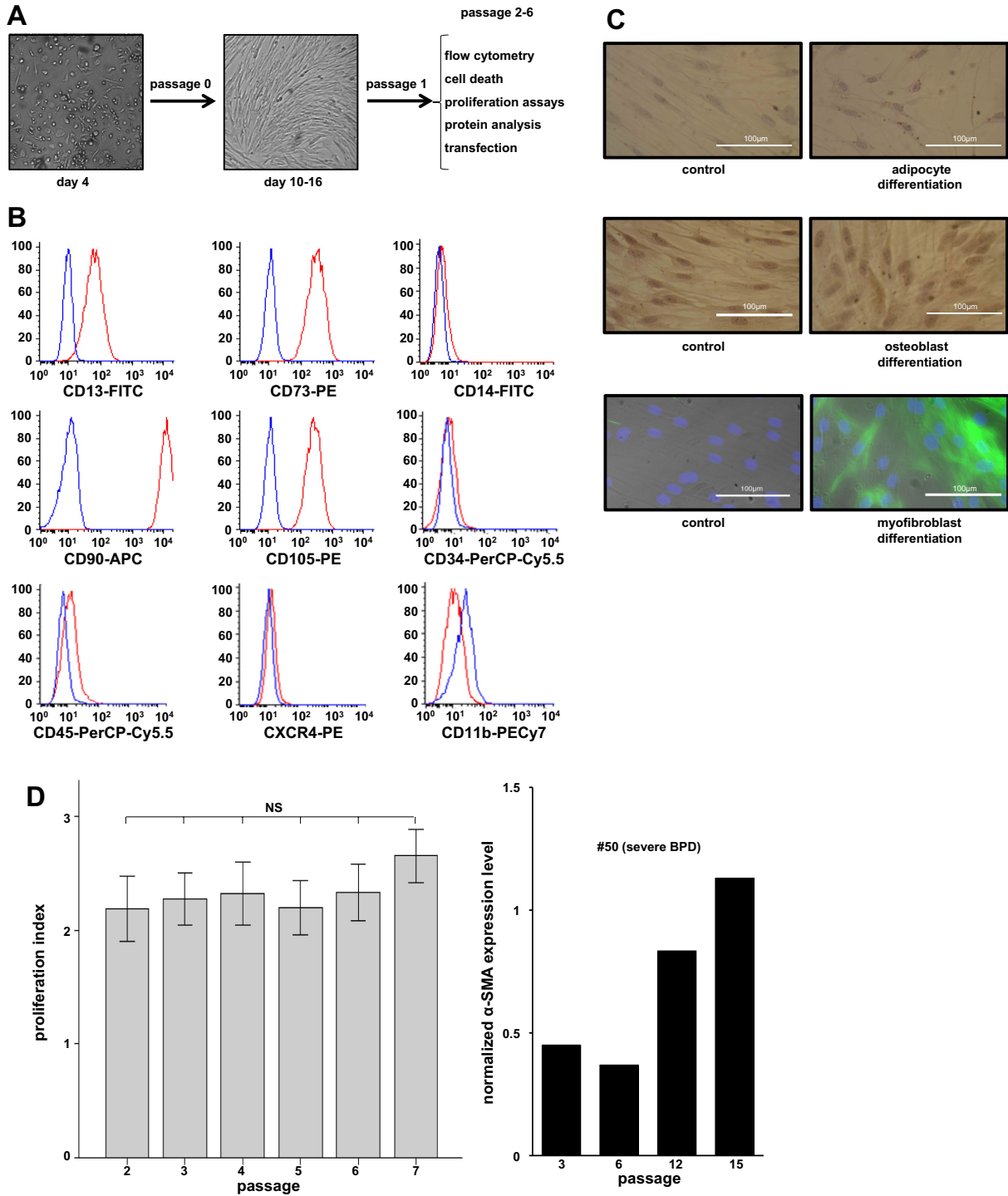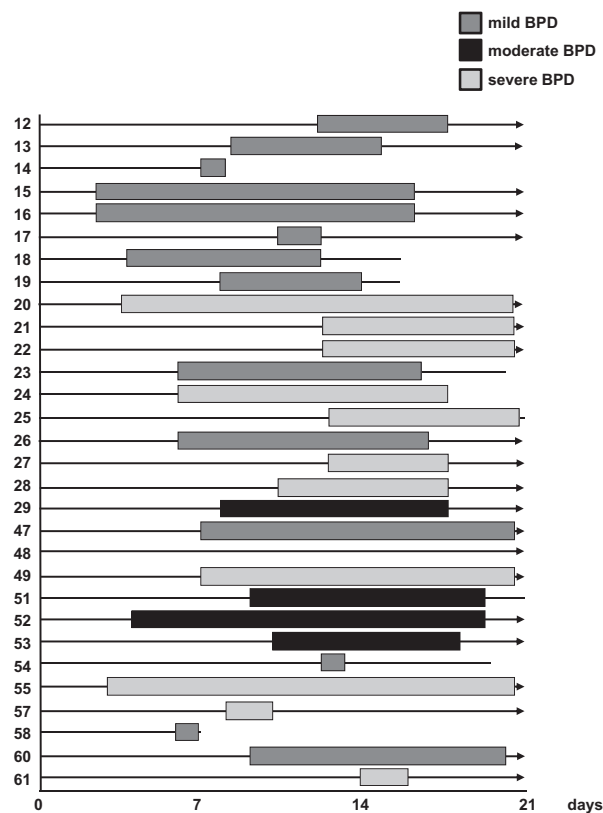
Fig. 2. Emergence and duration of the presence of mesenchymal stromal cells (MSCs) in tracheal aspirates. The time point of first detection of MSCs and the duration of successful cultivation did not differ between groups defined by disease severity. Tracheal aspirates were cultured every other day during the entire period of invasive mechanical ventilation. MSC outgrowth is indicated by bars.

used four different antibody panels: one containing CD13-FITC, CD73-PE, CD34-PerCP-Cy5.5, and CD14-APC-Cy7; one containing CD105-PE, CD45-PerCP-Cy5.5, CD14-APC-Cy7, and CD90-APC; one with CD45-PerCP-Cy5.5, CD90-APC, and CD14-APC-Cy7; and one containing CD95-FITC, CXCR4-PE, and CD11b-PECy7. Propidium iodide (1 µg/ml) was added to each panel to label and sort out dead cells. Negative controls were stained with an isotype control panel. Flow cytometry was performed using an LSR II device. Facs Diva software version 6.1.3 (BD Biosciences) was used for data acquisition, and FlowJo analysis-software version 8.8.6 (Tree Star, Ashland, VA) was used for analyses. Compensation was performed with leftover cells and compensation beads (BD Biosciences).

Cell proliferation assays. For quantification of cell proliferation, cells were plated in a 96-well plate, with density defined as 10–25% of the well area covered. The change in the well area covered was observed over time using a Cellscreen device and data acquisition using PA adhesion software (Innovatis, Bielefeld, Germany). Manual cell counts were performed in a Neubauer chamber after the addition of trypan blue.

Flow cytometry. The induction of apoptosis was determined using Nicoletti staining (32). For multicolor flow cytometry, cells were washed in a buffer containing 2% glucose, 1% BSA, 0.1% EDTA, and 0.1% sodium azide. Cells were resuspended and incubated with fluorochrome-conjugated antibodies at a concentration of 1:50. We

Western Blot Analysis

Cytosolic extracts were obtained by cell lysis in 10 mM 4-(2-hydroxyethyl)-1-piperazine ethanesulfonic acid (HEPES, pH 7.0), 1 mM KCl, 1.5 mM $MgCl_2$, and 0.5% Triton-X supplemented with a proteinase inhibitor cocktail I (Merck KGaA). Nuclear extracts were obtained after lysis of cell nuclei in 20 mM HEPES (pH 7.9), 400 mM KCl, 0.1 mM EDTA, and 25% glycerin. Protein density was quantified using AIDA imaging software version 2.50 (Raytest, Straubenhardt, Germany). An internal standard deposited on each gel enabled the comparison between different gels.

Histological Staining and Immunofluorescence

Cells were incubated for 9–18 days in a medium containing dexamethasone (10 µmol), isobutylmethylxanthine (100 µg/ml), indomethacin (50 µmol), and insulin (10 µg/ml, Sanofi-Aventis, Frankfurt, Germany) for adipocyte differentiation, and in a medium containing dexamethasone (0.1 µmol), β-glycerophosphate (10 mmol), and L-ascorbic acid (50 µg/ml) for osteoblast differentiation. Culture medium was exchanged every third day. For myofibroblast differentiation, cells were incubated with 1 ng/ml TGF-β added to the medium for 48 h (16, 36).

Histological detection of adipocytic and osteoblastic differentiation was conducted with Oil Red O or Alizarin Red staining, respectively. Immunofluorescence was performed using sterilized glass slides. Cells were fixed either in methanol or acetone, permeabilized with

Table 2. *Detection of mesenchymal stromal cells in tracheal aspirates: separation by BPD severity scores*

	BPD Grade			
	Mild	Moderate	Severe	P Value
No. of infants	19	13	17	>0.05
Gestational age, wk	25 + 3 (7 + 3)	25 + 1 (0 + 6)	25 + 3 (1 + 5)	>0.05
Birth weight, g	704 (145)	707 (137)	709 (165)	>0.05
Chorioamnionitis	9/19 (47.4%)	2/13 (15.4%)	4/14 (28.6%)	>0.05
Day of first MSC isolation	9 (5)	8 (4)	8 (4)	>0.05
Duration of presence of MSCs, days	8 (7)	12 (8)	12 (7)	>0.05
Maximum peak inspiratory pressure until culture establishment	14 (6)	13 (2)	16 (4)	>0.05
Maximum FI_{O_2} until culture establishment, %	29 (7)	33 (3)	40 (18)	>0.05
Mechanical ventilatory support, days	65 (13)	78 (13)	96 (33)	<0.05
Proliferation index	2.04 (0.55)	2.7 (0.69)	2.87 (1.0)	<0.05

Tracheal aspirates from 49 preterm infants were cultured at least every 2nd day during the period of mechanical ventilation and screened for the presence of mesenchymal stromal cells (MSCs). The mean values and SDs are presented. The number of patients with proven chorioamnionitis on pathological examination is presented in relation to the total number of patients. No pathological examination could be performed on the placenta of 3 patients with severe bronchopulmonary dysplasia (BPD) (2 home births and 1 outborn child, where placenta was not sent for workup). Statistical analysis was performed using ANOVA on ranks and χ^2 to analyze for the presence of chorioamnionitis. FI_{O_2}, fraction of oxygen in the breathing air.

Table 3. *Detection of MSCs in tracheal aspirates: separation by time point of first appearance*

	First Appearance Within		
	Days 0–7	*Days 8–21*	*P* Value
No. of infants	20	20	
Day of first MSC isolation	5 (2)	11 (4)	<0.05
Gestational age, wk	24 + 6 (7 + 2)	26 + 0 (7 + 2)	<0.05
Birth weight, g	630 (98)	746 (143)	<0.05
Mild BPD	7 (35%)	8 (40%)	>0.05
Moderate BPD	5 (25%)	4 (20%)	>0.05
Severe BPD	8 (40%)	8 (40%)	>0.05
Maximum peak inspiratory pressure until culture establishment	14 (3)	16 (3)	>0.05
Maximum FI$_{O_2}$ until culture establishment, %	34 (17)	34 (7)	>0.05
Mechanical ventilatory support , days	83 (33)	79 (15)	>0.05
Proliferation index	2.6 (0.13)	2.24 (0.77)	>0.05

Preterm infants were separated by the time point of the first appearance of mesenchymal stromal cells (MSCs). Parameters were analyzed as in Tables 1 and 2. Statistical analysis was performed using Student's *t*-test. BPD, bronchopulmonary dysplasia.
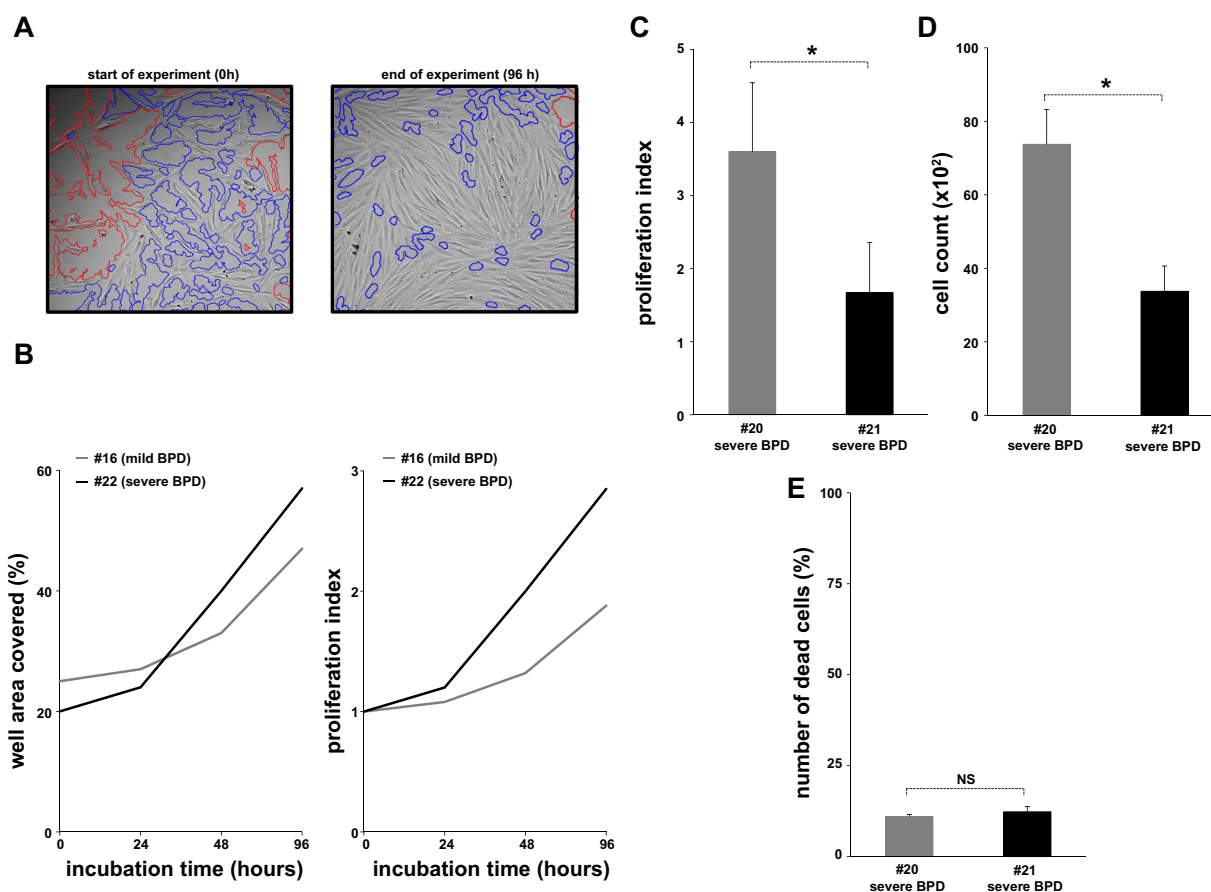
Fig. 3. Determination of proliferative capacity of mesenchymal stromal cells (MSCs) and induction of cell death. Cell proliferation was determined using Cellscreen automated computer-based light microscopy. Results were confirmed by complementary techniques. *A*: the proliferative capacity of MSCs was determined over time using Cellscreen. Red lines indicate the surface area covered by the cells, while blue lines indicate the uncovered surface area excluded from the red marked area. *B*: the proliferation index was introduced to standardize the well area covered at the start of experiments (*right*) as cell density varied between samples (*left*). Cellscreen analysis (*C*) and manual cell counts (*D*) yielded identical results in MSCs from different patients. *E*: the fraction of dead cells did not differ between samples. The mean from *n* = 3 independent measurements is shown. Statistical analysis was performed using Student's *t*-test. *$P < 0.05$, which indicates statistically significant differences. NS, not significant.

31

Triton-X, rinsed in phosphate-buffered saline (PBS), and stained with specific primary antibodies and fluorochrome-conjugated secondary antibodies. Cells were then mounted on slides, and the nuclei were counterstained using Vectashield mounting medium with DAPI (Vector, Burlingame, CA). Images were acquired using a Zeiss Axiovert 200 M fluorescent microscope (Zeiss, Jena, Germany) and OpenLab software version 3.0.8 (Improvision, Coventry, UK).

Determination of Cytokine Levels in Tracheal Aspirates

Protein expression of IL-1β was measured in tracheal aspirates using the IL-1β Quantikine ELISA kit (R&D Systems, Minneapolis, MN) according to the manufacturer's instructions. Standardization to sIgA (Immunodiagnostik, Bensheim, Germany) was performed to compensate for the dilution effects of the suctioning procedures (11).

Statistical Analysis

The proliferation index (PI) was calculated as the quotient of (well area covered at the end of the experiment)/(well area covered at the start of the experiment).

Student's *t*-test was used to test for statistically significant differences between two independent groups. Multivariate analyses were performed using an analysis of variance (ANOVA) test, and Bonferroni correction was used to adjust for multiple comparisons. Association studies were analyzed with Spearman's rank order correlation coefficient, and regression analyses were performed with a standard linear logistic model or a proportional odds model, depending on the type of the response variable (metric/binary/ordinal). We used a linear mixed model with random intercept to test for effects on batches of
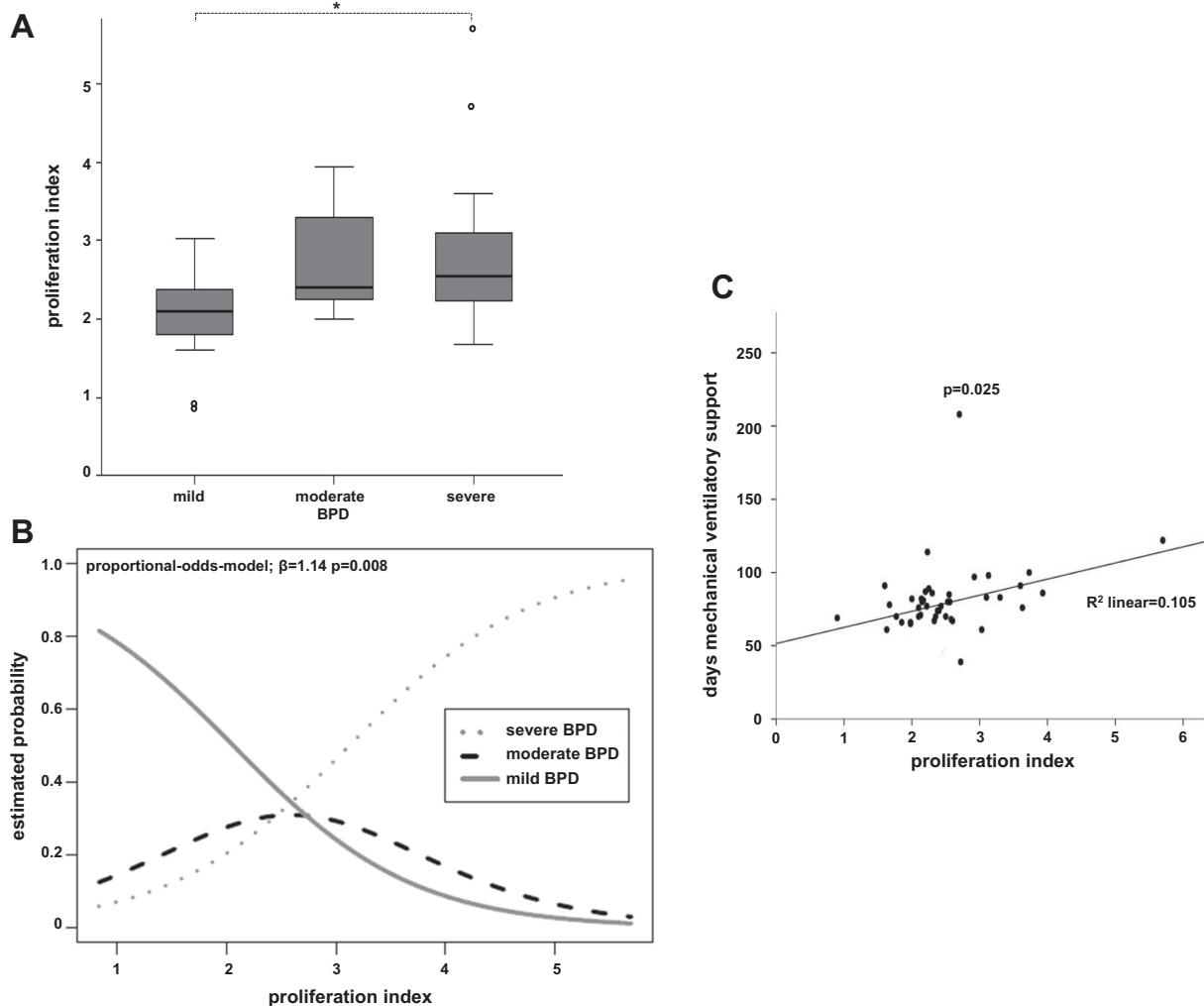

Fig. 4. The proliferative capacity of mesenchymal stromal cells (MSCs) as a predictor of the duration of mechanical ventilation and severity of bronchopulmonary dysplasia (BPD). The proliferation index was significantly increased in MSCs from preterms with severe BPD in the cohort from Table 1. *A*: statistical analysis was performed from 3 independent experiments performed between p2 and p6 using one-way ANOVA and post hoc pairwise comparisons by means of *t*-tests with Bonferroni adjustment. $*P < 0.05$ indicates statistically significant differences. *B*: the predictive value was verified using a proportional odds model. $P = 0.008$ indicates statistically significant differences. *C*: the association between the PI and days of mechanical ventilatory support was demonstrated using linear regression. $P = 0.025$ indicates statistically significant differences. The association remained statistically significant when the two outlying values were omitted from the analysis.

MSC cultures obtained from different children. A child-specific random intercept was included to account for dependencies between observations of the same child. Differences were considered statistically significant at P values < 0.05.

RESULTS

We performed an observational study of a prospective cohort of 112 preterm infants (<29 wk of gestation), and determined the phenotype of MSCs isolated from the tracheal aspirates of these infants. Patient characteristics are described in Table 1.

Presence and Characterization of MSCs

MSCs were detected in the tracheal aspirates of every preterm infant ventilated for at least the first 7 days of life (data not shown). Cells grew to confluence within $8-16$ days. Standardized protocols (depicted in Fig. 1A) were started at passage 2. Flow cytometric analyses confirmed the specific phenotype of MSCs and the high purity of cultured cells (9, 16, 33). MSCs were identified by flow cytometry. MSCs were positive for MSC surface markers CD13, CD73, CD90, and CD105 and negative for CD11b, CD14, CD34, CD45, and CXCR4; CD11b, CD14, CD34, CD45, and CXCR4 are markers of hematopoietic precursors, leukocytes, macrophages, dendritic cells, fibrocytes, and endothelial cells and are not expressed on MSCs (Fig. 1B) (9, 16, 26, 31, 34, 44). The characteristic pluripotency of MSCs was confirmed by adipocytic, osteoblastic, and myofibroblastic differentiation (Fig. 1C). Stability of cell characteristics was assured until passage 6 by testing the relevant phenotypic parameters (Fig. 1D).

Because 49 of the 50 infants fulfilled the criteria for having BPD, we focused on the degrees of BPD severity (Table 1) (21). Neither the day of first appearance nor the duration of successful cultivation from tracheal aspirates was predictive for the severity of BPD (Fig. 2 and Table 2). As expected, children with high severity of BPD needed prolonged ventilatory support. There was no difference in the distribution of BPD severity between preterm infants with MSC present in tracheal aspirates within the first 7 days of life and those with MSC present in tracheal aspirates only after *day 7* and before *day 21* of life (Table 3).

These data are in agreement with previous observations showing that the presence of MSCs is associated with the development of BPD (3, 16, 39). Therefore, we then evaluated characteristics that could be used to discriminate among MSCs derived from children with better and poorer pulmonary outcomes.

Proliferative Capacity of MSCs As a Predictor of the Duration of Mechanical Ventilation and Severity of BPD

MSCs were grouped according to disease severity into mild, moderate, and severe BPD. MSCs from the three groups did not differ in the density of surface receptor expression and potential for adipogenic, osteogenic, or myofibroblastic differentiation (data not shown). The duration for establishing a successful MSC culture at passage 0 varied highly among the cells obtained from different patients. This observation was reproduced under standardized conditions in cell culture. Automated repetitive light microscopy was used to determine the changes in well area covered over time (Fig. 3A). The proliferation index (PI) was introduced to compensate for differences in the well area covered at the start of the experimental procedures (Fig. 3B). Automated repetitive light microscopy (Fig. 3C) and manual cell counting (Fig. 3D) yielded identical results in selected experiments and indicated that the increase in the well area covered resulted from an increase in absolute cell numbers. Using Nicoletti staining, we ruled out the notion that the difference in absolute cell numbers was a consequence of variations in cell death (Fig. 3E). When MSC samples were separated by disease severity, statistically significant differences in the PI were observed between the groups (Fig. 4A). Using a proportional odds model and logistic regression, followed by inspection of the receiver operating characteristic (ROC) curve, the PI was predictive of BPD severity (Fig. 4B and data not shown). In agreement with this result, a higher PI was associated with longer duration of ventilatory support. The PI was not impacted by early or late time points of first establishing the MSC culture (Fig. 4C and Tables 2 and 3).

Thus the severity of BPD can be predicted from alterations in the proliferative capacity of MSCs.

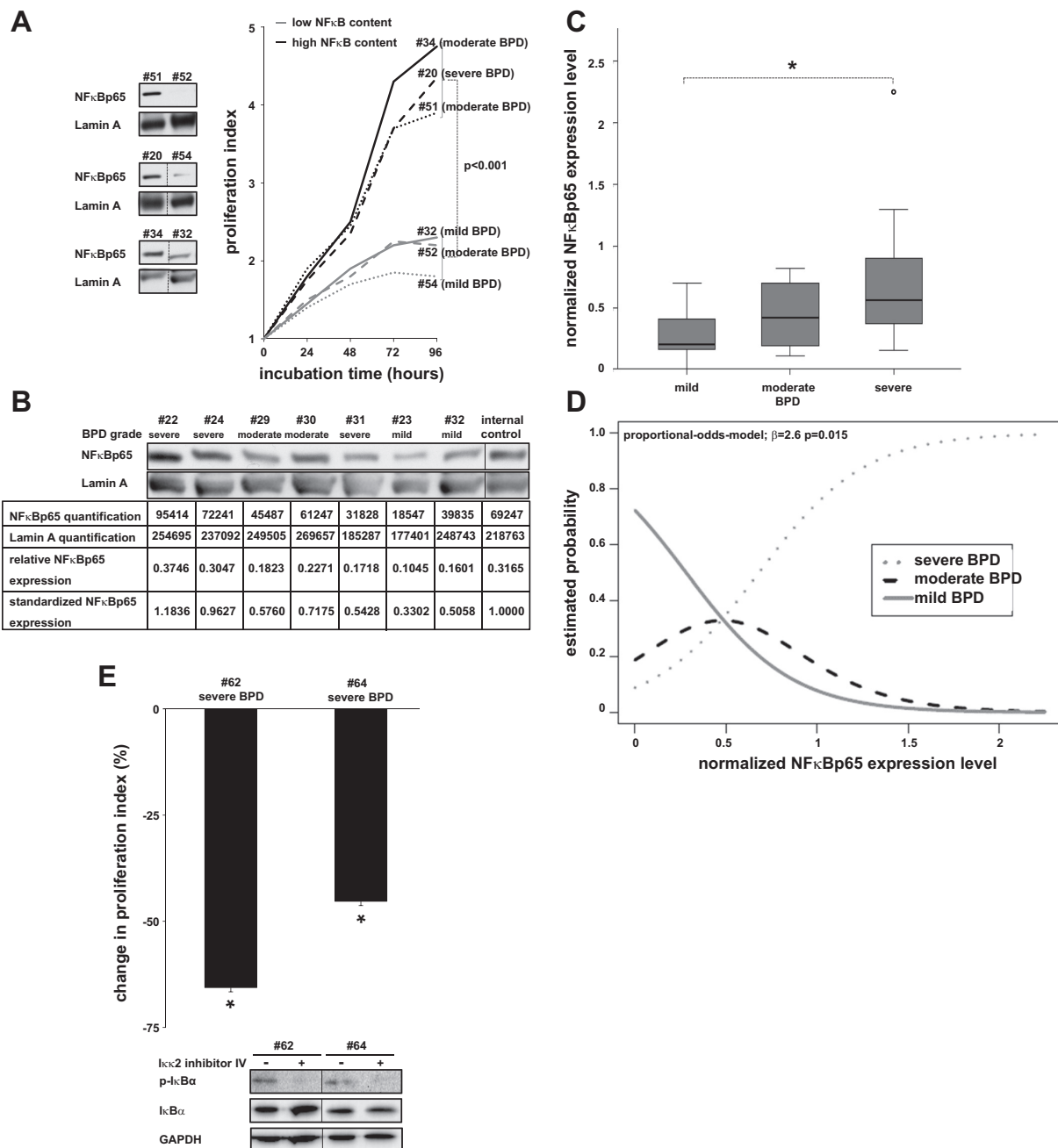### Proliferative Capacity of MSCs is Correlated with Accumulation of NFκBp65 and Downregulation of α-SMA

The earliest changes, observed in the lungs of preterm infants who later developed BPD, included the influx of inflammatory cells and an imbalance of inflammatory cytokines and growth factors. Because NF-κB is a central regulator of most inflammatory processes and proliferation (15, 41), we focused on the contribution of NF-κB to heterogeneous growth characteristics. MSC samples that displayed a particularly low

Fig. 5. The proliferative capacity of mesenchymal stromal cells (MSCs) is correlated with the nuclear accumulation of NFκBp65 and reduction in α-smooth muscle actin (α-SMA) expression. Nuclear accumulation of NFκBp65 was increased in MSCs with a higher PI. A: nuclear NFκBp65 was increased in MSCs (*left*) that were selected for their high spontaneous proliferation (*right*). Lamin A served as loading control. The order of samples from the identical blot was rearranged (*middle* and *bottom blot*) and indicated by separating lines without any further manipulation. Student's *t*-test was used to test for differences between groups; $P < 0.001$ indicates statistically significant differences. B: computer-based image quantification was introduced to compare protein density between different gels as presented for nuclear NFκBp65. An internal standard deposited on each gel enabled comparison of different gels (standardized expression level). The relative NFκBp65 expression was calculated as NFκBp65 quantification/Lamin A quantification; standardized quantification was calculated by division by the internal standard. Different sections from identical gels (indicated by separated lines) are presented without any further manipulation. C: the expression level of NFκBp65 was significantly higher in preterms with severe BPD when the technique described in B was applied to evaluate the total cohort. Nuclear extracts were available from $n = 42$ patients. Statistical analysis was performed using one-way ANOVA and post hoc pairwise comparisons by means of *t*-tests with Bonferroni adjustment. *$P < 0.05$ indicates statistically significant differences. D: the predictive accuracy of NFκBp65 was verified using the proportional odds model. $P = 0.015$ indicates statistically significant differences. E: inhibition of IκBα phosphorylation by IκK2 inhibitor IV (10 μM) reduced proliferation in MSCs after 72 h. Western blot analysis was performed after 48 h. Statistical analysis was performed using a post hoc Bonferroni adjusted pairwise comparison. The mean from $n = 3$ experiments is shown. *$P < 0.005$ indicates statistically significant differences.

or high PI were selected and assayed for nuclear accumulation of NFκBp65. Western blot analysis revealed clear differences in the levels of NFκBp65 (Fig. 5A). MSCs from the entire cohort were next assayed for the expression of NFκBp65 with the help of computer-based image quantification (Fig. 5B). Separating samples by disease severity revealed a significant difference in nuclear accumulation of NFκBp65 among samples of MSCs from preterm infants with mild and severe BPD

(Fig. 5C). Applying the proportional odds model revealed that high levels of NFκBp65 were predictive for the development of severe BPD (Fig. 5D). Biochemical inhibition of the phosphorylation of IκBα confirmed that NF-κB signaling is important for controlling proliferation in MSCs (Fig. 5E).

We next studied additional intracellular markers to detect correlations with the development of severe BPD. We assessed proteins typically expressed in mesenchymal cells including

BPD grade	#22 severe	#24 severe	#29 moderate	#30 moderate	#31 severe	#23 mild	#32 mild	internal control
NFκBp65 quantification	95414	72241	45487	61247	31828	18547	39835	69247
Lamin A quantification	254695	237092	249505	269657	185287	177401	248743	218763
relative NFκBp65 expression	0.3746	0.3047	0.1823	0.2271	0.1718	0.1045	0.1601	0.3165
standardized NFκBp65 expression	1.1836	0.9627	0.5760	0.7175	0.5428	0.3302	0.5058	1.0000

α-SMA, collagen Iα, myosin heavy chain, and PDGFR-α. Only the levels of α-SMA differed among the three groups (Fig. 6A). MSC samples revealed an inverse cytosolic expression level of α-SMA and nuclear NFκBp65 (Fig. 6B). As observed for the expression of PI and NFκBp65, the expression level of α-SMA was distinctly correlated with the degree of BPD severity (Fig. 6C). A high expression level of α-SMA was predictive of a good pulmonary outcome (Fig. 6D). The combined analysis of the levels of PI, NFκBp65, and α-SMA revealed good accuracy of prediction for moderate or severe BPD when logistic regression was used with an area under the curve (AUC) of 0.847 (Fig. 6E).

Taken together, the parameters PI, NFκBp65 accumulation, and expression of α-SMA are useful markers to predict the pulmonary prognosis.

Regulation of Proliferative Capacity of MSCs and α-SMA Expression by NFκBp65

We used RNA interference against NFκBp65 to substantiate our findings on the molecular level. The efficient delivery of siRNA against NFκBp65 inhibited spontaneous proliferation and led to increased expression of α-SMA in MSCs from preterm infants with moderate or severe BPD (Fig. 7).

These data suggest that NFκBp65 is responsible for the regulation of proliferation and expression of α-SMA in MSCs. We next focused on identifying the cause of the accumulation of NFκBp65.

Alterations in MSCs Characterized by Proinflammatory Cytokines

The pulmonary inflammatory response in preterm infants is characterized by an imbalance of proinflammatory cytokines and growth factors. IL-1β and TNF-α represent important contributors to the inflammatory response in the preterm lung (42, 43). Measurements of IL-1β in the supernatant of tracheal aspirates confirmed a positive association between higher levels of IL-1β and an increased PI (Fig. 8A). We next mimicked the in vivo environment and stimulated MSCs with recombinant IL-1β and TNF-α. Both cytokines consistently increased the PI in a panel of cultured MSCs (Fig. 8, B–D). Furthermore, both cytokines induced the accumulation of NFκBp65 and reduced the expression of α-SMA (Fig. 8, B and C). The effect of cytokine stimulation was accompanied by the nuclear translocation of NFκBp65 (Fig. 8E). Dose-response analyses revealed gradual transition to an inflammatory phenotype depending on the extent of the proinflammatory stimulus (Fig. 8F). A one-time cytokine stimulation was sufficient to induce persistent alterations in the phenotype of MSCs (Fig. 8G). These data agree with the previous observation indicating that phenotypic alterations in MSCs from preterm infants with severe BPD persisted for several passages under cell culture conditions.

Finally, RNA interference, used in the experimental setting shown in Fig. 7, was modified so that the baseline level of nuclear NFκBp65 was not affected. Subsequent stimulation with IL-1β or TNF-α markedly reduced the nuclear accumulation of NFκBp65 and the PI after cytokine stimulation (Fig. 9, A–D).

DISCUSSION

We identified a combination of phenotypic alterations in MSCs isolated from the tracheal aspirates of preterm infants; these MSCs allow for the prediction of better or worse pulmonary prognosis in these children. Surprisingly, we were able to clearly separate children with good and poor pulmonary prognosis in the relatively small patient cohort studied.

Molecular studies indicated a link between phosphorylation of IκBα, the nuclear accumulation of NFκBp65, and the development of severe BPD. The accumulation of NFκBp65, induced by IL-1β and TNF-α, was responsible for the increased proliferative capacity of MSCs and was accompanied by the reduced expression of α-SMA. Notably, a one-time in vitro stimulation led to persistent alterations in the MSC phenotype lasting for days. These alterations were identical to those observed in MSCs freshly isolated from preterm infants who later developed severe BPD. Taken together, our data clearly indicate that alteration in the MSC phenotype is a critical event in the development of BPD.

The data presented here support the dominant role of NF-κB within the cellular pulmonary inflammatory response; NF-κB represents a central transcription factor with respect to proliferation and inflammation in many inflammatory diseases (15, 18, 27). High expression levels of NF-κB within the total cellular fraction of tracheal aspirates are associated with later development of BPD, but the detailed analyses of specific cellular fractions have not yet been conducted. Cellular fractions possess a heterogeneous composition; hence, the predictive value was limited in previous studies (2, 5). Because MSCs represent a very small cellular fraction (data not shown), the determination of the expression level of NFκBp65 in MSCs was not achievable in previous studies. Using cell sorting and single cell analyses to optimize the procedure described here will enable early determination of proliferative capacity and expression of NF-κB and α-SMA in the majority of patients as

---

Fig. 6. Protein expression levels in mesenchymal stromal cells (MSCs) correlate with bronchopulmonary dysplasia (BPD) severity and can serve as predictive markers for pulmonary outcome. Reduced expression of α-SMA together with an increased PI and augmented nuclear accumulation of NFκBp65 can serve to predict severe BPD. The expression level of other proteins showed no differences between MSC cultures. A: using immunofluorescence, MSCs from 2 patients with mild or severe BPD did not differ in the expression levels of PDGF receptor-α (PDGFRα), collagen-Iα, myosin heavy chain, while α-SMA expression was reduced in MSCs obtained from the infant with severe BPD. B: in Western blot, α-SMA expression was reduced in cytosolic extracts of selected MSCs from preterms with moderate or severe BPD. GAPDH served as loading control. The order of samples in the blot was rearranged without any further manipulation (indicated by separated lines). C: the expression level of α-SMA was significantly reduced in preterms with severe BPD in the total cohort when the technique from Fig. 5B was applied to the total cohort. Cytosolic extracts were available from $n = 36$ patients. Statistical analysis was performed using one-way ANOVA and post hoc pairwise comparisons by means of t-tests with Bonferroni adjustment. *$P < 0.05$ indicates statistical significance. D: predictive accuracy of α-SMA was verified using the proportional odds model. $P = 0.018$ indicates statistically significant differences. E: the receiver operating characteristic curve (ROC) for combining PI, NFκBp65, and α-SMA data from Figs. 4A, 5C, and 6C in a logistic model predicted moderate/severe BPD with an area under the curve (AUC) of 0.847.

shown before (22, 48). Once this has been achieved, the determination of MSC phenotype may be a promising biomarker for predicting pulmonary outcome and establishing a protocol for early treatment decisions. The general applicabil-

ity of this biomarker approach requires validation in an independent cohort of patients (13).

Inflammation, infection, exposure to mechanical ventilation, and oxygen toxicity are important risk factors in the pathogen-
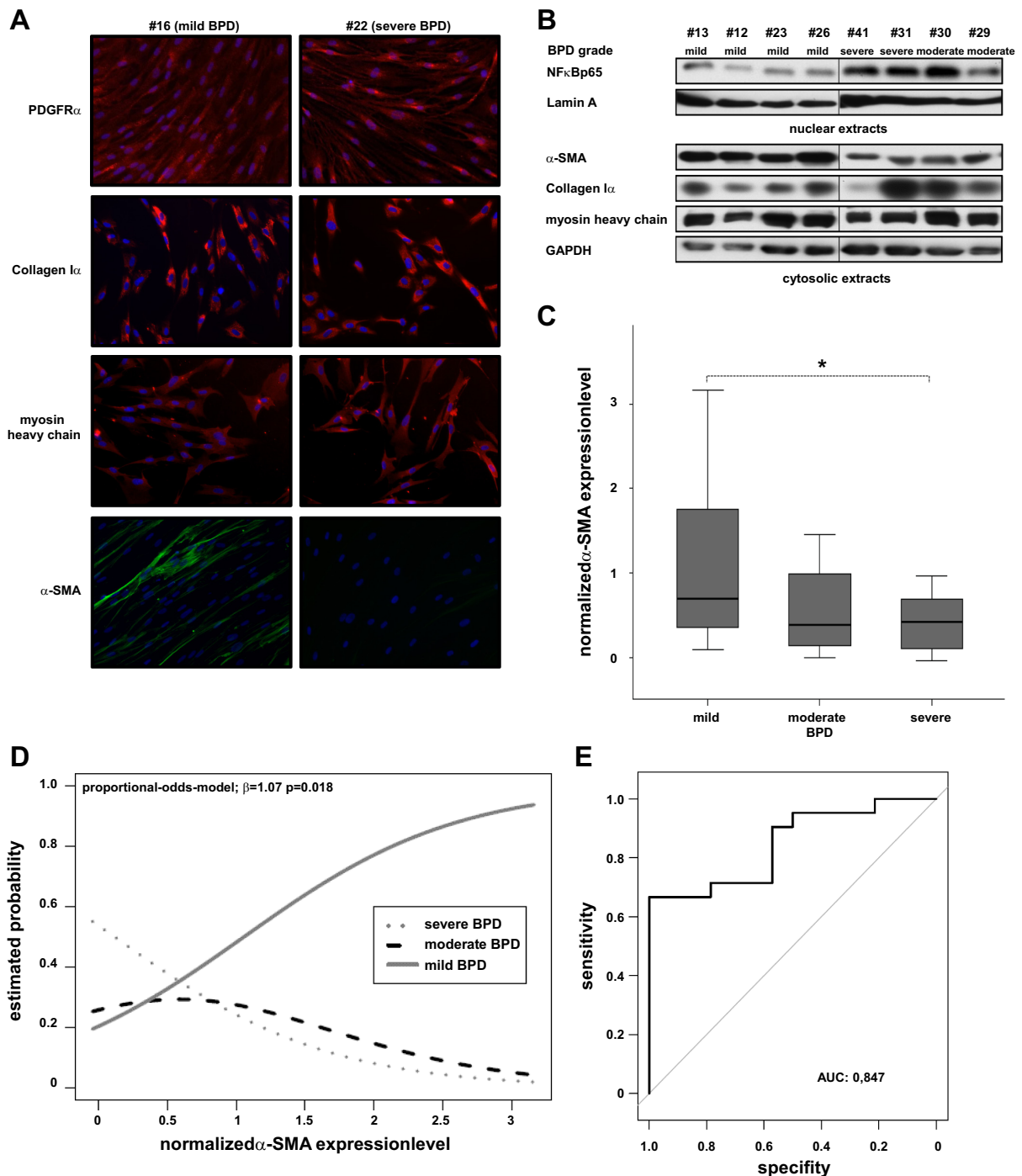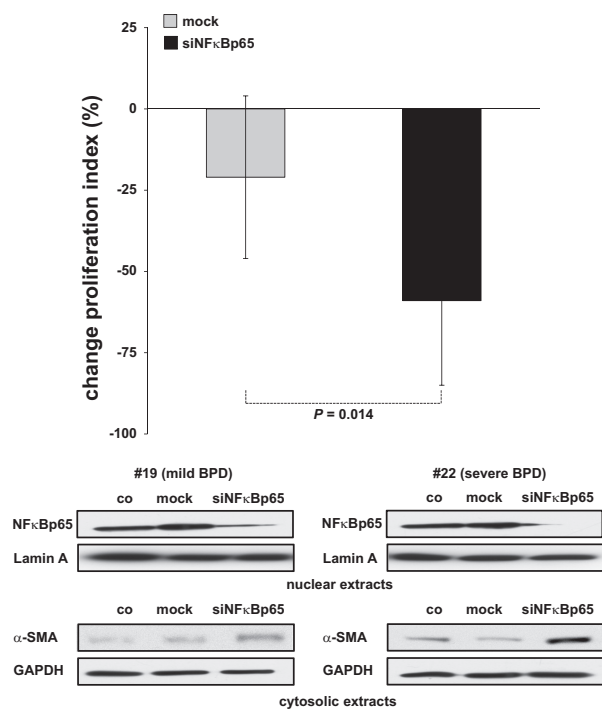
Fig. 7. Using RNA interference to confirm the central role of NFκBp65 in alteration of the mesenchymal stromal cell (MSC) phenotype. RNA interference against NFκBp65 reduced the proliferation of MSCs from $n = 15$ randomly selected preterm infants with moderate or severe bronchopulmonary dysplasia (BPD). Cell growth was assessed by Cellscreen analysis for 72 h starting 24 h after transfection. Western blot analyses for NFκBp65 expression were performed 24 h after transfection and for α-smooth muscle actin (α-SMA) after 72 h. The calculated relative change in the proliferation index (%) is presented as the mean and 95% confidence interval compared with those of the untreated control group. Statistical significance was tested using a post hoc Bonferroni adjusted pairwise comparison. *$P = 0.014$ indicates statistically significant differences.

esis of BPD. These factors induce excessive and prolonged secretion of proinflammatory cytokines. Therefore, dysregulation of cytokine and growth factor signaling is attributed to the development of BPD (13, 43). Under physiological conditions, resident pulmonary mesenchymal cells undergo a highly orchestrated process of myofibroblastic differentiation during lung development (24, 28, 40). Previous studies demonstrated substantial alterations in the pathways controlling the differentiation of MSCs into myofibroblasts; these pathways include PDGF receptor-α, β-catenin, and TGF-β1 signaling in BPD

(33, 37, 38, 40). Here we provide molecular evidence that exposure to proinflammatory cytokines leads to a persistent aberrant phenotype, with reduced expression of α-SMA, in pulmonary MSCs. This study was not designed to determine the precise origin of these cells from the proximal or distal airways of the immature lung; however, these cells are of pulmonary origin and display a lung-specific phenotype (3). It is possible that the distortion of myofibroblastic differentiation by pulmonary inflammatory response contributes to the distortion of septation and interstitial fibrosis (16, 29, 37, 38, 40). Our results provide a better understanding of how accumulation of NFκBp65 misdirects the functions of MSCs.

Conversely, NF-κB signaling is a key pathway and regulator in the regulation of development, growth, and resolution of inflammation (15, 18, 25, 41). Members of the TNF family are an important class of activators of NF-κB. The downstream effect of TNF family members depends on specific intracellular signal transduction and includes prosurvival functions (1, 10–12, 46). In accordance with this, animal studies have clearly demonstrated that a balanced activation status is critical for normal lung development, and that either overstimulation or inhibition of NF-κB signaling leads to distortion in normal lung development and a BPD-like phenotype (19, 27). A recent study demonstrated a connection between NF-κB signal transduction and the TGF-β pathway, which is another important signaling pathway involved in lung development (11). Not surprisingly, any distortion in the balance of these signaling pathways can lead to augmented lung injury, and can result in increased induction of apoptosis in mesenchymal progenitor cells (11). Therefore, the direct targeting of NF-κB can further distort lung development (19). However, selective targeting of NF-κB signaling in MSCs, or identifying decisive downstream signaling pathway(s) that lead to detrimental activity of NF-κB, can yield new therapeutic options.

MSCs are readily obtainable from tracheal aspirates of ventilated preterm infants. Studies on these cells can yield further valuable insights into the pathogenesis of BPD (3, 16, 33). Thorough evaluation of the physiological functions of these MSCs and their distortion in the injured lung is prerequisite for developing efficient therapeutic interventions. Our results indicate that distorted proliferation, nuclear accumulation of NFκBp65, and reduction in the α-SMA content of MSCs are early key events associated with the development of severe BPD. This study shows that future therapeutic approaches, aiming to prevent or reduce the burden of BPD, should include studies on phenotypic alterations in pulmonary MSCs. The following two scenarios should be considered: *1*) reversal of the inflammatory MSC phenotype as achieved using

Fig. 8. Increase in mesenchymal stromal cell (MSC) proliferation and NFκBp65 accumulation mediated by proinflammatory cytokines IL-1β and TNF-α. Proinflammatory cytokines induced the identical changes observed in MSCs from preterm infants with unfavorable pulmonary outcome. *A*: IL-1β (ng/ml) standardized to sIgA (U/ml) determined in tracheal aspirate supernatants correlated to the proliferation index. Supernatants were available from $n = 29$ infants. Statistical analysis was performed using linear regression. *$P < 0.05$ indicates statistically significant differences. Stimulation of MSCs with IL-1β (*B*, 300 ng/ml) or TNF-α (*C*, 300 ng/ml) increased proliferation and nuclear NFκBp65 and reduced the content of cytosolic α-smooth muscle actin (α-SMA). Different sections from the gel (indicated by separated lines) are presented without any further manipulation. Dots indicate the means of at least three different measurements ± SE. *D*: stimulation of $n = 12$ randomly selected cell cultures with IL-1β and TNF-α increased spontaneous proliferation. Statistical analysis was performed using a linear mixed model. *$P < 0.05$ indicates a statistically significant difference vs. control. *E*: nuclear translocation of NFκBp65 was induced after stimulation with IL-1β (300 ng/ml) for the time periods indicated. *F*: increasing the dosage of IL-1β from 3 to 300 ng/ml increased cell proliferation in MSCs. *G*: separation of data from *F* into 24-h time intervals revealed a persistent increase in proliferation and reduction in α-SMA content. Statistical analysis was performed using Student's *t*-test. NS, not statistically significant; BPD, bronchopulmonary dysplasia.
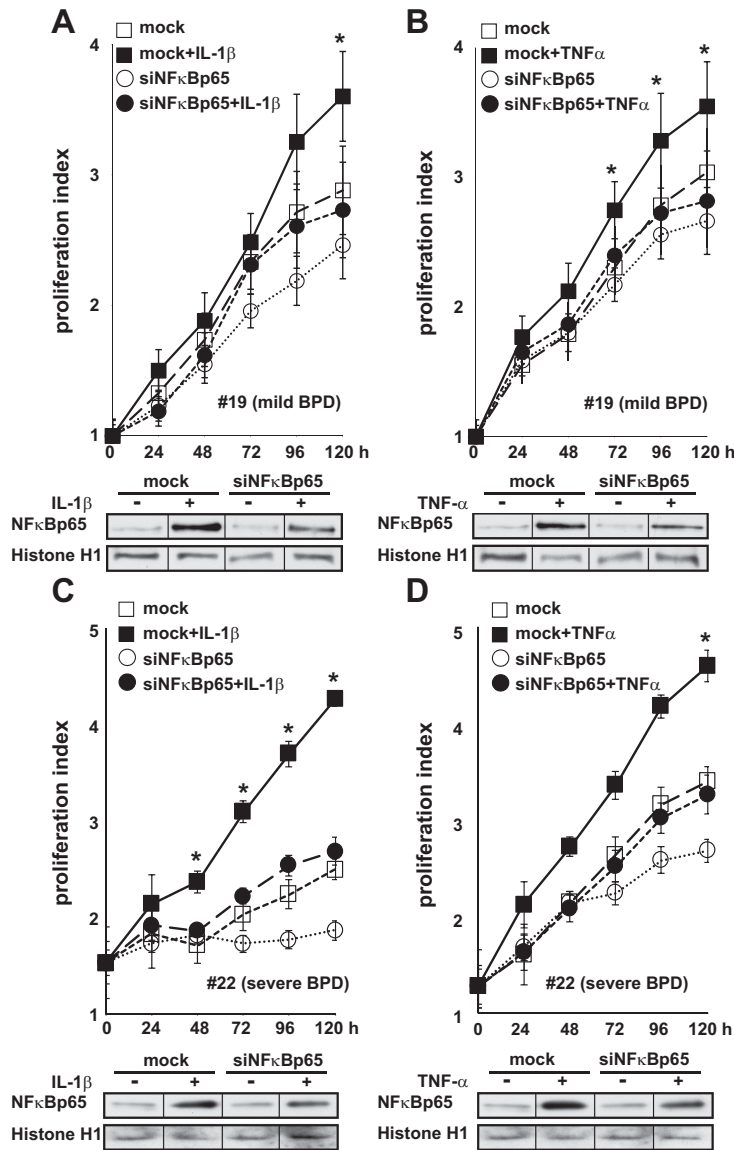
37

Fig. 9. Stimulation of mesenchymal stromal cells (MSCs) with pro-proliferative cytokines induces a phenotype that is stable for at least 120 h. Modified RNA interference against NFκBp65 before stimulation with IL-1β (300 ng/ml; A and C) or TNF-α (300 ng/ml; B and D) reduced the nuclear accumulation of NFκBp65 and the PI. The order of Western blot samples was rearranged as indicated by separated lines without any further manipulation. Statistical analysis was performed using ANOVA. *$P < 0.05$ indicates statistically significant differences.

RNA interference in this study; and 2) prophylactic prevention of phenotypic alterations in MSCs. In addition to the emerging beneficial role of allograft MSCs (35), the crucial role of resident lung MSCs has been discussed with respect to numerous pulmonary disease states of childhood and adolescence (6, 22, 23, 30, 45). Our results encourage future studies to further focus on resident pulmonary MSCs and their role in inflammation and subsequent development of BPD, and to further examine alterations in the MSC phenotype, which account for disease severity.

DISCLOSURES

No conflicts of interest, financial or otherwise, are declared by the authors.

AUTHOR CONTRIBUTIONS

T.R. and H.E. conceived and designed research; T.R., S.H., T.S., J. Gronbach, J.M., and H.E. performed experiments; T.R., S.H., C.H., U.H., J. Gertheiss, A.S., and H.E. analyzed data; T.R., S.H., J.M., J. Gertheiss, and H.E.

interpreted results of experiments; T.R., J. Gertheiss, and H.E. prepared figures; T.R. and H.E. drafted manuscript; T.R., S.H., T.S., J. Gronbach, J.M., C.H., U.H., J. Gertheiss, A.S., S.B., R.E.M., A.H., and H.E. approved final version of manuscript.

REFERENCES

1. **Baader E, Toloczko A, Fuchs U, Schmid I, Beltinger C, Ehrhardt H, Debatin KM, Jeremias I.** Tumor necrosis factor-related apoptosis-inducing ligand-mediated proliferation of tumor cells with receptor-proximal apoptosis defects. *Cancer Res* 65: 7888–7895, 2005. doi:10.1158/0008-5472.CAN-04-4278.

2. **Bourbia A, Cruz MA, Rozycki HJ.** NF-kappaB in tracheal lavage fluid from intubated premature infants: association with inflammation, oxygen, and outcome. *Arch Dis Child Fetal Neonatal Ed* 91: F36–F39, 2006. doi:10.1136/adc.2003.045807.

3. **Bozyk PD, Popova AP, Bentley JK, Goldsmith AM, Linn MJ, Weiss DJ, Hershenson MB.** Mesenchymal stromal cells from neonatal tracheal aspirates demonstrate a pattern of lung-specific gene expression. *Stem Cells Dev* 20: 1995–2007, 2011. doi:10.1089/scd.2010.0494.

4. **Bry K, Whitsett JA, Lappalainen U.** IL-1β disrupts postnatal lung morphogenesis in the mouse. *Am J Respir Cell Mol Biol* 36: 32–42, 2007. doi:10.1165/rcmb.2006-0116OC.

5. **Cheah FC, Hampton MB, Darlow BA, Winterbourn CC, Vissers MC.** Detection of apoptosis by caspase-3 activation in tracheal aspirate neutrophils from premature infants: relationship with NF-kappaB activation. *J Leukoc Biol* 77: 432–437, 2005. doi:10.1189/jlb.0904520.

6. **Chow K, Fessel JP, Kaoriihida-Stansbury, Schmidt EP, Gaskill C, Alvarez D, Graham B, Harrison DG, Wagner DH Jr, Nozik-Grayck E, West JD, Klemm DJ, Majka SM.** Dysfunctional resident lung mesenchymal stem cells contribute to pulmonary microvascular remodeling. *Pulm Circ* 3: 31–49, 2013. doi:10.4103/2045-8932.109912.

7. **Coalson JJ.** Pathology of bronchopulmonary dysplasia. *Semin Perinatol* 30: 179–184, 2006. doi:10.1053/j.semperi.2006.05.004.

8. **Collins JJ, Thébaud B.** Lung mesenchymal stromal cells in development and disease: to serve and protect? *Antioxid Redox Signal* 21: 1849–1862, 2014. doi:10.1089/ars.2013.5781.

9. **Dominici M, Le Blanc K, Mueller I, Slaper-Cortenbach I, Marini F, Krause D, Deans R, Keating A, Prockop D, Horwitz E.** Minimal criteria for defining multipotent mesenchymal stromal cells. The International Society for Cellular Therapy position statement. *Cytotherapy* 8: 315–317, 2006. doi:10.1080/14653240600855905.

10. **Ehrhardt H, Fulda S, Schmid I, Hiscott J, Debatin KM, Jeremias I.** TRAIL induced survival and proliferation in cancer cells resistant towards TRAIL-induced apoptosis mediated by NF-kappaB. *Oncogene* 22: 3842–3852, 2003. doi:10.1038/sj.onc.1206520.

11. **Ehrhardt H, Pritzke T, Oak P, Kossert M, Biebach L, Förster K, Koschlig M, Alvira CM, Hilgendorff A.** Absence of TNF-α enhances inflammatory response in the newborn lung undergoing mechanical ventilation. *Am J Physiol Lung Cell Mol Physiol* 310: L909–L918, 2016. doi:10.1152/ajplung.00367.2015.

12. **Ehrhardt H, Wachter F, Grunert M, Jeremias I.** Cell cycle-arrested tumor cells exhibit increased sensitivity towards TRAIL-induced apoptosis. *Cell Death Dis* 4: e661, 2013. doi:10.1038/cddis.2013.179.

13. **Förster K, Sass S, Ehrhardt H, Mous DS, Rottier RJ, Oak P, Schulze A, Flemmer AW, Gronbach J, Hübener C.** Early identification of bronchopulmonary dysplasia using novel biomarkers by proteomic screening. *Am J Respir Crit Care Med* 197: 1076–1080, 2018. doi:10.1164/rccm.201706-1218LE.

14. **Gough A, Linden M, Spence D, Patterson CC, Halliday HL, McGarvey LP.** Impaired lung function and health status in adult survivors of bronchopulmonary dysplasia. *Eur Respir J* 43: 808–816, 2014. doi:10.1183/09031936.00039513.

15. **Hayden MS, Ghosh S.** NF-κB, the first quarter-century: remarkable progress and outstanding questions. *Genes Dev* 26: 203–234, 2012. doi:10.1101/gad.183434.111.

16. **Hennrick KT, Keeton AG, Nanua S, Kijek TG, Goldsmith AM, Sajjan US, Bentley JK, Lama VN, Moore BB, Schumacher RE, Thannickal VJ, Hershenson MB.** Lung cells from neonates show a mesenchymal stem cell phenotype. *Am J Respir Crit Care Med* 175: 1158–1164, 2007. doi:10.1164/rccm.200607-941OC.

17. **Hilgendorff A, Reiss I, Ehrhardt H, Eickelberg O, Alvira CM.** Chronic lung disease in the preterm infant. Lessons learned from animal models. *Am J Respir Cell Mol Biol* 50: 233–245, 2014. doi:10.1165/rcmb.2013-0014TR.

18. **Imanifooladi AA, Yazdani S, Nourani MR.** The role of nuclear factor-kappaB in inflammatory lung disease. *Inflamm Allergy Drug Targets* 9: 197–205, 2010. doi:10.2174/187152810792231904.

19. **Iosef C, Alastalo TP, Hou Y, Chen C, Adams ES, Lyu SC, Cornfield DN, Alvira CM.** Inhibiting NF-κB in the developing lung disrupts angiogenesis and alveolarization. *Am J Physiol Lung Cell Mol Physiol* 302: L1023–L1036, 2012. doi:10.1152/ajplung.00230.2011.

20. **Islam JY, Keller RL, Aschner JL, Hartert TV, Moore PE.** Understanding the short- and long-term respiratory outcomes of prematurity and bronchopulmonary dysplasia. *Am J Respir Crit Care Med* 192: 134–156, 2015. doi:10.1164/rccm.201412-2142PP.

21. **Jobe AH, Bancalari E.** Bronchopulmonary dysplasia. *Am J Respir Crit Care Med* 163: 1723–1729, 2001. doi:10.1164/ajrccm.163.7.2011060.

22. **Jun D, Garat C, West J, Thorn N, Chow K, Cleaver T, Sullivan T, Torchia EC, Childs C, Shade T, Tadjali M, Lara A, Nozik-Grayck E, Malkoski S, Sorrentino B, Meyrick B, Klemm D, Rojas M, Wagner DH Jr, Majka SM.** The pathology of bleomycin-induced fibrosis is associated with loss of resident lung mesenchymal stem cells that regulate effector T-cell proliferation. *Stem Cells* 29: 725–735, 2011. doi:10.1002/stem.604.

23. **Khan P, Gazdhar A, Savic S, Lardinois D, Roth M, Tamm M, Geiser T, Hostettler K.** 118 Lung-derived mesenchymal stem cells exert anti-fibrotic effects in vitro. *Chest* 151: A15, 2017. doi:10.1016/j.chest.2017.04.016.

24. **Kugler MC, Loomis CA, Zhao Z, Cushman JC, Liu L, Munger JS.** Sonic hedgehog signaling regulates myofibroblast function during alveolar septum formation in murine postnatal lung. *Am J Respir Cell Mol Biol* 57: 280–293, 2017. doi:10.1165/rcmb.2016-0268OC.

25. **Lawrence T, Fong C.** The resolution of inflammation: anti-inflammatory roles for NF-kappaB. *Int J Biochem Cell Biol* 42: 519–523, 2010. doi:10.1016/j.biocel.2009.12.016.

26. **Lee B, Sharron M, Montaner LJ, Weissman D, Doms RW.** Quantification of CD4, CCR5, and CXCR4 levels on lymphocyte subsets, dendritic cells, and differentially conditioned monocyte-derived macrophages. *Proc Natl Acad Sci USA* 96: 5215–5220, 1999. doi:10.1073/pnas.96.9.5215.

27. **Londhe VA, Maisonet TM, Lopez B, Jeng JM, Xiao J, Li C, Minoo P.** Conditional deletion of epithelial IKKβ impairs alveolar formation through apoptosis and decreased VEGF expression during early mouse lung morphogenesis. *Respir Res* 12: 134, 2011. doi:10.1186/1465-9921-12-134.

28. **McGowan SE.** Paracrine cellular and extracellular matrix interactions with mesenchymal progenitors during pulmonary alveolar septation. *Birth Defects Res A Clin Mol Teratol* 100: 227–239, 2014. doi:10.1002/bdra.23230.

29. **Möbius MA, Rüdiger M.** Mesenchymal stromal cells in the development and therapy of bronchopulmonary dysplasia. *Mol Cell Pediatr* 3: 18, 2016. doi:10.1186/s40348-016-0046-6.

30. **Möbius MA, Thébaud B.** Bronchopulmonary dysplasia–where have all the stem cells gone? Origin and (potential) function of resident lung stem cells. *Chest* 152: 1043–1052, 2017. doi:10.1016/j.chest.2017.04.173.

31. **Nestle FO, Zheng XG, Thompson CB, Turka LA, Nickoloff BJ.** Characterization of dermal dendritic cells obtained from normal human skin reveals phenotypic and functionally distinctive subsets. *J Immunol* 151: 6535–6545, 1993.

32. **Nicoletti I, Migliorati G, Pagliacci MC, Grignani F, Riccardi C.** A rapid and simple method for measuring thymocyte apoptosis by propidium iodide staining and flow cytometry. *J Immunol Methods* 139: 271–279, 1991. doi:10.1016/0022-1759(91)90198-O.

33. **Oak P, Pritzke T, Thiel I, Koschlig M, Mous DS, Windhorst A, Jain N, Eickelberg O, Foerster K, Schulze A, Goepel W, Reicherzer T, Ehrhardt H, Rottier RJ, Ahnert P, Gortner L, Desai TJ, Hilgendorff A.** Attenuated PDGF signaling drives alveolar and microvascular defects in neonatal chronic lung disease. *EMBO Mol Med* 9: 1504–1520, 2017. doi:10.15252/emmm.201607308.

34. **Pilling D, Fan T, Huang D, Kaul B, Gomer RH.** Identification of markers that distinguish monocyte-derived fibrocytes from monocytes, macrophages, and fibroblasts. *PLoS One* 4: e7475, 2009. doi:10.1371/journal.pone.0007475.

35. **Pittenger MF, Le Blanc K, Phinney DG, Chan JK.** MSCs: Scientific Support for Multiple Therapies. *Stem Cells Int* 2015: 280572, 2015. doi:10.1155/2015/280572.

36. **Pittenger MF, Mackay AM, Beck SC, Jaiswal RK, Douglas R, Mosca JD, Moorman MA, Simonetti DW, Craig S, Marshak DR.** Multilineage potential of adult human mesenchymal stem cells. *Science* 284: 143–147, 1999. doi:10.1126/science.284.5411.143.

37. **Popova AP, Bentley JK, Anyanwu AC, Richardson MN, Linn MJ, Lei J, Wong EJ, Goldsmith AM, Pryhuber GS, Hershenson MB.** Glycogen synthase kinase-3β/β-catenin signaling regulates neonatal lung mesenchymal stromal cell myofibroblastic differentiation. *Am J Physiol Lung Cell Mol Physiol* 303: L439–L448, 2012. doi:10.1152/ajplung.00408.2011.

38. **Popova AP, Bentley JK, Cui TX, Richardson MN, Linn MJ, Lei J, Chen Q, Goldsmith AM, Pryhuber GS, Hershenson MB.** Reduced platelet-derived growth factor receptor expression is a primary feature of human bronchopulmonary dysplasia. *Am J Physiol Lung Cell Mol Physiol* 307: L231–L239, 2014. doi:10.1152/ajplung.00342.2013.

39. **Popova AP, Bozyk PD, Bentley JK, Linn MJ, Goldsmith AM, Schumacher RE, Weiner GM, Filbrun AG, Hershenson MB.** Isolation of tracheal aspirate mesenchymal stromal cells predicts bronchopulmonary dysplasia. *Pediatrics* 126: e1127–e1133, 2010. doi:10.1542/peds.2009-3445.

40. **Popova AP, Bozyk PD, Goldsmith AM, Linn MJ, Lei J, Bentley JK, Hershenson MB.** Autocrine production of TGF-β1 promotes myofibroblastic differentiation of neonatal lung mesenchymal stem cells. *Am J Physiol Lung Cell Mol Physiol* 298: L735–L743, 2010. doi:10.1152/ajplung.00347.2009.

41. **Rahman A, Fazal F.** Blocking NF-κB: an inflammatory issue. *Proc Am Thorac Soc* 8: 497–503, 2011. doi:10.1513/pats.201101-009MW.

42. **Ryan RM, Ahmed Q, Lakshminrusimha S.** Inflammatory mediators in the immunobiology of bronchopulmonary dysplasia. *Clin Rev Allergy Immunol* 34: 174–190, 2008. doi:10.1007/s12016-007-8031-4.

43. **Shahzad T, Radajewski S, Chao CM, Bellusci S, Ehrhardt H.** Pathogenesis of bronchopulmonary dysplasia: when inflammation meets organ development. *Mol Cell Pediatr* 3: 23, 2016. doi:10.1186/s40348-016-0051-9.

44. **Simmons DL, Walker C, Power C, Pigott R.** Molecular cloning of CD31, a putative intercellular adhesion molecule closely related to carcinoembryonic antigen. *J Exp Med* 171: 2147–2152, 1990. doi:10.1084/jem.171.6.2147.

45. **Sinclair K, Yerkovich ST, Chambers DC.** Mesenchymal stem cells and the lung. *Respirology* 18: 397–411, 2013. doi:10.1111/resp.12050.

46. **Wachter F, Grunert M, Blaj C, Weinstock DM, Jeremias I, Ehrhardt H.** Impact of the p53 status of tumor cells on extrinsic and intrinsic apoptosis signaling. *Cell Commun Signal* 11: 27, 2013. doi:10.1186/1478-811X-11-27.

41

Research Article

Attenuated PDGF signaling drives alveolar and microvascular defects in neonatal chronic lung disease

Prajakta Oak[1,†], Tina Pritzke[1,†], Isabella Thiel[1], Markus Koschlig[1], Daphne S Mous[2], Anita Windhorst[3], Noopur Jain[1,4], Oliver Eickelberg[1], Kai Foerster[5], Andreas Schulze[5], Wolfgang Goepel[6], Tobias Reicherzer[5], Harald Ehrhardt[7], Robbert J Rottier[2], Peter Ahnert[8], Ludwig Gortner[9], Tushar J Desai[10,*] & Anne Hilgendorff[1,4,5,11,**]

Abstract

Neonatal chronic lung disease (nCLD) affects a significant number of neonates receiving mechanical ventilation with oxygen-rich gas (MV-O_2). Regardless, the primary molecular driver of the disease remains elusive. We discover significant enrichment for SNPs in the PDGF-Rα gene in preterms with nCLD and directly test the effect of PDGF-Rα haploinsufficiency on the development of nCLD using a preclinical mouse model of MV-O_2. In the context of MV-O_2, attenuated PDGF signaling independently contributes to defective septation and endothelial cell apoptosis stemming from a PDGF-Rα-dependent reduction in lung VEGF-A. TGF-β contributes to the PDGF-Rα-dependent decrease in myofibroblast function. Remarkably, endotracheal treatment with exogenous PDGF-A rescues both the lung defects in haploinsufficient mice undergoing MV-O_2. Overall, our results establish attenuated PDGF signaling as an important driver of nCLD pathology with provision of PDGF-A as a protective strategy for newborns undergoing MV-O_2.

Introduction

Positive pressure mechanical ventilation with O_2-rich gas (MV-O_2) offers life-saving treatment for respiratory failure due to lung immaturity and insufficient respiratory drive in preterm infants. Unfortunately, this therapy significantly increases the risk for an important number of preterm infants and a subset of newborns to develop neonatal chronic lung disease (nCLD), that is, bronchopulmonary dysplasia (BPD; Hargitai *et al*, 2001; Merritt & Boynton, 2009; Jobe, 2011; Konig & Guy, 2014). Characterized by defective alveolar septation and impaired vascularization, nCLD is associated with poor pulmonary and neurological long-term outcomes in affected infants (Ehrenkranz *et al*, 2005; Doyle & Anderson, 2009). The adverse effects of positive pressure MV-O_2 on pulmonary development have been reproduced in experimental models of the disease (Scherle, 1970; Hamilton *et al*, 2003; Ehrenkranz *et al*, 2005; Bland *et al*, 2008; Hilgendorff *et al*, 2011), manifesting as increased lung apoptosis and disordered matrix elastin characteristic of nCLD. Because a myriad of developmental signals are perturbed in the setting of active disease, it is difficult to distinguish primary drivers of pathology from secondary effectors or compensatory responses. Yet, if a defect in a specific signaling pathway underlies the susceptibility to developing nCLD and orchestrates the multiple processes that execute disease pathology, it would be critical to identify this potential therapeutic target.

An essential role for platelet-derived growth factor (PDGF) signaling in alveolar development was established by the discovery that

1 Comprehensive Pneumology Center, University Hospital of the University of Munich and Helmholtz Zentrum Muenchen, Munich, Germany
2 Department of Pediatric Surgery, Erasmus Medical Center – Sophia Children's Hospital, Rotterdam, The Netherlands
3 Institute for Medical Informatics, Justus-Liebig-University, Giessen, Germany
4 Department of Pediatrics, Stanford University School of Medicine, Stanford, CA, USA
5 Department of Neonatology, Perinatal Center Grosshadern, Ludwig-Maximilians University, Munich, Germany
6 Department of General Pediatrics, University Clinic of Schleswig-Holstein, Campus Lübeck, Lübeck, Germany
7 Department of General Pediatrics and Neonatology, Justus-Liebig-University and Universities of Giessen and Marburg Lung Center (UGMLC), Giessen, Germany
8 Institute for Medical Informatics, Statistics, and Epidemiology (IMISE), University of Leipzig, Leipzig, Germany
9 Department of Pediatrics and Neonatology, Medical University Vienna, Vienna, Austria
10 Department of Internal Medicine, Pulmonary and Critical Care, Stanford University School of Medicine, Stanford, CA, USA
11 Center for Comprehensive Developmental Care, Dr. von Haunersches Children's Hospital, University Hospital Ludwig-Maximilians University, Munich, Germany
*Corresponding author. Tel: +1 650 723 1696; Fax: +1 650 498 6288; E-mail: tdesai@stanford.edu
**Corresponding author. Tel: +49 89 3187 4675; Fax: +49 89 3187 4661; E-mail: a.hilgendorff@med.uni-muenchen.de
†These authors contributed equally to this work

lungs of "knockout" mice lacking PDGF-A failed to form alveoli, with animals that survived infancy demonstrating an emphysema-like phenotype of enlarged distal air sacs (Bostrom *et al*, 1996; Lindahl *et al*, 1997). This lung pathology was attributed to failure of migration of PDGF-Rα-positive alveolar smooth muscle progenitor cells (also known as myofibroblasts) into the distal embryonic lung. Because myofibroblasts are believed to drive normal subdivision of primitive air sacs into mature alveoli ("secondary septation"), their absence presumably resulted in abnormally large distal air sacs due to a failure to execute this process. Deletion of the cognate receptor, PDGF-Rα, resulted in death in mid-gestation before air sac morphogenesis initiated (Bostrom & Betsholtz, 2002), but transgenic rescue of the profound craniofacial abnormalities and spina bifida enabled survival through birth. Distal lungs in these mutants also lacked myofibroblasts and failed to undergo secondary septation (Sun *et al*, 2000).

When the PDGF signaling pathway was examined in the lungs of animal models of nCLD employing mechanical ventilation (MV-O_2), reduced abundance of PDGF-A and PDGF-Rα proteins or mRNA was observed (Bland *et al*, 2003, 2007, 2008), similar to the lungs of neonatal rats exposed to hyperoxia (Powell *et al*, 1992) and preterm infants developing nCLD (Popova *et al*, 2014). These findings suggest that reduced PDGF signaling may be involved in the air sac morphogenesis defect of nCLD, but a causal role has not yet been demonstrated. Furthermore, since microvascular defects were not reported in the lungs of PDGF mouse mutants that failed to undergo secondary septation, the position of this pathway in the hierarchy of perturbed signaling in nCLD is uncertain. Here, in a case–control study of infants with nCLD, we discover significant enrichment for SNPs in the PDGF-Rα gene associated with reduced PDGF-R levels and diminished migration of lung fibroblasts suggesting that impairment of this pathway might be a primary driver of disease. We confirm this model using gene-targeted mice haploinsufficient for PDGF-Rα, showing an interaction with an established model of MV-O_2 that reproduces the multiple pathologies of nCLD, all of which are ameliorated by exogenous administration of PDGF-A protein during MV-O_2. We also dissect the molecular crosstalk that mediate nCLD pathology, showing that attenuated PDGF-Rα signaling results in a reduction of VEGF-A expression, likely responsible for the vasculature phenotype through increased endothelial cell apoptosis. We also find that increased TGF-β and mechanical stretch, driving lung injury in the newborn lung, act in concert to reduce PDGF-Rα signaling, exacerbating the underlying basal reduction in PDGF-Rα to a level sufficient to result in disease. Our work implicating attenuated PDGF signaling as a driver of the air sac and vasculature defects of nCLD, along with our demonstration that both pathologies can be ameliorated by exogenous PDGF-A protein, provides a strong rationale for pursuing augmentation of PDGF signaling as a potential targeted therapy for this serious disease.

Results

Enrichment of PDGF-Rα SNPs associated with reduced protein levels and migration of lung fibroblasts from ventilated preterm infants developing nCLD

We confirm reduced PDGF-Rα expression in lung fibroblasts isolated from ventilated preterm infants. This reduction in PDGF-Rα expression was correlated with increased duration of MV-O_2, as quantified by immunofluorescence and immunoblot analysis (Fig 1A). Further, a case–control analysis of PDGF-Rα in 1,061 newborns ($n = 492$ with moderate or severe BPD) identified 14 SNPs out of 117 with nominal significance ($P \leq 0.05$; Fig 1B). Three of these SNPs were highly statistically significant, with *P*-values below 0.001 (Appendix Table S1). The presence of at least one SNP at these three positions (rs12506783) was associated with reduced PDGF-Rα gene expression and PDGF-R as well as VEGF-A protein levels in blood from ventilated preterm infants (Fig 1C–E, Appendix Fig S1). In human lung fibroblast, this SNP is associated with reduced PDGF-Rα protein level in accordance with reduced migration (Fig 1F and G). Analysis of SNPs cis-regulating gene expression for genes in the PDGF pathway and its downstream pathways showed enrichment of low *P*-values for SNPs linked to the MAPKKK-cascade, JAK/STAT-cascade, apoptosis, cell cycle, DNA metabolism, lipid metabolism, protein metabolism, and actin and calcium ion homeostasis (Appendix Table S2). Together, these experiments indicate that MV-O_2 in humans results in a reduction of PDGF-Rα expression by alveolar fibroblasts, and suggests that genetic risk factors for reduced PDGF signaling in human infants is associated with an increased risk of developing nCLD.

PDGF-Rα haploinsufficiency drives the air sac pathology of nCLD in neonatal mice undergoing MV-O_2

In order to test whether attenuated PDGF signaling was indeed a risk factor for the development of nCLD as suggested by our human SNP data and not restricted to the air sac component, we obtained gene-targeted mice lacking one allele of PDGF-Rα and subjected them to MV-O_2 using a unique preclinical mouse model. We found that lungs of PDGF-Rα haploinsufficient newborn mice undergoing MV-O_2 for 8 h showed a significant increase in distal airspace size and decrease in radial alveolar counts resembling nCLD pathology as assessed by quantitative morphometry when compared to unventilated controls (Fig 2A–C), whereas their ventilated WT littermates were unaffected. As expected with this phenotype, there were fewer secondary septae in PDGF-Rα$^{+/-}$ neonatal mice after MV-O_2 for 8 h as compared to WT mice (Fig 2D), with no significant difference in lung volumes between the groups (WT control 55.3 $\pm$ 7.0 μl/g bw; WT MV-O_2 56.2 $\pm$ 14.2 μl/g bw; PDGF-Rα$^{+/-}$ control 59.7 $\pm$ 11.9 μl/g bw; PDGF-Rα$^{+/-}$ MV-O_2 57.6 $\pm$ 23.7 μl/g bw; mean and SD each). Atelectasis, as analyzed using ImageJ, involved 14–18% of the total lung in both groups undergoing MV-O_2 (WT MV-O_2 17.2 $\pm$ 9.6%; PDGF-Rα$^{+/-}$ MV-O_2 22.8 $\pm$ 10.4%; $P = 0.61$).

Immunoblot and mRNA analysis confirmed reduced pulmonary PDGF-Rα level (Figs 2G and EV1D), reflected by the reduced number of myofibroblasts localized on septal crests in ventilated PDGF-Rα$^{+/-}$ mice lungs compared to WT littermates (Fig 2E and F). Diminished JAK-2 and STAT-3 in ventilated PDGF-Rα$^{+/-}$ mice reflects reduced PDGF-Rα downstream signaling (Fig 2H and I).

PDGF-Rα haploinsufficiency drives reduced pulmonary micro-vessel density with increased endothelial cell apoptosis in neonatal mice undergoing MV-O_2

We next asked whether attenuated PDGF signaling would also reproduce the vascular defect of nCLD. Indeed, we demonstrated by
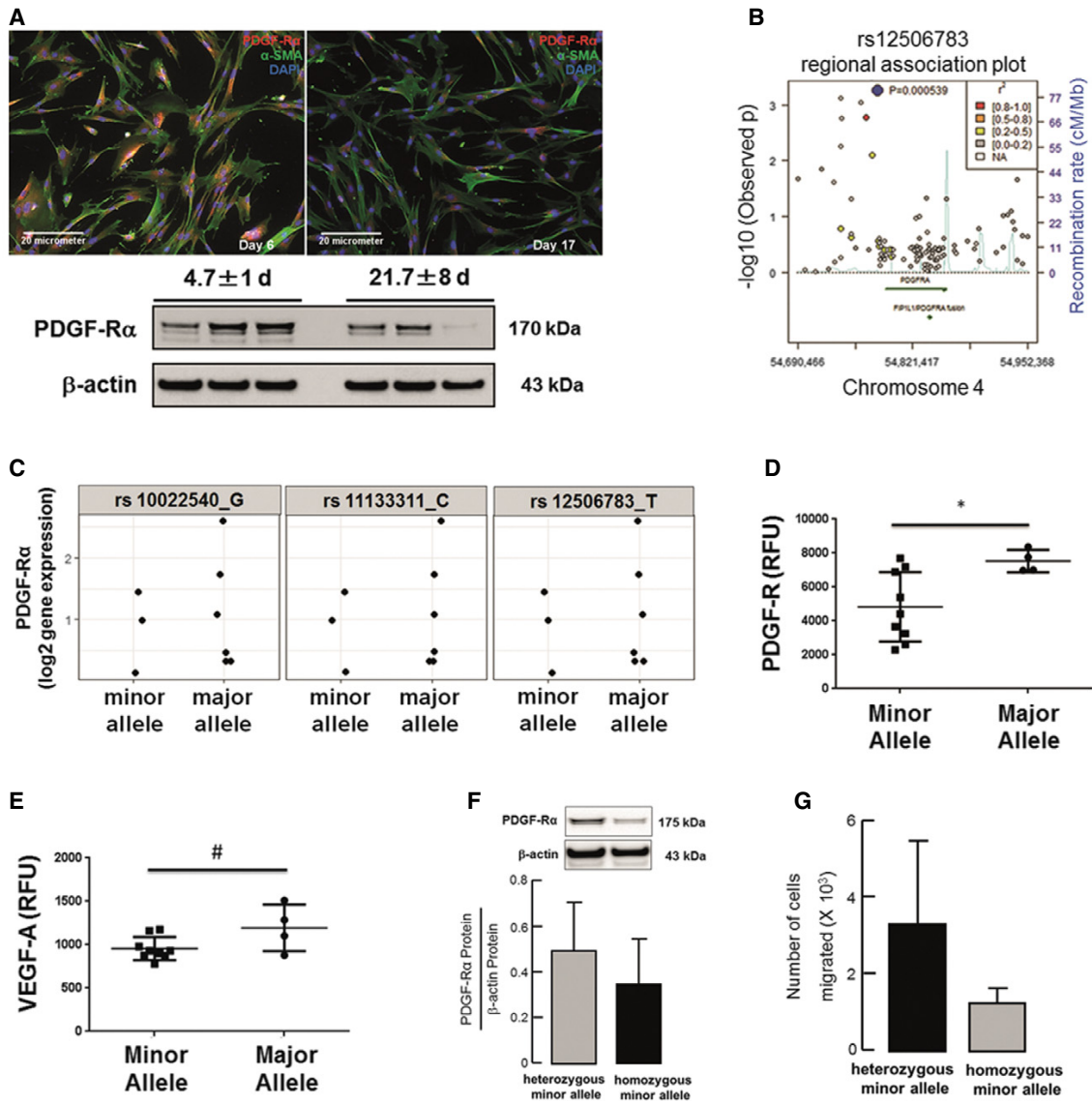
Figure 1. Enrichment of PDGF-Rα SNPs associated with reduced protein levels and migration of lung fibroblasts from ventilated preterm infants developing nCLD.

A   Decreased PDGF-Rα expression in human lung fibroblasts (hMFBs) from preterms undergoing MV-O_2 (21.7 $\pm$ 8 vs. 4.7 $\pm$ 1 day of life; serial samples 2 & 5, 3 & 6; n = 3 patients/group).

B   Regional association plot showing $-\log10$ *P*-values (*y*-axis) of SNPs according to chromosomal positions (*x*-axis). Light blue: estimated recombination rate (cM/Mb, HapMap CEU population); blue: most significant SNP (rs12506783); red: $r^2 \geq 0.8$; orange: $0.8 > r^2 \geq 0.5$, yellow: $0.5 > r^2 \geq 0.2$, gray: $0.2 > r^2 \geq 0$. *P*-values were determined using R by case-control analysis with a logistic regression model including case/control status, sex, gestational age at birth, status "small for gestational age", and country of origin of the mother. Analysis was adjusted for relatedness to account for multiple births (R-package GenABEL).

C   Levels of PDGF-Rα gene expression in patients (n = 9), which are carrying at least one SNP (minor allele) compared to patients with no SNPs (major allele). Major alleles are given in the figure labels. Minor alleles in rs10022540 are A, in rs11133311 are T, and in rs12506783 are C**.**

D, E   PDGF-R (D) and VEGF-A (E) protein levels in separate patient cohort (n = 13) carrying at least one SNP (minor allele) at position rs12506783 compared to patients with no SNPs (major allele). Protein levels were quantified using SOMAlogic technique. Data are presented as mean $\pm$ SD. Two-tailed unpaired Student's *t*-test (*P = 0.0336; $^\#P$ = 0.0863).

F, G   Representative PDGF-Rα levels (F) and migratory potential assessed by Boyden chamber assay (G) in fibroblasts isolated from tracheal aspirates of patients with nCLD. The fibroblast carrying SNP at both alleles (homozygote minor allele) displayed reduced PDGF-Rα levels and migration when compared to fibroblasts from patients carrying SNP at one allele (heterozygote minor allele). Data are presented as mean $\pm$ SD (n = 3/4 replicates).

Source data are available online for this figure.
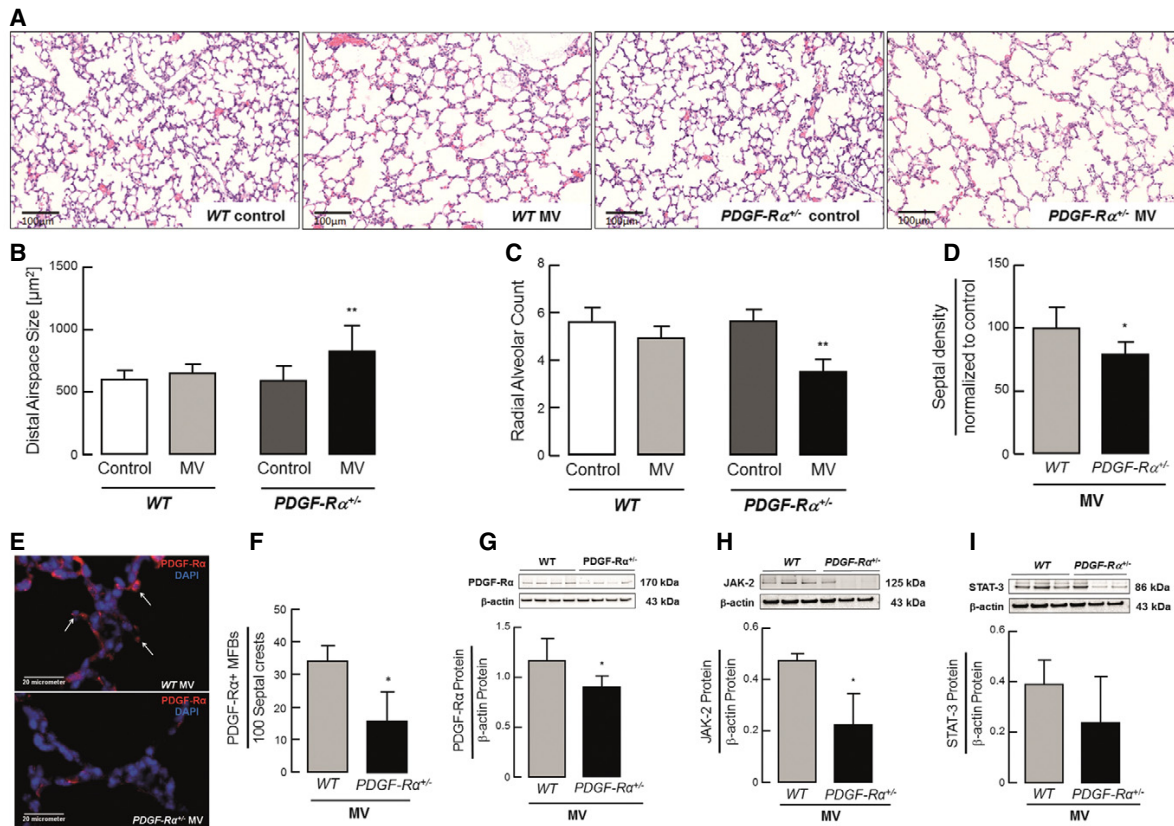
Figure 2. PDGF-Rα haploinsufficiency drives the air sac pathology of nCLD in neonatal mice undergoing MV-O_2.

A   Representative lung tissue sections (200×) from 5–8-day-old PDGF-Rα$^{+/+}$ (WT) and PDGF-Rα$^{+/−}$ mice after 8 h of MV-O_2 showing increased air space size compared to respective controls (O_2-control) spontaneously breathing 40% O_2 for 8 h.

B   Quantitative analysis of lung tissue sections showed increased alveolar area after 8 h of MV-O_2 in PDGF-Rα$^{+/−}$ mice, whereas no significant change was observed in WT mice when compared to respective controls (n = 6–11 mice/group).

C   Radial alveolar counts (alveolar number) in lung tissue sections from WT and PDGF-Rα$^{+/−}$ mice were reduced after 8 h of MV-O_2 when compared to respective controls (n = 6–11 mice/group).

D   Septal density was significantly reduced in PDGF-Rα$^{+/−}$ mice when compared to WT littermates after 8 h of MVO_2 (n = 6–8 mice/group).

E   Immunofluorescence staining (400×, merged) for PDGF-Rα (red, white arrows; blue: DAPI) with decreased stain from the septal crests in lungs of ventilated PDGF-Rα$^{+/−}$ (lower panel) and WT (upper panel) mice undergoing MV-O_2.

F   Quantitative analysis of the immunofluorescence images showed reduced number of PDGF-Rα$^+$ myofibroblasts located at the septal crests (presented myofibroblasts number per 100 septal crests; 10 fields of view in PDGF-Rα and α-smooth muscle actin co-stained sections/animal, 4 animals/group).

G–I Immunoblot analysis of PDGF-Rα (G) and its downstream proteins JAK-2 (H) and STAT-3 (I) showing a significant reduction in protein level in PDGF-Rα$^{+/−}$ neonatal mice in contrast to WT mice after MV-O_2 for 8 h (n = 3 mice/group). PDGF-Rα levels are displayed as fold change of control. Panels (H) and (I) are from same blot hence having same β-actin bands.

Data information: In (B–D) and (F–I), data are presented as mean ± SD. **P < 0.01, *P < 0.05. Statistical analysis was performed for (B–D) by ordinary one-way ANOVA with Bonferroni's correction (P = 0.0012–0.0293) and for (F–I) by two-tailed unpaired Student's t-test or Mann–Whitney test (P = 0.024–0.028).
Source data are available online for this figure.

histological analysis of PDGF-Rα$^{+/−}$ mice undergoing MV-O_2, a significant reduction in the number of alveolar micro-vessels (20–100 μm), notably exceeding the effect observed in WT pups (Fig 3A). This finding was corroborated by immunoblot analysis showing reduced lung protein levels of the endothelial cell markers, VEGF-R2 (Fig 3B), and VE-cadherin (Fig 3C) in ventilated neonatal PDGF-Rα$^{+/−}$ mice, suggesting a net loss of endothelial cells. Co-staining for apoptosis and endothelial cell markers demonstrated significantly increased vascular endothelial cell death in the lung

periphery of ventilated neonatal PDGF-Rα$^{+/−}$ mice compared with WT littermates (Fig 3E and F).

To further explore the link between reduced PDGF signaling and endothelial cell apoptosis, we focused on VEGF-A, a critical regulator of pulmonary microvascular development (Nauck *et al*, 1997; Compernolle *et al*, 2002; Kamio *et al*, 2008; Ding *et al*, 2010; Prochilo *et al*, 2013). With MV-O_2, pulmonary VEGF-A protein level was significantly reduced in PDGF-Rα$^{+/−}$ mice compared to WT littermates (Fig 3D). Interestingly, vessel number
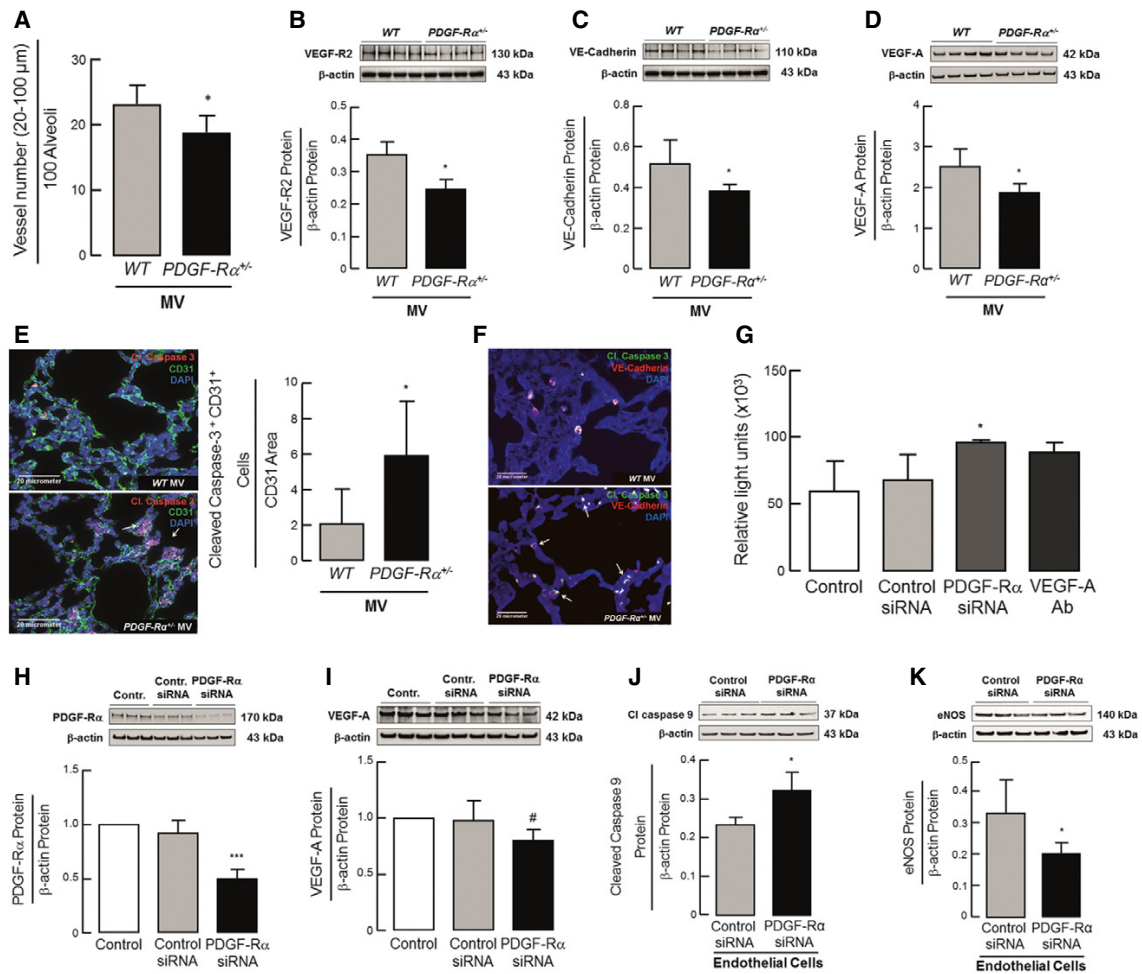
Figure 3. PDGF-Rα haploinsufficiency drives reduced pulmonary micro-vessel density with increased endothelial cell apoptosis in neonatal mice undergoing MV-O₂.

A–D Histologic and immunoblot analysis displayed reduced small vessel number (20–100 μm diameter) normalized to 100 alveoli as well as reduced pulmonary VEGF-R2, VE-cadherin, and VEGF-A protein levels, respectively (n = 6–8 mice/group). Panels (B) and (C) are from same blot hence having same β-actin bands.

E Immunofluorescence images of lung tissue (400×; merged) from neonatal PDGF-Rα$^{+/-}$ mice indicating increased cleaved caspase-3 (red, white arrows; lower panel) after 8 h of MV-O₂ in contrast to WT mice (upper panel; green: CD31; blue: DAPI). Double stain revealed increased cleaved caspase-3$^+$/CD31$^+$ cells normalized to CD31 area in PDGF-Rα$^{+/-}$ mice after 8 h of MV-O₂ (n = 4 mice/group, 4 sections/mice, and 10 images/section).

F Representative image confirming increased endothelial apoptosis in neonatal PDGF-Rα$^{+/-}$ mice after 8 h of MV-O₂ (lower panel; white arrows) with VE-cadherin (red) and cleaved caspase-3 (green) and nucleus stained with DAPI (blue) when compared to WT mice (upper panel) (n = 2 mice/group).

G Increased caspase-3 activation in HUVECs upon incubation with supernatants for 6 h obtained from lung mouse myofibroblasts after PDGF-Rα siRNA treatment when compared to control siRNA (n = 3 experiments).

H, I *In vitro* application of PDGF-Rα siRNA to primary lung mouse myofibroblasts from WT mice diminished PDGF-Rα (H) protein (normalized to control), associated with reduced VEGF-A protein (I) (n = 3 mice/group).

J, K Increased cleaved caspase-9 and reduced eNOS protein levels in HUVECs upon incubation with supernatants for 6 h obtained from lung mouse myofibroblasts after PDGF-Rα siRNA treatment when compared to control siRNA (n = 3 mice/group).

Data information: Data are presented as mean ± SD. ***P < 0.001, *P < 0.05 vs. control, #P vs. control siRNA. Statistical test in (A–E) is two-tailed unpaired Student's t-test or Mann–Whitney test, in (J, K) one-tailed Mann–Whitney test (P = 0.02–0.05), in (G) is Kruskal–Wallis H-test (P = 0.027), and in (H, I) is ordinary one-way ANOVA with Bonferroni's correction (#P = 0.0889).
Source data are available online for this figure.

did not differ compared to unventilated PDGF-Rα$^{+/-}$ mice (Appendix Fig S2).

In order to determine whether this reduction was a direct consequence of reduced PDGF-Rα signaling in myofibroblasts, we isolated primary lung myofibroblasts from WT mice and measured their production of VEGF-A at baseline as well as following siRNA mediated knockdown of PDGF-Rα expression *in vitro* (Fig 3H and I). We also administered conditioned supernatant from PDGF-Rα

46

siRNA-treated mouse myofibroblasts to human umbilical vein endothelial cells (HUVECs) in culture, and found reduced endothelial cell survival due to an increase in apoptosis (Fig 3G and J) and a reduction in the permeability factor eNOS (Fig 3K), comparable to the effect seen with an anti-VEGF-A antibody. These experiments together with Fig 2G–I indicate that PDGF-Rα signaling in the myofibroblasts promotes VEGF-A expression, and corroborates that the microvascular phenotype is downstream of attenuated PDGF signaling.

Supplemental PDGF-A rescues both the air sac and microvascular nCLD phenotypes induced by MV-O$_2$ in neonatal PDGF-Rα haploinsufficient mice

As suggested by the human SNP data and our experiments above, if the attenuated PDGF signaling drives the pathogenesis of nCLD in all its manifestations, experimentally augmenting PDGF signaling in the lungs of ventilated haploinsufficient mice should ameliorate both the air sac and microvascular phenotypes. To directly test this prediction, we administered exogenous PDGF-A protein by endotracheal delivery at the onset of MV-O$_2$. The results showed both an increase in peripheral lung micro-vessel number (20–100 μm) in treated vs. un-treated PDGF-Rα$^{+/-}$ neonatal mice undergoing MV-O$_2$, as well as a normalization of air sac defects, with increased alveolar and micro-vessel number compared with untreated controls (Fig 4A–C). The reduction in JAK-2, STAT-3, VE-cadherin, and VEGF-A protein expression in the lungs of ventilated mice was also ameliorated with PDGF-A treatment, supporting reversal of the endothelial cell apoptosis (Fig 4E–H). PDGF-A treatment further enhanced PDGF-Rα protein, associated with increased levels of AKT, suggesting a feed-forward mechanism where increased endosomal internalization leads to PDGF-Rα recycling in lung myofibroblasts with subsequent increase in receptor expression (Wang *et al*, 2004; Heldin, 2013) (Fig 4D and I). The lung periphery of mechanically ventilated PDGF-Rα$^{+/-}$ neonatal mice also exhibited an increase in (secreted) VEGF-A protein immunolocalized near myofibroblasts, providing further support (Fig 4J and M, upper panel). Quantification of immunofluorescent staining confirmed a pronounced reduction in apoptotic (cleaved caspase-3 positive) surface area and individual cells, with dramatically increased CD31 surface area in PDGF-A-treated mice

(Fig 4K–M lower panel). A physiological rescue was also observed, with an improvement in quasi-static compliance by lung function testing in neonatal mice pretreated with PDGF-A (Fig 4N), with no significant difference in lung volume (PDGF-A 49.8 ± 5.6 μl/g bw vs. no-PDGF-A 49.3 ± 3.9 μl/g bw; mean ± SD, *P* = 0.99, two-tailed Mann–Whitney test).

Elevated TGF-β levels causally relate with reduced PDGF-Rα expression in nCLD patients and mice undergoing MV-O$_2$, reducing downstream signaling and migration in pulmonary myofibroblasts

Clinical and experimental studies have consistently demonstrated activation of pulmonary TGF-β signaling with MV-O$_2$ (Assoian *et al*, 1987; Groneck *et al*, 1994; Zhao *et al*, 1997; Yamamoto *et al*, 2002; Schultz *et al*, 2003; Vozzelli *et al*, 2004; Xu *et al*, 2006; Wu *et al*, 2008). We therefore investigated how reduced PDGF signaling and its demonstrated consequences are provoked in the neonatal lung. Hence, we characterized the two potential players mechanical stretch and TGF-β alone and in combination, with respect to their effect on primary mouse and human lung myofibroblasts.

Immunofluorescent images of tissue sections from nCLD patients (*n* = 7) showed reduced expression of PDGF-Rα associated with increased expression of pSMAD-2 compared with a control lung, supporting the relevance of the findings to patients suffering from nCLD (Fig 5A). In parallel, we performed gene expression microarray analysis of blood samples obtained from 20 preterm infants in the first 72 h after birth, which similarly demonstrated an inverse correlation between the levels of TGF-β1 and PDGF-Rα in patients who went on to develop nCLD that was not observed in patients who did not (Fig 5B). We next analyzed TGF-β signaling activity in the lungs of ventilated WT mice, which demonstrated increased pSMAD 2/3 protein with a concomitant reduction in PDGF-Rα$^+$ alveolar myofibroblasts (Fig 5C). To test the impact of TGF-β on PDGF-Rα promoter activity, we conducted a luciferase assay by transfecting CCL206 cells with a pGal vector carrying a PDGF-Rα promoter insert. Administration of TGF-β caused a 50% reduction in luciferase activity (Fig 5D), indicating that TGF-β affects PDGF-Rα gene transcription, supporting the inverse relationship observed in nCLD is causal.

Figure 4. Supplemental PDGF-A rescues both the air sac and microvascular nCLD phenotypes induced by MV-O$_2$ in neonatal PDGF-Rα haploinsufficient mice. ▶

A–C Improved alveolar structure in 5–8-day-old PDGF-Rα$^{+/-}$ mice undergoing 8 h of MV-O$_2$ after intra-tracheal treatment with PDGF-A (10 μl/g bw, 25 ng/ml PDGF-A) when compared to mice receiving sterile saline (200×), confirmed by quantitative image analysis with increased alveolar counts (B) as well as vessel number normalized to 100 alveoli (C) (20–100 μm; *n* = 2–4 mice/group).

D–I Immunoblot analysis of total lung homogenates showed increased PDGF-Rα (D) together with increased JAK-2 (E), STAT-3 (F), VEGF-A (G), VE-cadherin (H), and AKT (I) protein levels in PDGF-A-treated PDGF-Rα$^{+/-}$ mice after 8 h of MV-O$_2$ when compared to WT littermates (*n* = 3–4 mice/group). Panels (D, H) and (E, F) are from same blot hence having same β-actin bands.

J–M Quantitative image analysis indicated increased VEGF-A to PDGF-Rα protein levels (J, M upper panel) together with an increase in CD31 expression in relation to total tissue (K, M lower panel) and a decrease in apoptotic (cleaved caspase-3) CD31-expressing cells (L) in the lungs of PDGF-A-treated PDGF-Rα$^{+/-}$ mice when compared to saline-treated controls after 8 h of MV-O$_2$ (*n* = 2–4 mice/group). Upper panel in (M) shows sections from PDGF-Rα$^{+/-}$ mice treated with NaCl (left) or PDGF-A (right) stained with VEGF-A (green), PDGF-Rα (red) dual positive (orange, white arrows), and inserts show VEGF-A stain (green). Lower panel shows sections from PDGF-Rα$^{+/-}$ mice treated with NaCl (left) or PDGF-A (right) stained with cleaved caspase-3 (green), CD31 (red) dual positive (orange, white arrows). Nucleus is stained with DAPI (blue).

N Treatment with PDGF-A in ventilated neonatal PDGF-Rα$^{+/-}$ mice led to improved lung compliance displayed as a function of airway pressure (Ptramax) and tidal volume when compared to untreated mice (*n* = 4 mice/group).

Data information: In (B–L, N), the data are presented as mean ± SD. ***P < 0.001, **P < 0.01, *P < 0.05, #P < 0.067. Statistical test used is one-tailed unpaired Student's *t*-test (P = 0.0001–0.065), in (C) and (G) is two-tailed Mann–Whitney and unpaired Student's *t*-test (P = 0.02–0.067).
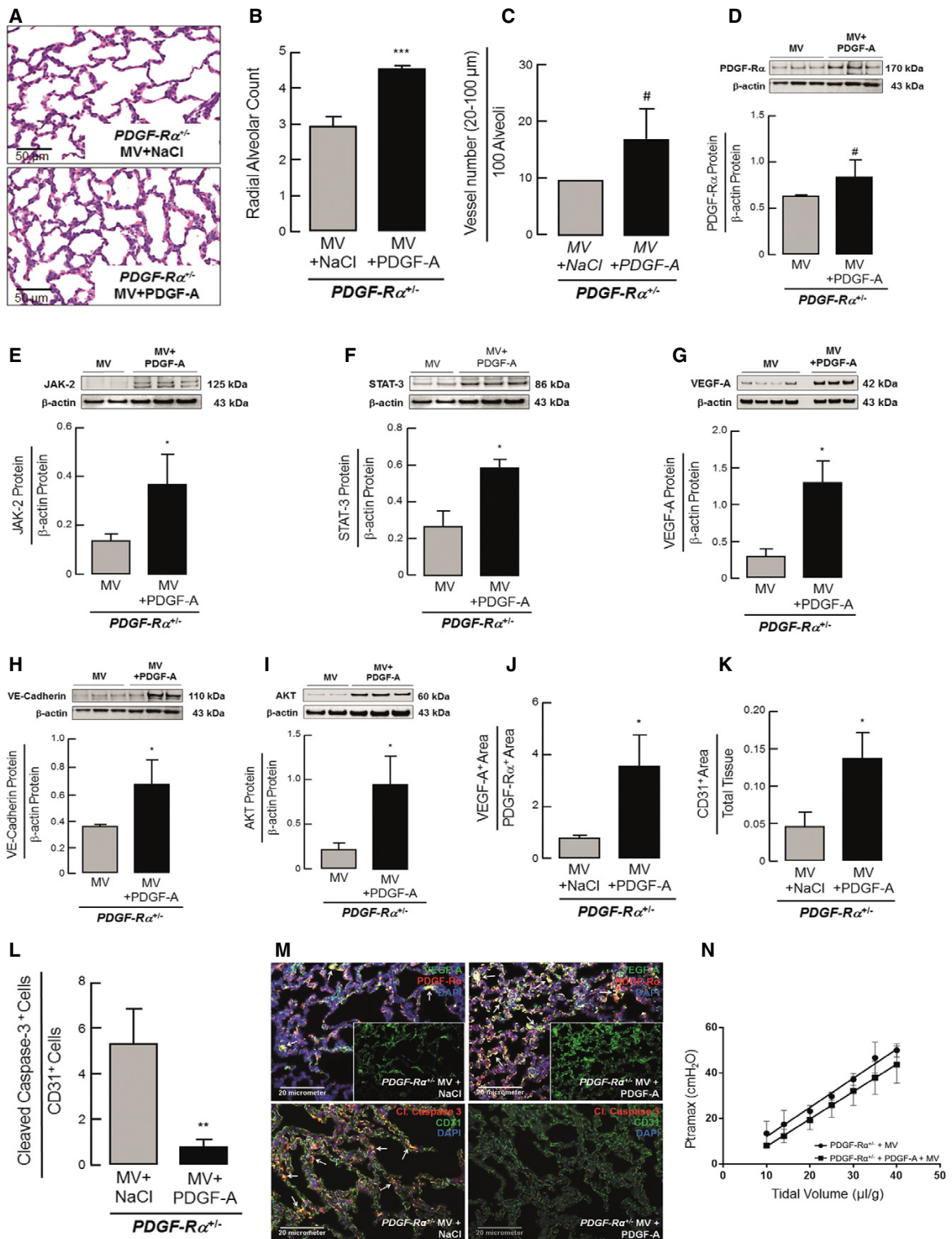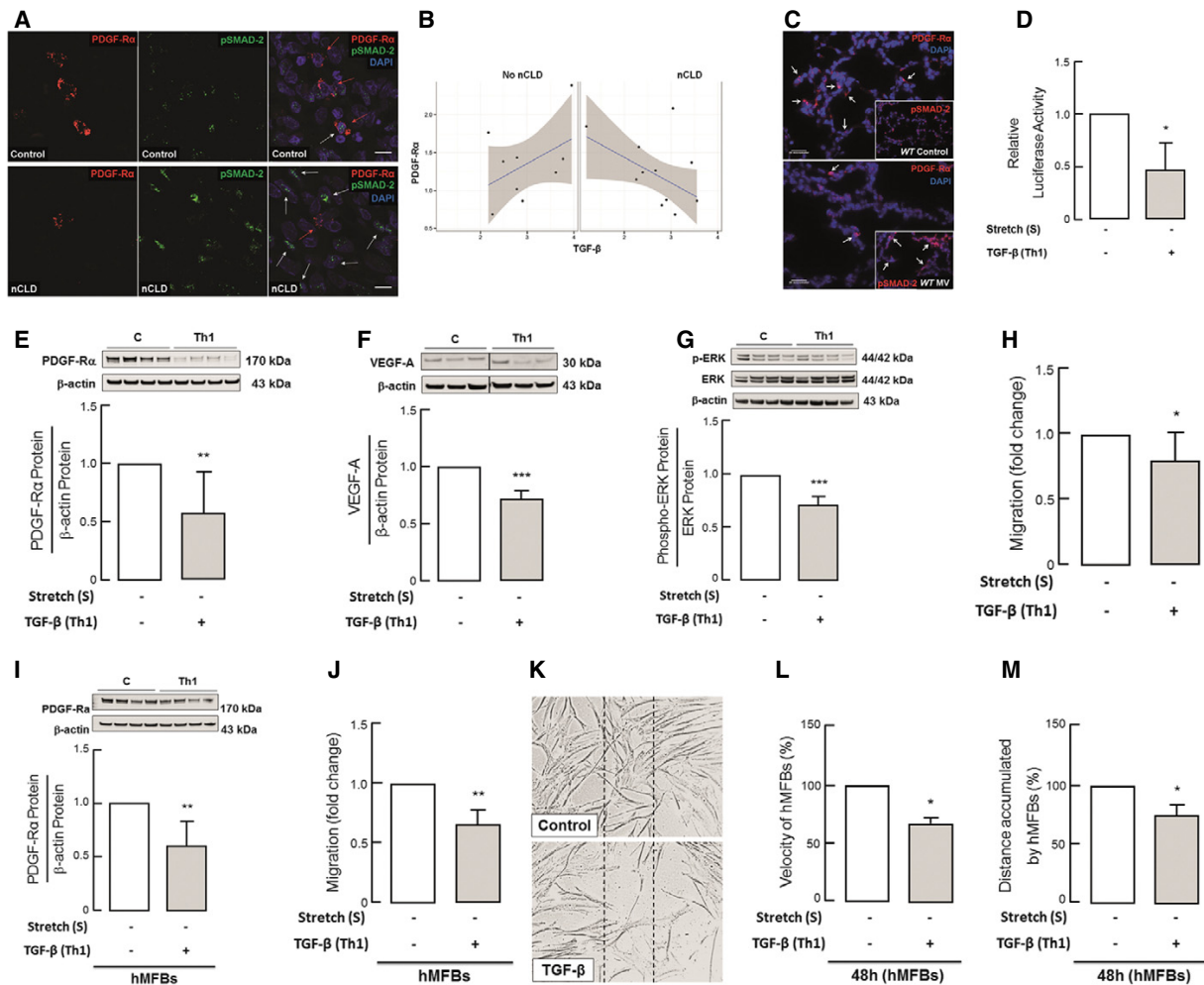Source data are available online for this figure.
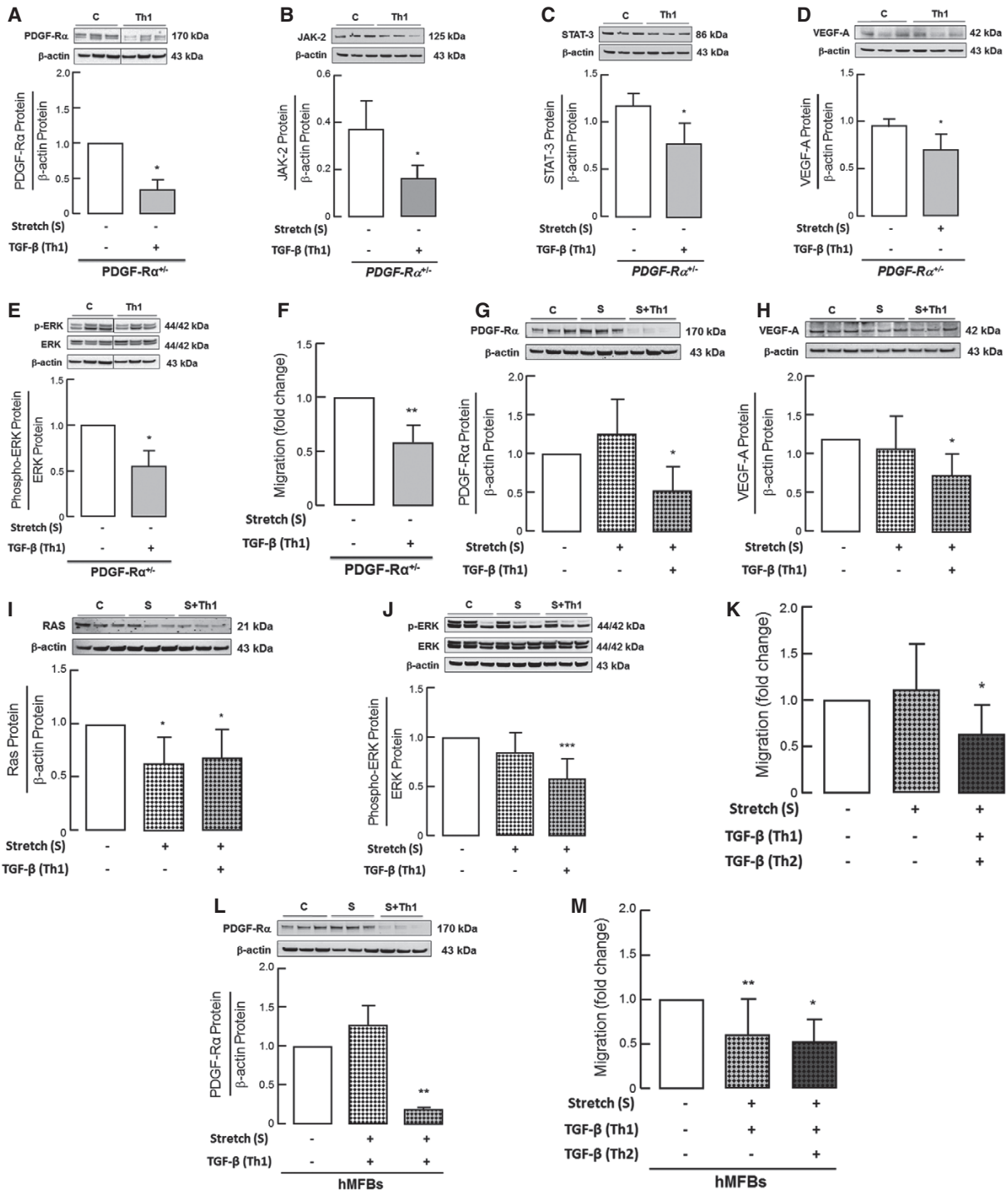
Figure 4.

Figure 5. Elevated TGF-β levels causally relate with reduced PDGF-Rα expression in nCLD patients and mice undergoing MV-O₂, reducing downstream signaling and migration in pulmonary myofibroblasts.

A   Representative immunofluorescence images showing reduced expression of PDGF-Rα (red) in the lungs of patients ($n = 7$) developing nCLD (lower left panel, red stain; white arrows) together with increased pSMAD-2 expression (lower middle panel, green stain; white arrows) as compared to lung sections from a non-nCLD patient ($n = 1$) (upper panel) (200×).

B   Negative correlation between PDGF-Rα and TGF-β1 in transcriptome analysis 72 h after birth in preterms with nCLD ($n = 11$) in contrast to non-nCLD ($n = 9$); z test of the difference of the Fisher's z transformed correlations divided by the standard error of the difference ($P = 0.048$); scatter plots log2-gene expression; linear regression (blue), with 95% CI (gray).

C   MV-O₂ reduced lung PDGF-Rα (main: red stain; white arrows) and increased pSMAD-2 levels (insert: red stain; white arrows) in ventilated neonatal WT (lower panel) when compared to control WT mice (upper panel); ($n = 4$ mice/group; 10 images/mouse; 200×).

D   Luciferase assay of CCL-206 cells transfected with pGL4.14 containing PDGF-Rα promoter revealing reduced promoter activity upon TGF-β application (normalized to control) ($n = 3$ experiments).

E–G   Immunoblot analysis showing reduced PDGF-Rα (E), VEGF-A (F), and pERK/EKR (G) protein levels upon TGF-β application alone in primary pulmonary myofibroblasts from 5–7-day-old WT mice ($n = 6$–9 mice/group).

H   Reduced migration of myofibroblasts (MFBs) from neonatal WT mice upon TGF-β application alone ($n = 5$ mice/group, 3 technical replicates).

I, J   Translation of the results in fibroblasts isolated from tracheal aspirates of ventilated preterm infants (hMFBs) displayed reduced PDGF-Rα levels (I) and migration assessed by Boyden chamber assay (J) upon TGF-β application ($n = 3$–5 patients/group).

K–M   Representative phase contrast images (100×) of scratch migration assays in human lung fibroblasts (hMFBs) after 48 h of TGF-β incubation indicating decreased wound closure (K) quantified by reduced velocity (L) and distance travelled (M) ($n = 3$ patients/group).

Data information: In (D–J) and (L, M), data are presented as mean ± SD and normalized to control. Statistical test used is two-tailed unpaired Student's t-test or Mann–Whitney test ($P = 0.0002$–0.039). ***$P < 0.001$, **$P < 0.01$, *$P < 0.05$. C, un-stretched untreated control; Th1, un-stretched myofibroblasts subjected to 5 ng/ml TGF-β (24 h).

Source data are available online for this figure.

Figure 6.

We further confirmed the effect of TGF-β on PDGF-Rα signaling in primary pulmonary myofibroblasts isolated from WT neonatal mice and fibroblasts isolated from tracheal aspirates of nCLD patients. This analysis showed a significant downregulation in PDGF-Rα level, its signaling measure by pERK/ERK and impaired function displayed as reduced migration (Fig 5E, F and H). In accordance with the *in vivo*

50

◄

Figure 6. Pronounced effect of TGF-β on pulmonary myofibroblasts from PDGF-Rα⁺/⁻ mice and in concert with mechanical stretch on both mice and human myofibroblasts.

A–E   TGF-β application (Th1) to myofibroblasts (MFBs) isolated from neonatal PDGF-Rα⁺/⁻ mice reduced PDGF-Rα (A), JAK-2 (B), STAT-3 (C), VEGF-A (D), and pERK/ERK (E) protein levels when compared to control (*n* = 3–6 mice/group). Panels (A, E) and (B, C) are from same blot hence having same β-actin bands.

F   Reduced migration assessed by Boyden chamber in myofibroblasts (MFBs) isolated from PDGF-Rα⁺/⁻ mice compared to WT mice (*n* = 5 mice/group).

G–J   TGF-β application in combination with mechanical stretch (S+Th1) in myofibroblasts (MFBs) isolated from neonatal WT mice showed reduced PDGF-Rα (G) and VEGF-A (H) protein levels as well as migratory RAS (I) and pERK/ERK (J) protein levels when compared to control myofibroblasts as assessed by immunoblot assay (*n* = 6–9 mice/group).

K   TGF-β application (Th1) as an additional dose (Th2) on stretched myofibroblasts (MFBs) from WT mice reduced migration as assessed by Boyden chamber assay (*n* = 5 mice/group).

L, M   TGF-β application in combination with stretch (S+Th1) reduced PDGF-Rα protein levels in fibroblasts (hMFBs) isolated from tracheal aspirates of nCLD patients when compared to control (C) or stretched (S) myofibroblasts (L) and as an additional dose (Th2) to stretched fibroblasts reduced migration (M) (*n* = 3–6 patients/group).

Data information: Values are normalized to the respective controls except for (B–D). Data are presented as mean ± SD. Statistical test used in (A, D–F) is two-tailed and in (B, C) is one-tailed Student's *t*-test or Mann–Whitney test (*P* = 0.004–0.05) and in (G–M) is ordinary one-way ANOVA with Bonferroni's correction (*P* = 0.0001–0.04). ***P < 0.001, **P < 0.01, *P < 0.05. C, un-stretched untreated control; S, stretched myofibroblasts (24 h); Th1, un-stretched myofibroblasts subjected to 5 ng/ml TGF-β (24 h); S+Th1, myofibroblasts stretched in parallel to TGF-β application (5 ng/ml) (24 h); Th2, re-incubation with 5 ng/ml TGF-β (8 h).

Source data are available online for this figure.

data, VEGF-A signaling associated with micro-vessel development was also diminished by 20% in pulmonary myofibroblasts from neonatal WT mice incubated with TGF-β (Fig 5G). Translating this finding in human, we demonstrate diminished PDGF-Rα levels and migration of fibroblasts (Fig 5I). Reduced migration upon TGF-β was confirmed by Boyden chamber and wound migration assays showing significantly abrogated velocity and distance travelled by fibroblasts in comparison to untreated controls (Fig 5J–M).

Pronounced effect of TGF-β on pulmonary myofibroblasts from PDGF-Rα⁺/⁻ mice and in concert with mechanical stretch on both mice and human myofibroblasts

The inhibitory effect of TGF-β on PDGF-Rα level and downstream proteins JAK-2, STAT-3, and pERK/ERK was dramatic in myofibroblasts isolated from PDGF-Rα⁺/⁻ mice with more than 30–50% reduction in the respective proteins (Fig 6A–C and E). This was accompanied by reduction in vascular marker VEGF-A and diminished migration (Fig 6D and F).

Mechanical ventilation has been demonstrated to exert significant strain forces on the developing lung in infants requiring invasive and even non-invasive respiratory support (Konig & Guy, 2014). We therefore dissected the contribution of mechanical stretch and the impact of growth factor exposure on PDGF signaling *in vitro*. Here we found that mechanical stretch in combination with TGF-β significantly reduced PDGF-Rα level in mouse myofibroblasts together with a matched reduction in VEGF-A expression confirming our *in vivo* findings (Fig 6G and H). With respect to myofibroblast function, we found that mechanical stretch in the presence of single or repeat doses of TGF-β significantly reduced migration in primary pulmonary myofibroblasts from WT mice together with a significant reduction in RAS and downstream pERK/ERK protein level, a signaling downstream of PDGF-Rα with a crucial role in myofibroblasts migration (Fig 6I–K; Liu *et al*, 2007; Fuentes-Calvo *et al*, 2013). In addition, mechanical stretch in the presence of TGF-β increased myofibroblast proliferation, together with proteins associated with proliferation PI3K and PCNA level (Fig EV2B–F). Whereas TGF-β in the absence of mechanical stretch was able to achieve comparable effects on myofibroblast migration, PDGF-Rα, and VEGF-A protein level (Fig 5E, G and H), mechanical stretch alone did not alter the migratory behavior or protein expression in the lung myofibroblasts

but did increase their proliferative behavior (Figs 6G and H, and EV2A and C).

Translating these effects to primary human fibroblasts obtained from tracheal aspirates of preterm nCLD patients, we found a significant reduction in PDGF-Rα protein level and migration by TGF-β in combination with stretch (Fig 6L and M). In line with this, repeat application of TGF-β in combination with stretch markedly reduced the migration of human lung fibroblasts (Fig 6M).

Taken together, these results indicate that elevated TGF-β signaling in the setting of MV-O₂ contributes to the development of nCLD, exacerbating the deficiency in PDGF signaling by inhibiting expression of PDGF-Rα on lung myofibroblasts.

The central role of the PDGF signaling cascade closely intertwined with upstream effectors and downstream effects with critical consequences for cellular functions in the injured neonatal lung as well as its recue with administration of PDGF-A is depicted in Fig 7.

Discussion

Neonatal chronic lung disease (nCLD), formerly known as bronchopulmonary dysplasia, has long-term health consequences not only for pulmonary but also neurologic function. Invasive and non-invasive mechanical ventilation with oxygen-rich gas (MV-O₂) is necessary for the survival of preterm babies suffering from respiratory failure due to lung immaturity and insufficient respiratory drive after birth. Nonetheless, both treatments are known to contribute to adverse pulmonary outcome, that is, the development of nCLD (Konig & Guy, 2014). Hence, it is critical to pursue medical treatments that can prevent or treat nCLD in neonates requiring ventilatory support. Here, we provide causal evidence supporting a surprising cellular and molecular model for the development of nCLD. As shown in mouse and human, PDGF signaling not only affects secondary septation but significantly impacts the microvascular structure in close relation with the omnipresent TGF in the injured neonatal lung (Fig 7A). This close intertwinement of growth factor signaling in nCLD pathology with PDGF as a central driver holds promising potential for therapeutic approaches.

The integration of PDGF-Rα haploinsufficient mice with a unique preclinical model of nCLD, together with tailored biochemical and *in vitro* assays of human and mouse primary lung cells, allowed us
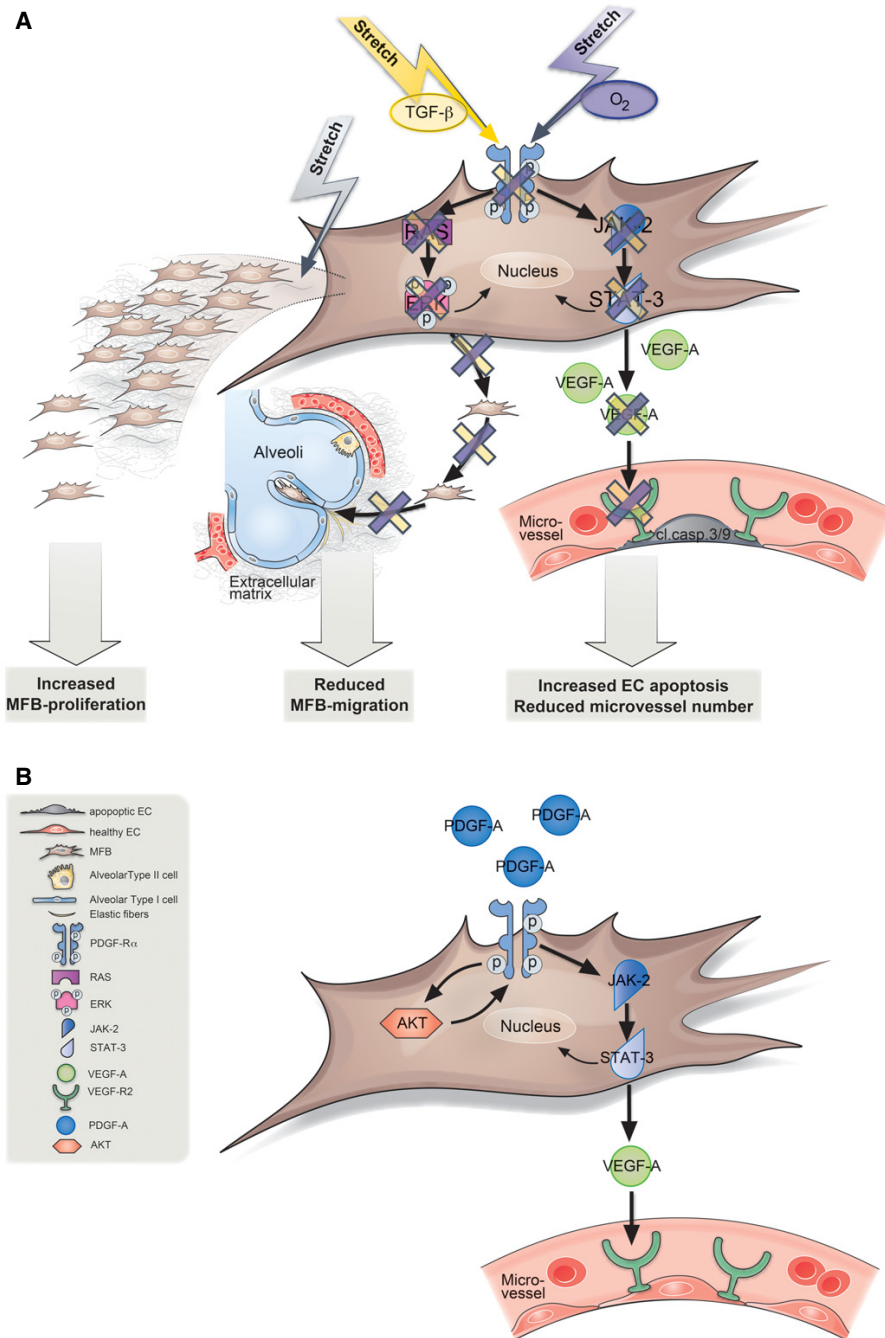
Figure 7.   Model for how attenuated PDGF signaling and positive pressure ventilation interact to produce the distinct phenotypic manifestations of nCLD.

A   MV-O$_2$ *in vivo*, a combination of O$_2$, that is, oxygen and stretch (purple arrow) and/or TGF-β alone or in combination with mechanical stretch *in vitro* (yellow arrow), reduces platelet-derived growth factor receptor α (PDGF-Rα) levels and its downstream signaling through JAK-2 and STAT-3 in the pulmonary myofibroblast (MFB). This reduction in turn abrogates vascular endothelial growth factor expression (VEGF-A and VEGF-R2), leading to increased apoptosis in pulmonary endothelial cells (EC). Whereas myofibroblast migration is diminished through reduced RAS and pERK/ERK signaling, stretch alone increases their proliferation, hence depicting the differential effect of the most important denominators of nCLD development in the premature lung undergoing MV-O$_2$.

B   Application of PDGF-A to premature lung increases PDGF-Rα levels in an AKT-dependent manner in turn activating the downstream cascade through JAK-2, STAT-3 signaling. This then activates VEGF-A secretion and VEGF-R2 activity reducing apoptosis in endothelial cells (ECs).

to elucidate the molecular pathogenesis of this disease to an unprecedented level of understanding. Building upon previous observations suggesting a role for reduced PDGF-Rα signaling in lung pathology (Bostrom *et al*, 1996; Lindahl *et al*, 1997; Bostrom & Betsholtz, 2002; Lau *et al*, 2011; Chen *et al*, 2012; Popova *et al*, 2014), we dissected upstream and downstream molecular regulators of nCLD, including a crosstalk with VEGF-A and TGF-β with mechanical stretch (Fig 7A).

Our finding that impairment of the PDGF signaling pathway—previously associated only with myofibroblast migration and secondary septation of air sacs—is capable to produce both the alveolar structural and microvascular pathology of nCLD is surprising. Is it possible that due to the dynamic intercellular crosstalks required to generate the highly stereotyped and architecturally complex arrangement of alveoli, disruption of a single program indirectly disrupts closely coordinated, but distinct, processes? There is some precedent for this model, since inhibition of VEGF in lung development has been shown to result in reduced epithelial proliferation and impaired sacculation (Zhao *et al*, 2005). However, as we show in the case of PDGF-Rα, the causal relationship may be more direct, since VEGF-A is apparently produced not only by lung epithelial cells, but also by myofibroblasts in response to PDGF and its downstream signaling through JAK and STAT (Niu *et al*, 2002; Yu & Jove, 2004). Perhaps this additional level of patterned VEGF-A production is important for ensuring proper investment of newly forming secondary septal walls by the microvascular network. In any case, our demonstration of the therapeutic activity of exogenously administered PDGF-A (Fig 7B) for rescuing both the air sac septation and microvascular defects is highly promising, particularly since previous attempts to improve vascularization by administering exogenous VEGF-A not only failed to rescue nCLD, but actually induced capillary leakage (Akeson *et al*, 2005).

Materials and Methods

All the antibodies used in the manuscript could be found in 1DegreeBio database. Study design for the manuscript experiments is described in Appendix Supplementary Methods.

Human studies

Patient characteristics
Two study cohorts comprising of 1,061 preterm infants at or less than 32 weeks of gestational age (GA) with and without nCLD, that is, BPD grade 2 or 3 according to Jobe & Bancalari (2001) [Pneumonia Research Network on Genetic Resistance and Susceptibility for the Evolution of Severe Sepsis (PROGRESS); German Neonatal Network (GNN)], were included in the SNP analysis (Ethics Approval #65/07, Homburg, University of Saarland; #145-07, Munich, Ludwig Maximillian's University of Munich and #File 79/01, Giessen, University of Giessen, Germany). Detailed patient characteristics are in Appendix Supplementary Methods. Nine patients out of this cohort were subjected to PDGF-Rα transcriptome analysis in association with the presence of single nucleotide polymorphism (SNPs). Patient characteristics of this cohort are in Appendix Table S3A. A separate study cohort was obtained from Perinatal Center of the Ludwig-Maximilians-University, Campus

Grosshadern (Ethics Approval #195-07, Munich, Ludwig Maximillian's University of Munich, Germany) for SNP and protein analysis using SOMAscan (*n* = 13). The patient characteristics are in Appendix Table S3B. Tracheal aspirates of few patients from this patient cohort were used to isolate primary fibroblasts (*n* = 6). Patient characteristics of this cohort are in Appendix Table S3C. Sections from human lung were available through the Department of Pediatric Surgery at the Erasmus Medical Center. Lung samples were retrieved from the archives of the Department of Pathology of the Erasmus MC, Rotterdam, following approval by the Erasmus MC Medical Ethical Committee. Patient characteristics of this cohort are in Appendix Table S3D. According to Dutch law following consent to perform autopsy, no separate consent is needed from the parents to perform additional staining of tissues. A group of 20 preterm infants from Giessen was subjected to microarray analysis (Ethics Approval #File 79/01, Giessen, University of Giessen, Germany). The clinical course of all infants was comprehensively monitored. Approval of the local ethics committee and written informed parental consent was obtained for all samples studied. All the experiments conformed to the principles set out in the WMA Declaration of Helsinki and Department of Health and Human Services Belmont Report. The limitation of human material to be tested in case of neonatal chronic lung disease is well known; hence, analysis was performed with samples available in maximum capacity. Samples were collected from patients randomly. Our datasets were obtained from subjects who have consented to the use of their individual genetic data for biomedical research, but not for unlimited public data release. Therefore, we submitted it to the European Genome-phenome Archive (accession number—EGAS00001002586, study unique name—ena-STUDY-IMI-24-07-2017-10:03:30:362-576), through which researchers can apply for access of the raw data.

SNP and protein analysis
Cord blood samples of 1,061 preterm infants at or below 32 weeks of gestational age (*n* = 492 BPD cases) were collected in ethylenediaminetetraacetic acid (EDTA) neonatal collection tubes. Genotypes of this patient cohort for PDGF-Rα SNPs (single nucleotide polymorphisms) were determined using Affymetrix Axiom microarrays based on the Axiom CEU array supplemented with some custom content. Matched controls were selected according to gender, GA, birth weight < 10th percentile, and country of maternal origin. Case–control analysis adjusted for relatedness; 117 SNPs were measured in or near the PDGF-Rα. Whole-blood samples collected from a separate patient cohort (*n* = 13) that were analyzed for three significant SNPs by Eurofins Genomics were subjected to proteomic screening for PDGF-R and VEGF-A (SOMAscan™, SomaLogic, Boulder, USA). For a detailed description, please refer to Appendix Supplementary Methods.

Human primary lung fibroblasts
Human primary lung fibroblasts were extracted from serial tracheal aspirate samples obtained from ventilated preterm infants (mean GA 24.9 ± 1 weeks, *n* = 6) later developing nCLD, at 4.7 ± 1 and 21.7 ± 8 day of life (Ethics Approval #195-07, Munich, Ludwig Maximillian's university of Munich, Germany). Human lung fibroblasts were cultured until 80% confluency in DMEM medium with 2 mM L-glutamine, Pen/Strep, and 20% FCS (PAN Biotech GmbH).

Purity of cell cultures was > 95% and FACS verified expression of CD11b (< 3%) (eBiosciences #48-0112-80), CD11c (< 3%) (BD Biosciences #557401), CD14 (< 5%) (BD Biosciences #09475A), CD45 (< 5%) (BD Biosciences #552848), CD90 (> 95%) (eBiosciences#48-0900-80), and CD105 (> 95%) (Miltenyi Biolabs #130-092-930); differences between patient samples were < 5% (Appendix Fig S3A). All fibroblast cultures expressed α-SMA as detected in cytosolic cell lysates by immunoblot analysis. This section is further described in Appendix Supplementary Methods.

Gene expression microarray analysis

250–300 μl of whole cord blood was obtained from 20 preterm infants 72 h after birth and directly transferred to 750–900 μl of the PAXgene Blood RNA System (PreAnalytiX, Heidelberg, Germany). RNA was isolated using PAXgene Blood RNA System (PreAnalytiX) and was subjected to CodeLink Human Whole Genome Bioarrays (GE Healthcare). PDGF-Rα gene expression in GWAS patient cohort was measured by the expression of NM_006206 on the human whole genome bioarray and human 10 k I bioarray by Codelink. For details of blood sampling and RNA analysis, please refer to Appendix Supplementary Methods.

Human lung slides

Human slides were obtained from paraformaldehyde-fixed and paraffin-embedded autopsy lungs from preterm infants with different BPD grades ($n = 7$) and an infant that died from a non-pulmonary cause. Tissue sections were stained for PDGF-Rα and TGF-β for further quantification. Please refer to Appendix Supplementary Methods for details of patient characteristics.

In vivo studies

All the studies were performed as per ARRIVE guidelines.

Gene-targeted mice

Gene-targeted mice (B6.129S4-Pdgfra$^{tm11(EGFP)Sor}$/J) referred to in manuscript as PDGF-Rα$^{+/-}$ or PDGF-Rα haploinsufficient mice were purchased from Jackson laboratories (Bar Harbor, ME, USA). Heterozygous mice are healthy and viable and reported to have no lung abnormalities (Hamilton *et al*, 2003). Co-staining for PDGF-Rα and α-SMA showed a reduction in myofibroblasts (double-positive), and mRNA and immunoblot analysis confirmed the reduced abundance of pulmonary PDGF-Rα expression in unventilated PDGF-Rα$^{+/-}$ mice when compared to WT littermates (Fig EV1A–C). For the study, 5–8-day-old neonatal mice both males and females were used. The experimental protocols were approved by the Bavarian government (TVA no. 55.2-1-54-2532-117-2010). The mice were kept under specified pathogen-free (SPF) conditions in a 12/12-h light cycle in the fully climate-controlled rooms having set points to the new conventions 2007/526 EC in our central mouse facility. Mice had a 2-week adaptation phase to their new environment and a handling by new nurses before putting them into the experiment. For each experiment, appropriate sample size ($n = 6$–12) was estimated considering the effect of MV-O$_2$ on viability of newborn mice.

Mechanical ventilation

We used 5–8-day-old (newborn/neonatal) C57B6 wild-type (PDGF-Rα$^{+/+}$) and PDGF-Rα haploinsufficient (PDGF-Rα$^{+/-}$) mice, all born at term gestation weighing 4 g [WT 3.98 ± 0.55 g; PDGF-Rα$^{+/-}$ 3.93 ± 0.66 g bodyweight (bw)] to perform experiments in four groups of mice (14–16 mice per group). WT and PDGF-Rα$^{+/-}$ pups received mechanical ventilation with oxygen-rich gas (40% O$_2$) (MV-O$_2$) for 8 h at 180 breaths/min (MicroVent 848; Harvard Apparatus) after tracheotomy under sedation with ketamine and xylazine (60 and 12 μg/g bw), as previously described (Hilgendorff *et al*, 2011). The ventilator setting mimicked the clinical setting to avoid severe lung injury (mean tidal volume 8 μl/g bw; mean airway pressure (11–12 cmH$_2$O)). Tidal volumes were similar between the MV-O$_2$ groups (WT 8.3 ± 0.5 μl/g bw; PDGF-Rα$^{+/-}$ 7.9 ± 0.3 μl/g bw). The ventilation protocol was designed to avoid severe lung injury typically occurring in response to MV with very high inflation pressures and extreme hyperoxia. Hence, we used modest tidal volumes (mean 8.7 μl/g bw) and airway pressures (peak 12–13 cmH$_2$O, mean 11–12 cmH$_2$O), and limited the FiO$_2$ to 40%, thereby simulating the MV strategy of choice for preterm infants with respiratory failure. Respective controls spontaneously breathed 40% O$_2$ for 8 h after receiving sham surgery (superficial neck incision) under mild sedation. During MV-O$_2$, mice were maintained at neutral thermal environment; sedation with ketamine and xylazine (10 μg/g bw and 2 μg/g bw, respectively) was repeated as needed to minimize spontaneous movement and assure comfort. At the end of each study, pups were euthanized with an intraperitoneal overdose of sodium pentobarbital, ~150 μg/g bw, and lungs were excised for various studies as described below including histological analysis, as well as protein measurement and RNA expression analysis from frozen lung tissue. For PDGF-A treatment, 10 μl/g bw of sterile saline containing 25 ng/ml PDGF-A was administered through the endotracheal tube immediately before the onset of MV-O$_2$ as described previously. In a subgroup of mice with or without PDGF-A treatment, tidal volume and maximum tracheal pressure (Ptramax) was measured by whole-body plethysmography (Pulmodyn, Harvard Apparatus). Stepwise increase in the tidal volume allowed to assess quasi-static compliance (Hilgendorff *et al*, 2011).

All animals were viable with response to tactile stimulation and adequate perfusion at the end of each experiment. All surgical and animal care procedures were reviewed and approved by the Institutional Animal Care and Use Committee (Bavarian Government). Upon ventilation, both the mouse strains showed similar activation of pSMAD-2, while neonatal PDGF-Rα$^{+/-}$ mice displayed increased apoptosis when compared to wild-type mice (Fig EV3A–C). Allocation of the newborn mice to the groups was performed on the basis of similarity in weight and age. When newborn mice from more than one cage were used for the experiments, all pups were randomized before distribution in the groups. Investigators were blinded for the sex of mice during allocation. Further, the analysis of lungs was performed based on internal serial numbers allotted to mice blinding the investigator for genetic background and treatment (e.g., controls or ventilated). All experimental procedures were carried out in a laboratory-controlled environment during daytime.

Quantitative histology and immunostaining

Lungs ($n = 6$–11/group) were fixed intra-tracheally with 4% paraformaldehyde overnight at 20 cmH$_2$O, as previously described (Bland *et al*, 2008). Fixed lungs were then excised, and their volume was measured by fluid displacement (Scherle, 1970). Lungs were embedded in paraffin for isotropic uniform random

(IUR) sectioning, as described previously (Scherle, 1970). Tissue sections (4 μm) were stained with hematoxylin and eosin (H&E) for quantitative assessment of alveolar area and number of incomplete and complete alveolar walls (septal density) in 2–3 independent random tissue sections per animal using the CAST image analysis system (CAST-Grid 2.1.5; Olympus, Ballerup, Denmark). Alveolar area, number of incomplete and complete alveolar walls (septal density), and radial alveolar counts providing an index of alveolar number were assessed. A minimum of 30 fields of view were quantitatively assessed in 2–3 independent random 4-μm H&E stained tissue sections per animal (CAST-Grid 2.1.5; Olympus; Emery & Mithal, 1960). Tissue sections were stained for PDGF-Rα, VEGF-A, cleaved caspase-3, CD31, and αSMA for further quantification (see Appendix Supplementary Methods for detailed description).

Quantification of micro-vessels (20–100 μm)

20- to 100-μm-diameter blood vessels were assessed in H&E (normalized to 100 alveoli)- and CD-31-stained slides obtained from 8-h studies ($n = 6$–8/group) applying a previously described immunohistochemical and morphometric approach (Hilgendorff *et al*, 2011) in 30 fields of view in the distal lung/animal (400× magnification).

Protein extraction and immunoblot analysis

After 8 h of MV-O_2, protein extraction from snap-frozen total lungs was done using high urea buffer (KPO_4, Urea, AppliChem) with Halt Protease Inhibitor (#1861280, Thermo Fisher Scientific). Primary lung fibroblasts were lysed with RIPA buffer with Halt Protease Inhibitor (mouse) or sodium vanadate (human) (#S6508, Sigma) and complete mini (#11836170001, Roche) followed by sonication. After measurement of protein concentrations (BCA, #23227, Pierce Scientific), immunoblots were performed using a Bis-Tris or a Tris-Acetate gel (#NP0321BOX, #EA0375BOX, Life Technologies) using the following antibodies: PDGF-Rα (C-20, Santa Cruz Biotechnology #338), VEGF-A (147, Santa Cruz Biotechnology #507), VEGF-R2 (Abcam, Cambridge, USA #Ab2349), VE-cadherin (H-72, Santa Cruz Biotechnology #28644), cleaved caspase-3 (Cell Signaling Technology #9661), cleaved caspase-9 (Cell Signaling Technologies #7237), eNOS (Cell Signaling Technologies #5880), phospho-ERK (Cell Signaling Technologies #4370), total ERK (Cell Signaling Technologies #4695), RAS (Cell Signaling Technologies #8955), PI3K (Cell Signaling Technologies #13666), JAK-2 (Cell Signaling Technologies #3230), STAT-3 (Cell Signaling Technologies #9139). Images were detected by chemiluminescence (#RPN2232, GE Healthcare) and quantified by densitometry (Bio Rad). Details of immunoblot analysis could be found in Appendix Supplementary Methods.

In vitro experiments

Mouse primary pulmonary myofibroblasts

Mouse myofibroblasts (MFBs) were extracted by excising lungs of 5–7-day-old C57BL6 wild-type mice after intraperitoneal overdose of sodium pentobarbital (~150 μg/g bodyweight). Under sterile conditions, lungs were flushed with PBS after cannulation of the right ventricle. Flushed lungs were then excised, diced into 1-mm pieces, and distributed on a petri dish (Corning #430167, Tewksbury, MA,

USA). Attachment to the dish was accomplished by incubation for 15–20 min at 37°C. Afterward, the tissue pieces were gently submerged in media (Gibco #41966-029, Darmstadt, Germany) containing Pen/Strep (Gibco, #15140-122) and Gentamycin (Lonza #BE02-012E, Basel, Switzerland) for 48 h before changing to fresh media. Experiments were started at 70–80% confluency. Myofibroblasts were characterized with fluorescence-activated cell sorter (FACS LSRII) using multicolor staining technique. Briefly myofibroblasts were resuspended in FACS buffer (PBS + 2% FCS + 10 mM HEPES + 0.1% Na-Azide) and stained with CD90.2 APC FITC (BD Pharmingen, Heidelberg, Germany #561974), CD 105 PE (BD Pharmingen #562759), CD45 FITC (BD Pharmingen #553080), CD11b V450 (BD horizon, Heidelberg, Germany #560455), CD11c PerCpCy5.5 (Biolegend, Fell, Germany #117328). For detection of internal markers, myofibroblasts were fixed with 4% PFA (Alfa Aesar GmbH, Germany #43368) followed by permeabilization with 0.2% Triton X-100 (Carl Roth GmbH + Co.KG, Karlsruhe, Germany #3051.2) and blocking with 1% BSA (Sigma) in PBS. Myofibroblasts were then stained in blocking solution with PDGF-Rα APC (eBiosciences #17-1401-81), α-Smooth Muscle Actin PE (R&D systems, Minneapolis, MN, USA #IC1420P), and Vimentin Alexa 488. Stained myofibroblasts were then acquired through BD™ LSR II utilizing BD FACSDiva™ software version 6.0 and analyzed using Flowjo version 9.6.1. As displayed in Appendix Fig S3B, myofibroblast culture constituted leukocytes ($0.6 \pm 0.5\%$ $CD45^+$), mesenchymal-like cells ($8.5 \pm 4.5\%$ $CD105^+$, $32 \pm 8.6\%$ $CD90^+$), and myofibroblasts ($77.2 \pm 14\%$ PDGF-$Rα^+$/$Vimentin^+$, $16.7 \pm 12\%$ $Vimentin^+$, and $77.6 \pm 27\%$ $αSMA^+$). Antibodies used were CD45 (BD Pharmingen #553080), CD105 (BD Pharmingen #562759), CD90 (BD Pharmingen #561974), PDGF-Rα (eBiosciences #17-1401), Vimentin (Cell Signaling #9854), and α-SMA (R&D systems #IC1420P).

Mechanical stretch

Myofibroblasts were seeded on flexible-bottomed laminin-coated culture plates (#BF-3001L, Flex Cell International Corporation) and stretched at 70–80% confluency (shape/sine; elongation min 0%, max 8%; frequency 2 Hz; duty cycle 50%; cycles 43216) for 24 h. A detailed description of mechanical stretch experiment is available in the Appendix Supplementary Methods.

Protein analysis

Cells were lysed with RIPA buffer including Halt Protease Inhibitor Cocktail (mouse myofibroblasts) or sodium vanadate (catalog #S6508, Sigma) and complete mini (Roche, Penzberg, Germany #11836170001; human lung fibroblasts). After storage at −80°C, cell lysates were sonicated and processed for immunoblot analysis (as described in "*in vivo*" methods).

siRNA transfection of pulmonary mouse myofibroblasts

Primary neonatal mouse myofibroblasts were transfected with either 100 nM specific siRNA against PDGF-Rα (Santa Cruz Biotechnology, Inc., Germany #sc-29444) or 100 nM control siRNA B (Santa Cruz Biotechnology #sc-44230) suspended in TurboFect (Thermo Fisher Scientific, Waltham, MA, USA #R0531) or remained untreated controls in siRNA transfection media (Santa Cruz Biotechnology, Inc., #sc-36868). Transfection with siRNA was repeated after 17 h.

Caspase activity and immunoblot analysis in human umbilical vein endothelial cells

Mycoplasma tested human umbilical vein endothelial cells (HUVECs; Commercially obtained from Lonza #CC-2935) were cultured in EBM-2 Basal Media (#00190860, #cc-4176, Lonza, mycoplasma free) with EGM-2 Single Quots supplements (Lonza #cc-4176) on 0.2% gelatin (Sigma Aldrich #G1393)-coated 96-well plates (5,000 cells/well) or 6-well plates (150,000 cells/well). After obtaining stable culture conditions, HUVECs were incubated with culture supernatants collected from three groups of mouse myofibroblasts: (i) untreated myofibroblasts (TurboFect), (ii) control siRNA-treated myofibroblasts, and (iii) myofibroblasts treated with siRNA against PDGF-Rα. For caspase activity assay, incubation with 40 μg/ml anti-VEGF (C-1) antibody (#sc-7269, Santa Cruz) served as a positive control. Caspase activity was assessed after 6 h using the Caspase-Glo 3/7 assay kit (#G8091, Promega). After 6 h of incubation, caspase activity was assessed using the Caspase-Glo 3/7 assay kit (Promega GmbH, Germany #G8091) according to the manufacturer's instructions. Cells plated in 6-well plate were lysed after 6-h incubation, and lysate was processed for immunoblot analysis with cleaved caspase-9 (Cell Signaling Technologies #9509) and eNOS (Cell Signaling Technologies #880) protein.

Luciferase assay

PDGF-Rα promoter inserted in a reporter plasmid was transfected in CCL206 stimulated with TGF-β1. Luciferase activity was assessed the next day using dual luciferase assay. For generation of reporter, please refer to Appendix Supplementary Methods.

Functional assays for myofibroblasts

Mouse and human myofibroblasts or lung fibroblasts were subjected to analysis of proliferation (Cell titer Glo assay and manual counting) and migration (Boyden chamber assay and scratch migration assay) followed by the application of stretch and TGF-β as shown in Appendix Fig S3C. Proliferation assay and scratch migration assay were performed after 48 h of application, while migration assay was done after 8 h. For detailed description of proliferation, Boyden chamber and scratch migration assays please refer to Appendix Supplementary Methods.

Statistical analysis

All datasets are presented as mean ± SD. Statistical analysis was performed using Prism 5 and 6 software package (GraphPad, San Diego, CA, USA). Two-way analysis of variance (ANOVA) and *post hoc* test with Bonferroni correction were performed to compare controls and mechanically ventilated WT (PDGF-Rα$^{+/+}$) and haploinsufficient (PDGF-Rα$^{+/-}$) newborn mice. For *in vitro* experiments, one-way ANOVA and *post hoc* test with Bonferroni correction were performed to compare more than two groups of myofibroblasts (immunoblot, migration, and proliferation analysis). For analysis of caspase activity to HUVECs, nonparametric Kruskal–Wallis test was performed. To compare datasets from two groups of either WT or PDGF-Rα$^{+/-}$ mice (immunoblot, migration and proliferation analysis, reporter assays), parametric unpaired Student's *t*-test with Welch's correction or the nonparametric Mann–Whitney test (for datasets with a skewed distribution) was performed with two-tailed or one-tailed analysis. Test groups were always compared

The paper explained

Problem

Neonatal chronic lung disease (nCLD) exhibits significant structural alveolar and vascular defects and frequently occurs in susceptible babies born prematurely and treated with mechanical ventilation with oxygen-rich gas (MV-O$_2$). Little is known about genetic risk factors or the hierarchy of molecular and cellular events that drive nCLD, resulting in serious health consequences for this significant patient population.

Results

This study demonstrates the significant association of SNPs in the PDGF-Rα gene with the development of nCLD and show the functional relevance of the genetic variants. Our data based on human studies, our preclinical mouse model and extensive *in vitro* studies in primary lung cells confirm that impaired PDGF-Rα and its downstream signaling drives alveolar and microvascular injury induced by MV-O$_2$.

Impact

Findings derived from this study will impact the understanding of nCLD pathophysiology and at the same time enable the development of new treatment.

to control group. Differences were considered statistically significant when the *P*-value was < 0.05. For microarray, data were analyzed in a target gene approach using the Pearson's correlation coefficient to correlate expression of PDGF-Rα and TGF-β in preterm infants with and without BPD. Correlation coefficients in preterm infants with and without BPD were tested using the R-packages *psych*. Statistical methods applied for the SNP analysis are outlined above.

Expanded View for this article is available online.

Author contributions

The conception and design of the manuscript was done by AH, TJD, and OE; data were acquired by PO, IT, MK, TP, KF, RJR, and DSM; followed by analysis and interpretation done by AH, TJD, HE, AW, PA, WG, LG, PO, TP, TR, DSM, and NJ; finally, the manuscript was drafted for important intellectual content by AH, TJD, OE, AS, PO, and TP.

Conflict of interest

The authors declare that they have no conflict of interest.

References

Akeson AL, Cameron JE, Le Cras TD, Whitsett JA, Greenberg JM (2005) Vascular endothelial growth factor-A induces prenatal neovascularization and alters bronchial development in mice. *Pediatr Res* 57: 82–88

56

Assoian RK, Fleurdelys BE, Stevenson HC, Miller PJ, Madtes DK, Raines EW, Ross R, Sporn MB (1987) Expression and secretion of type beta transforming growth factor by activated human macrophages. *Proc Natl Acad Sci USA* 84: 6020–6024

Bland RD, Albertine KH, Pierce RA, Starcher BC, Carlton DP (2003) Impaired alveolar development and abnormal lung elastin in preterm lambs with chronic lung injury: potential benefits of retinol treatment. *Biol Neonate* 84: 101–102

Bland RD, Mokres LM, Ertsey R, Jacobson BE, Jiang S, Rabinovitch M, Xu L, Shinwell ES, Zhang F, Beasley MA (2007) Mechanical ventilation with 40% oxygen reduces pulmonary expression of genes that regulate lung development and impairs alveolar septation in newborn mice. *Am J Physiol Lung Cell Mol Physiol* 293: L1099–L1110

Bland RD, Ertsey R, Mokres LM, Xu L, Jacobson BE, Jiang S, Alvira CM, Rabinovitch M, Shinwell ES, Dixit A (2008) Mechanical ventilation uncouples synthesis and assembly of elastin and increases apoptosis in lungs of newborn mice. Prelude to defective alveolar septation during lung development? *Am J Physiol Lung Cell Mol Physiol* 294: L3–L14

Bostrom H, Willetts K, Pekny M, Leveen P, Lindahl P, Hedstrand H, Pekna M, Hellstrom M, Gebre-Medhin S, Schalling M *et al* (1996) PDGF-A signaling is a critical event in lung alveolar myofibroblast development and alveogenesis. *Cell* 85: 863–873

Bostrom HG-LA, Betsholtz C (2002) PDGF-A/PDGF alpha-receptor signaling is required for lung growth and the formation of alveoli but not for early lung branching morphogenesis. *Dev Dyn* 223: 155–162

Chen L, Acciani T, Le Cras T, Lutzko C, Perl AK (2012) Dynamic regulation of platelet-derived growth factor receptor alpha expression in alveolar fibroblasts during realveolarization. *Am J Respir Cell Mol Biol* 47: 517–527

Compernolle V, Brusselmans K, Acker T, Hoet P, Tjwa M, Beck H, Plaisance S, Dor Y, Keshet E, Lupu F *et al* (2002) Loss of HIF-2alpha and inhibition of VEGF impair fetal lung maturation, whereas treatment with VEGF prevents fatal respiratory distress in premature mice. *Nat Med* 8: 702–710

Ding W, Knox TR, Tschumper RC, Wu W, Schwager SM, Boysen JC, Jelinek DF, Kay NE (2010) Platelet-derived growth factor (PDGF)-PDGF receptor interaction activates bone marrow-derived mesenchymal stromal cells derived from chronic lymphocytic leukemia: implications for an angiogenic switch. *Blood* 116: 2984–2993

Doyle LW, Anderson PJ (2009) Long-term outcomes of bronchopulmonary dysplasia. *Semin Fetal Neonatal Med* 14: 391–395

Ehrenkranz RA, Walsh MC, Vohr BR, Jobe AH, Wright LL, Fanaroff AA, Wrage LA, Poole K, National Institutes of Child H, Human Development Neonatal Research N (2005) Validation of the National Institutes of Health consensus definition of bronchopulmonary dysplasia. *Pediatrics* 116: 1353–1360

Emery JL, Mithal A (1960) The number of alveoli in the terminal respiratory unit of man during late intrauterine life and childhood. *Arch Dis Child* 35: 544–547

Fuentes-Calvo I, Crespo P, Santos E, Lopez-Novoa JM, Martinez-Salgado C (2013) The small GTPase N-Ras regulates extracellular matrix synthesis, proliferation and migration in fibroblasts. *Biochem Biophys Acta* 1833: 2734–2744

Groneck P, Gotze-Speer B, Oppermann M, Eiffert H, Speer CP (1994) Association of pulmonary inflammation and increased microvascular permeability during the development of bronchopulmonary dysplasia: a sequential analysis of inflammatory mediators in respiratory fluids of high-risk preterm neonates. *Pediatrics* 93: 712–718

Hamilton TG, Klinghoffer RA, Corrin PD, Soriano P (2003) Evolutionary divergence of platelet-derived growth factor alpha receptor signaling mechanisms. *Mol Cell Biol* 23: 4013–4025

Hargitai BSV, Hajdú J, Harmath A, Pataki M, Farid P, Papp Z, Szende B (2001) Apoptosis in various organs of preterm infants: histopathologic study of lung, kidney, liver, and brain of ventilated infants. *Pediatr Res* 1: 110–114

Heldin CH (2013) Targeting the PDGF signaling pathway in tumor treatment. *Cell Commun Signal* 11: 97

Hilgendorff A, Parai K, Ertsey R, Jain N, Navarro EF, Peterson JL, Tamosiuniene R, Nicolls MR, Starcher BC, Rabinovitch M *et al* (2011) Inhibiting lung elastase activity enables lung growth in mechanically ventilated newborn mice. *Am J Respir Crit Care Med* 184: 537–546

Jobe AH, Bancalari E (2001) Bronchopulmonary dysplasia. *Am J Respir Crit Care Med* 163: 1723–1729

Jobe AH (2011) The new bronchopulmonary dysplasia. *Curr Opin Pediatr* 23: 167–172

Kamio K, Sato T, Liu X, Sugiura H, Togo S, Kobayashi T, Kawasaki S, Wang X, Mao L, Ahn Y *et al* (2008) Prostacyclin analogs stimulate VEGF production from human lung fibroblasts in culture. *Am J Physiol Lung Cell Mol Physiol* 294: L1226–L1232

Konig K, Guy KJ (2014) Bronchopulmonary dysplasia in preterm infants managed with non-invasive ventilation or surfactant and a brief period of mechanical ventilation: a 6-year cohort study. *J Matern Fetal Neonatal Med* 27: 608–611

Lau M, Masood A, Yi M, Belcastro R, Li J, Tanswell AK (2011) Long-term failure of alveologenesis after an early short-term exposure to a PDGF-receptor antagonist. *Am J Physiol Lung Cell Mol Physiol* 300: L534–L547

Lindahl P, Karlsson L, Hellström M, Gebre-Medhin S, Willetts K, Heath JK, Betsholtz C (1997) Alveogenesis failure in PDGF-A-deficient mice is coupled to lack of distal spreading of alveolar smooth muscle cell progenitors during lung development. *Development* 124: 3943–3953

Liu J, Li M, Cheng BL, Zeng WS, Zou ZP, Luo SQ (2007) [Effects of blocking phospholipase C-gamma1 signaling pathway on proliferation and apoptosis of human colorectal cancer cell line LoVo]. *Ai Zheng* 26: 957–962

Merritt TADD, Boynton BR (2009) The 'new' bronchopulmonary dysplasia: challenges and commentary. *Semin Fetal Neonatal Med* 14: 345–357

Nauck M, Roth M, Tamm M, Eickelberg O, Wieland H, Stulz P, Perruchoud AP (1997) Induction of vascular endothelial growth factor by platelet-activating factor and platelet-derived growth factor is downregulated by corticosteroids. *Am J Respir Cell Mol Biol* 16: 398–406

Niu G, Wright KL, Huang M, Song L, Haura E, Turkson J, Zhang S, Wang T, Sinibaldi D, Coppola D *et al* (2002) Constitutive Stat3 activity up-regulates VEGF expression and tumor angiogenesis. *Oncogene* 21: 2000–2008

Popova AP, Bentley JK, Cui TX, Richardson MN, Linn MJ, Lei J, Chen Q, Goldsmith AM, Pryhuber GS, Hershenson MB (2014) Reduced platelet-derived growth factor receptor expression is a primary feature of human bronchopulmonary dysplasia. *Am J Physiol Lung Cell Mol Physiol* 307: L231–L239

Powell PP, Wang CC, Jones R (1992) Differential regulation of the genes encoding platelet-derived growth factor receptor and its ligand in rat lung during microvascular and alveolar wall remodeling in hyperoxia. *Am J Respir Cell Mol Biol* 7: 278–285

Prochilo T, Savelli G, Bertocchi P, Abeni C, Rota L, Rizzi A, Zaniboni A (2013) Targeting VEGF-VEGFR pathway by sunitinib in peripheral primitive neuroectodermal tumor, paraganglioma and epithelioid hemangioendothelioma: three case reports. *Case Rep Oncol* 6: 90–97

Scherle W (1970) A simple method for volumetry of organs in quantitative stereology. *Mikroskopie* 26: 57–60

Schultz C, Tautz J, Reiss I, Moller JC (2003) Prolonged mechanical ventilation induces pulmonary inflammation in preterm infants. *Biol Neonate* 84: 64–66

Sun T, Jayatilake D, Afink GB, Ataliotis P, Nister M, Richardson WD, Smith HK
(2000) A human YAC transgene rescues craniofacial and neural tube
development in PDGFRalpha knockout mice and uncovers a role for
PDGFRalpha in prenatal lung growth. *Development* 127: 4519 – 4529

Vozzelli MA, Mason SN, Whorton MH, Auten RL Jr (2004) Antimacrophage
chemokine treatment prevents neutrophil and macrophage influx in hyperoxia-
exposed newborn rat lung. *Am J Physiol Lung Cell Mol Physiol* 286: L488 – L493

Wang Y, Pennock SD, Chen X, Kazlauskas A, Wang Z (2004) Platelet-derived
growth factor receptor-mediated signal transduction from endosomes. *J
Biol Chem* 279: 8038 – 8046

Wu S, Capasso L, Lessa A, Peng J, Kasisomayajula K, Rodriguez M, Suguihara
C, Bancalari E (2008) High tidal volume ventilation activates Smad2 and
upregulates expression of connective tissue growth factor in newborn rat
lung. *Pediatr Res* 63: 245 – 250

Xu L, Rabinovitch M, Bland R (2006) Altered expression of key growth factors
(TGF{alpha}, TGFß1, PDGF-A) and flawed formation of alveoli and elastin
(Eln) in lungs of preterm (PT) lambs with chronic lung disease (CLD).
FASEB J 20 meeting abstract: A1442 – A1443

Yamamoto H, Teramoto H, Uetani K, Igawa K, Shimizu E (2002) Cyclic stretch
upregulates interleukin-8 and transforming growth factor-beta1
production through a protein kinase C-dependent pathway in alveolar
epithelial cells. *Respirology* 7: 103 – 109

Yu H, Jove R (2004) The STATs of cancer–new molecular targets come of age.
Nat Rev Cancer 4: 97 – 105

Zhao Y, Gilmore BJ, Young SL (1997) Expression of transforming growth
factor-beta receptors during hyperoxia-induced lung injury and repair. *Am
J Physiol* 273: L355 – L362

Zhao L, Wang K, Ferrara N, Vu TH (2005) Vascular endothelial growth factor
co-ordinates proper development of lung epithelium and vasculature.
Mech Dev 122: 877 – 886

58

10 Danksagung

11 Publikationsliste

Originalarbeiten

Oak P., Pritzke T., Thiel I., Koschlig M., Mous D. S., Windhorst A., Jain N., Eickelberg O., Förster K., Schulze A., Goepel W., **Reicherzer T**., Ehrhardt H., Rottier R.J., Ahnert P., Gortner L., Desai T.J. und Hilgendorff A. (2017). „Attenuated PDGF signaling drives alveolar and microvascular defects in neonatal chronic lung disease". In: *EMBO molecular medicine* 9(11), S. 1504-1520. (Impact-Factor 2017: 10,3)

Reicherzer T., Häffner S., Shahzad T., Gronbach J., Mysliwietz J., Hübener C., Hasbargen U., Gertheiss J., Schulze A., Bellusci S., Morty R.E., Hilgendorff A. und Ehrhardt H. (2018). „Activation of the NFκB pathway alters the phenotype of MSCs in the tracheal aspirates of preterm infants with severe BPD". In: *American Journal of Physiology-Lung Cellular and Molecular Physiology.* L87-L101 (Impact-Factor 2017: 4,1)

Reviews und Buchbeiträge

Reicherzer T. (2009). „Checklisten Anatomie und Physiologie". *Elsevier, Urban & Fischer.*

Herzig D., Delius M., Hasbargen U., Hübener C., **Reicherzer T.** und Schulze A. (2014). „Zwillingsschwangerschaften und feto-fetales Transfusionssyndrom". In: *Neonatologie Scan*, 3(03), 217-231.

Gronbach J., Shahzad T., Radajewski S., Chao C-M., Bellusci S., Morty R.E., **Reicherzer T.** und Ehrhardt H. (2018). „The Potentials and Caveats of Mesenchymal Stromal Cell-Based Therapies in the Preterm Infant". In: *Stem Cells Int*, Article ID 9652897.

Abstracts

Reicherzer T., Schulze A. und Ehrhardt H. (2010). „Phänotypische Charakterisierung der Lungenfibroblasten aus dem Trachealaspirat von Frühgeborenen <29

vollendete SSW". In: *Klinische Pädiatrie*, Volume 222 S 01

Reicherzer T., Schulze A. und Ehrhardt H. (2011). „NFκB als zentraler Mediator der Spontanproliferation der Lungenfibroblasten von Frühgeborenen". In: *Monatsschr Kinderheilkd,* May 2011, Issue 2 Supplement, 159:20-140

Reicherzer T., Häffner S., Müller C., Gertheiss J., Schulze A. und Ehrhardt H. (2012). „Identifikation von intrazellulären Markern des Trachealaspirates als Prädiktoren des Schweregrades der chronischen Lungenerkrankung von Frühgeborenen <29 SSW". In: *Monatsschr Kinderheilkd*, September 2012 [Suppl 1] 160:1–260

Ehrhardt H., Häffner S., Müller C., **Reicherzer T.** und Schulze A. (2012). „Veränderung der Charakteristika der Lungenfibroblasten von Frühgeborenen <29 SSW durch die pro-inflammatorischen Zytokine der pulmonalen Inflammationsreaktion". In: *Monatsschr Kinderheilkd*, September 2012 [Suppl 1] 160:1–260

Oak P., Jain N., Koschlig M., **Reicherzer T.**, Ehrhardt H.und Hilgendorff A. (2013). „Impact on shear stress and transforming growth factor on pulmonary (myo)fibroblasts of newborn mice and humans". In: *Am J Respir Crit Care Med* 187; 2013: A3256

Reicherzer T., Häffner S., Gertheiss J., Schulze A. und Ehrhardt, H. (2016). „Phenotype of lung Mesenchymal Stromal Cells predicts severity of BPD in extremely preterm infants". In: *Eur J Pediatr*; 2016: 175: 1393.

Reicherzer T., Schütze G., Vogeser M., Schulze A. und Flemmer A.W. (2017). „Copper and Zinc content of breast milk from women suffering from Wilson's disease". In: *JPNIM*, 2017; 6(2):e060238

Preise

Bengt Robertson Award 2016 der European Society for Paediatric Research (ESPR) für "Phenotype of lung Mesenchymal Stromal Cells predicts severity of BPD in extremely preterm infants" (Genf, 2016)

12 Eidesstattliche Versicherung

Ich, Tobias Reicherzer, erkläre hiermit an Eides statt, dass ich die vorliegende Dissertation mit dem Thema

Mesenchymale Stromazellen aus der Lunge extrem unreifer Frühgeborener und ihre Wechselwirkung mit der pulmonalen Entzündungsreaktion

selbständig verfasst, mich außer der angegebenen keiner weiteren Hilfsmittel bedient und alle Erkenntnisse, die aus dem Schrifttum ganz oder annähernd übernommen sind, als solche kenntlich gemacht und nach ihrer Herkunft unter Bezeichnung der Fundstelle einzeln nachgewiesen habe. Ich erkläre des Weiteren, dass die hier vorgelegte Dissertation nicht in gleicher oder in ähnlicher Form bei einer anderen Stelle zur Erlangung eines akademischen Grades eingereicht wurde

München, 26.01.2020
Ort, Datum

Tobias Reicherzer
Unterschrift Verfasser